

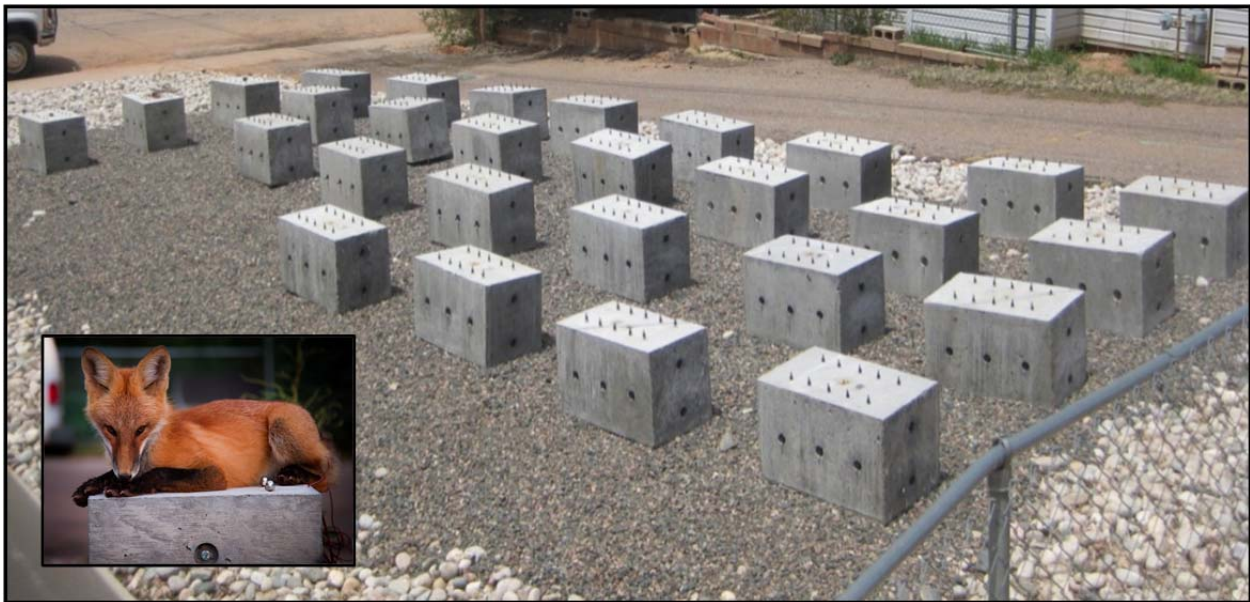


FINAL REPORT

FHWA-WY-13/04F

State of Wyoming
Department of Transportation

U.S. Department of Transportation
Federal Highway Administration



EVALUATION OF ASR POTENTIAL IN WYOMING AGGREGATES

By:

Department of Civil and Architectural Engineering
University of Wyoming
1000 East University Avenue, Dept. 3295
Laramie, WY 82071

October 2013

Notice

This document is disseminated under the sponsorship of the U.S. Department of Transportation in the interest of information exchange. The U.S. Government assumes no liability for the use of the information contained in this document.

The contents of this report reflect the views of the author(s) who are responsible for the facts and accuracy of the data presented herein. The contents do not necessarily reflect the official views or policies of the Wyoming Department of Transportation or the Federal Highway Administration. This report does not constitute a standard, specification, or regulation.

The United States Government and the State of Wyoming do not endorse products or manufacturers. Trademarks or manufacturers' names appear in this report only because they are considered essential to the objectives of the document.

Quality Assurance Statement

The Federal Highway Administration (FHWA) provides high-quality information to serve Government, industry, and the public in a manner that promotes public understanding. Standards and policies are used to ensure and maximize the quality, objectivity, utility, and integrity of its information. FHWA periodically reviews quality issues and adjusts its programs and processes to ensure continuous quality improvement.

Report No. FHWA-WY-13/04F	Government Accession No.	Recipients Catalog No.	
Title and Subtitle: Evaluation of ASR Potential in Wyoming Aggregates		Report Date October 2013	Performing Organization Code
Author(s) Ryan Fertig, Angela Jones, Margaret Kimble, Darby Hacker, Saadet Toket, Jennifer Eisenhauer Tanner		Performing Organization Report No.	
Performing Organization Name and Address Department of Civil and Architectural Engineering University of Wyoming, Dept 3295 Laramie, WY 82071-3295		Work Unit No. Job No.	Contact or Grant No. RSO6212
Sponsoring Agency Name and Address Wyoming Department of Transportation 5300 Bishop Blvd. Cheyenne, WY 82009-3340 WYDOT Research Center (307) 777-4182		Type of Report and Period Covered Final Report Jan 2006 – September 2013	Sponsoring Agency Code
Supplementary Notes WYDOT Project Manager: Bob Rothwell, Assistant State Materials Engineer			
Abstract: A comprehensive study was performed to evaluate the ASR reactivity of eight Wyoming aggregates. State-of-the-art and standardized test methods were performed and results were used to evaluate these aggregate sources. Of the eight aggregates: four are reactive; two are moderately reactive and two are nonreactive. The Concrete Prism Test (CPT) and large scale field blocks provided the most accurate data.			
Key Words Wyoming, Alkali silica reaction, expansion, aggregate, concrete, durability		Distribution Statement Unlimited	
Security Classif. (of this report) Unclassified	Security Classif. (of this page) Unclassified	No. of Pages 162	Price

Form DOT F 1700.7 (8-72) Reproduction of form and completed page is authorized.

SI* (Modern Metric) Conversion Factors

Approximate Conversions from SI Units

Symbol	When You Know	Multiply By	To Find	Symbol
Length				
mm	millimeters	0.039	inches	in
m	meters	3.28	feet	ft
km	kilometers	0.621	miles	mi
Area				
mm ²	square millimeters	0.0016	square inches	in ²
m ²	square meters	10.764	square feet	ft ²
km ²	square kilometers	0.386	square miles	mi ²
Volume				
ml	milliliters	0.034	fluid ounces	fl oz
l	liters	0.264	gallons	gal
m ³	cubic meters	35.71	cubic feet	ft ³
m ³	cubic meters	1.307	cubic yards	yd ³
Mass				
g	grams	0.035	ounces	oz
kg	kilograms	2.202	pounds	lb
Temperature (exact)				
°C	Centigrade temperature	1.8 C + 32	Fahrenheit temperature	°F
Force and Pressure or Stress				
N	newtons	0.225	poundforce	lbf
kPa	kilopascals	0.145	pound-force per square inch	psi

Approximate Conversions to SI Units

Symbol	When You Know	Multiply By	To Find	Symbol
Length				
in	inches	25.4	millimeters	Mm
ft	feet	0.305	meters	M
mi	miles	1.61	kilometers	Km
Area				
in ²	square inches	645.2	square millimeters	mm ²
ft ²	square feet	0.093	square meters	m ²
mi ²	square miles	2.59	square kilometers	km ²
Volume				
fl oz	fluid ounces	29.57	milliliters	MI
gal	gallons	3.785	liters	L
ft ³	cubic feet	0.028	cubic meters	m ³
yd ³	cubic yards	0.765	cubic meters	m ³
Mass				
oz	ounces	28.35	grams	G
lb	pounds	0.454	kilograms	Kg
Temperature (exact)				
°F	Fahrenheit temperature	5(F-32)/9 or (F-32)/1.8	Celsius temperature	°C
Force and Pressure or Stress				
lbf	pound-force	4.45	newtons	N
psi	pound-force per square inch	6.89	kilopascals	kPa

II:

Executive Summary

Alkali-silica reactivity (ASR) is a global concrete durability problem that continues to plague concrete around Wyoming. One particularly expansive aggregate exists in the Cheyenne area that has caused damage in residential, commercial and governmental projects. Although this aggregate is not typically specified for WYDOT highway projects, it was evaluated because of the widespread damage observed in Cheyenne and the surrounding area.

Currently WYDOT evaluates ASR potential in aggregates using the Accelerated Mortar Bar Test (AMBT) before using them in new concrete. Although, this test is appealing because of its relatively short duration (16 days), it is a harsh test that has been known to produce both false positives and negatives. After an initial study of existing ASR damage in the Big Horn Basin, eight aggregate sources were selected for evaluation. Tested aggregates include: Blackrock; Devries Farm; Harris; Goton; Knife River; Labarge; Lamax; and Worland. Researchers classified each aggregate on the basis of both standardized and state-of-the art methods including: the Concrete Prism Test (CPT); the Accelerated Mortar Bar Test (AMBT); the Kinetic Method; a modified Chinese Accelerated Mortar Bar Test (CAMBT); and real-time field exposure. The CAMBT method is as harsh as the AMBT because there is an unlimited supply of alkalis present in the solution. It is not surprising that all aggregates failed both ABMT and CAMBT methods. In addition, all eight aggregates failed the Kinetic Method which is based on the AMBT. Despite the one-year time frame to complete CPTs of standard aggregates, it is still considered the best accelerated test method because it correlates well with field performance.

A large scale, outdoor exposure, real-time field site was developed at the Civil and Architectural Engineering Research Facility. A total of 28 blocks measuring 380 x 380 x 660 mm (15 x 15 x 26 in.) specimens were built in order to measure expansions over a period of 10 years. Results from the first 54 months of exposure are presented in this report.

All eight aggregates are classified based on the CPT and field expansions. Goton, Knife River, Labarge and Worland sources are reactive. Harris and Devries Farm aggregates are nonreactive. Blackrock and Lamax are moderately reactive. A mitigation study for the moderately reactive

aggregates is underway at the University of Wyoming and results are anticipated at the end of 2014.

Table of Contents

Chapter 1	Introduction.....	1
Chapter 2	Objectives.....	3
Chapter 3	Background and Literature Review.....	5
3.1	Mechanism of reaction.....	5
3.1.1	Reactive Aggregate.....	5
3.1.2	Alkalies	6
3.1.3	Moisture.....	7
3.2	Test Methods.....	8
3.2.1	Mortar Bar Method - ASTM C227.....	8
3.2.2	Chemical Method - ASTM C289.....	8
3.2.3	Accelerated Mortar Bar Test (AMBT) - ASTM C1260	9
3.2.4	Kinetic Method	10
3.2.5	Concrete Prism Test (CPT) - ASTM C1293.....	10
3.2.6	Chinese Accelerated Mortar Bar Test (CAMBT) and Modifications	11
3.2.7	Large Scale Field Exposure Testing.....	12
3.3	Summary	13
Chapter 4	Materials and Methods.....	15
4.1	Accelerated Testing Methods	16
4.1.1	Concrete Prism Test (ASTM C1293).....	17
4.1.2	Accelerated Mortar Bar Test (ASTM C1260)	23
4.1.3	Modified CAMBT.....	27
4.2	Large Scale Field Exposure.....	30
4.2.1	Exposure Site.....	32
4.2.2	Casting	33

4.2.3	Measurement Stud Installation	34
4.2.4	Measurement.....	35
4.2.5	Labeling	37
4.2.6	Demec Measurement Technique	38
Chapter 5	Results	41
5.1	Accelerated Test Methods	41
5.1.1	Concrete Prism Test (ASTM C1293)	41
5.1.2	Accelerated Mortar Bar Test (ASTM C1260)	44
5.1.3	Kinetic Method	46
5.1.4	Modified CAMBT.....	47
5.2	Field Specimens	51
5.3	Petrography Results.....	52
5.4	Discussion of Results	56
5.4.1	Accelerated test methods.....	56
5.4.2	Field specimen results	60
5.4.3	Final classifications.....	62
5.4.4	Rate of Reaction.....	63
Chapter 6	Conclusions and Recommendations.....	67
References	69
Acknowledgements	73
Appendix A	Field Study.....	74
Appendix B	Weather Data	100
Appendix C	Aggregate Expansions	102
Appendix D	Petrography.....	147

List of Figures

Figure 1. Wyoming map showing location of each aggregate..... 2

Figure 2. Equation. Sodium oxide equivalent equals percent sodium oxide plus 0.658 times percent potassium oxide. 6

Figure 3. Aggregate gradations. 16

Figure 4. Mold for ASTM C1293 with four measurement pin inserts..... 20

Figure 5. Length comparator with reference bar. 21

Figure 6. Top portion of rack (left) and bottom portion of rack shown upside-down (right)... 22

Figure 7. CPT storage environment without lid. 22

Figure 8. Equation. Percent expansion at day subscript i equals the quantity day subscript i measurement minus day subscript 0 measurement end of quantity divided by the gage length. 25

Figure 9. Equation. Percent expansion equals quantity a time b plus c times t to the d power end of quantity divided by quantity b times t to the d power end of quantity. 25

Figure 10. Equation. Alpha equals one plus alpha subscript naught minus e raised to the quantity negative k times the quantity t minus t subscript naught end of quantity raised to the M power end of quantity..... 26

Figure 11. Equation. M times natural log of the quantity t minus t naught equals the natural log of the natural log of the quantity of one divided by the quantity one plus

alpha subscript naught minus alpha end of quantity, end of quantity minus natural log of k.....	26
Figure 12. Compacting mortar (left), finished CAMBT specimen (right).....	28
Figure 13. Length comparator setup (left) and specimen in measurement position (right).	29
Figure 14. Tolerance gained from offset orientation.	32
Figure 15. Outdoor exposure site.	32
Figure 16. Threaded steel insert assembly.....	33
Figure 17. Portion of the insert assembly on the inside of the form (left) and the outside of the form (right).....	33
Figure 18. Field specimen immediately after casting.	34
Figure 19. Setting out bar.....	35
Figure 20. Side of field specimen (left) and close up of installed measurement stud (right).	35
Figure 21. Field specimen diagram showing the layout of the measurement locations.	37
Figure 22. Using labeling system to measure side of block.	38
Figure 23. Orientation of strain gauge based on indicator arrow.....	38
Figure 24. Photo of Demec instrument.	39
Figure 25. Invar reference bar.....	39
Figure 26. Average expansion for eight aggregates subjected to the CPT.	41
Figure 27. Average one year expansion in the CPT with error bars showing standard deviation.....	42
Figure 28. ASTM C 1293 Black Rock Test Results (Fertig 2008).	43
Figure 29. ASTM C 1293 Black Rock Test Results.	44
Figure 30. Average expansions for eight aggregates subjected to AMBT.....	45

Figure 31. Average 14 day expansion in the AMBT with error bars showing standard deviation.....	45
Figure 32. t_o versus $\ln(k)$ for eight aggregates analyzed using the Kinetic Method.....	47
Figure 33. Average expansions for eight aggregates subjected to the modified CAMBT....	48
Figure 34. Average 14 day expansion in the CAMBT with error bars showing standard deviation.....	49
Figure 35. Average mass changes for eight aggregates subjected to the modified CAMBT.	50
Figure 36. Potentially Reactive Aggregates – a) Unboosted b) Boosted.	51
Figure 37. Nonreactive Aggregates – a) Unboosted b) Boosted.....	52
Figure 38. Comparison of the CPT and the AMBT expansions with error bars for each aggregate.....	54
Figure 39. Standard deviation values versus accelerated test method.....	60
Figure 40. Expansion Limits for Field Specimens – a) Unboosted and b) Boosted.	61
Figure 41. Expansion to date of unboosted field specimens.....	62
Figure 42. Expansion rates for eight aggregates subjected to the CPT.	64
Figure 43. Rate of expansion for unboosted field specimens.	65
Figure 44. Average daily maximum and minimum temperature in Laramie.....	100
Figure 45. Average daily relative humidity in Laramie.	101
Figure 46. Total monthly precipitation in Laramie.	101
Figure 47. ASTM C1293 results for Blackrock aggregate.	102
Figure 48. Typical Blackrock prism after test (BR-2 pictured).....	103
Figure 49. ASTM C1260 average Blackrock mortar bar expansion.....	104

Figure 50. Average actual expansion and MMF approximation for Blackrock aggregate.	105
.....	
Figure 51. Modified CAMBT mortar bar expansion for Blackrock.....	106
Figure 52. Expansion ratio comparison for Blackrock.	107
Figure 53. ASTM C1293 results for Devries Farm aggregate.	108
Figure 54. ASTM C1260 average Devries Farm mortar bar expansion.....	109
Figure 55. Average actual expansion and MMF approximation for Devries Farm aggregate.....	110
Figure 56. CAMBT Mortar bar expansion for Devries Farm.	111
Figure 57. Mass change (%) for Devries Farm mortar bars in the modified CAMBT.....	112
Figure 58. Expansion ratio comparison for Devries Farm.	113
Figure 59. ASTM C1293 results for Goton aggregate.	114
Figure 60. ASTM C1260 average Goton mortar bar expansion.	115
Figure 61. Average actual expansion and MMF approximation for Goton aggregate.	116
Figure 62. CAMBT Mortar bar expansion for Goton.....	117
Figure 63. Mass change (%) for Goton mortar bars in the modified CAMBT.	118
Figure 64. Expansion ratio comparison for Goton.	119
Figure 65. ASTM C1293 expansion for Harris.	120
Figure 66. ASTM C1260 average Harris mortar bar expansion.....	121
Figure 67. Average actual expansion and MMF approximation for Harris aggregate.....	122
Figure 68. CAMBT Mortar bar expansion for Harris.	123
Figure 69. Mass change (%) for Harris mortar bars in the modified CAMBT.....	124
Figure 70. Expansion ratio comparison for Harris.....	125

Figure 71. ASTM C1293 results for Knife River aggregate.....	126
Figure 72. ASTM C1260 average Knife River mortar bar expansion.	127
Figure 73. Average actual expansion and MMF approximation for Knife River aggregate.	128
Figure 74. CAMBT Mortar bar expansion for Knife River.	129
Figure 75. Mass change (%) for Knife River mortar bars in the modified CAMBT.....	130
Figure 76. Expansion ratio comparison for Knife River.....	130
Figure 77. ASTM C1293 results for Labarge aggregate.	131
Figure 78. ASTM C1260 average Labarge mortar bar expansion.....	132
Figure 79. Average actual expansion and MMF approximation for Labarge aggregate. .	133
Figure 80. CAMBT Mortar bar expansion for Labarge.	134
Figure 81. Mass change (%) for Labarge mortar bars in the modified CAMBT.....	135
Figure 82. Expansion ratio comparison for Labarge.	136
Figure 83. ASTM C1293 expansion for Lamax.....	137
Figure 84. ASTM C1260 average Lamax mortar bar expansion.	138
Figure 85. Average actual expansion and MMF approximation for Lamax aggregate.	139
Figure 86. CAMBT Mortar bar expansion for Lamax.	140
Figure 87. Mass change (%) for Lamax mortar bars in the modified CAMBT.	141
Figure 88. Expansion ratio comparison for Lamax.....	142
Figure 89. ASTM C1293 results for Worland aggregate.	143
Figure 90. ASTM C1260 average Worland mortar bar expansion.....	144
Figure 91. Average actual expansion and MMF approximation for Worland aggregate..	145
Figure 92. CAMBT Mortar bar expansion for Worland.	146

Figure 93. Mass change (%) for Worland mortar bars in the modified CAMBT..... 147
Figure 94. Expansion ratio comparison for Worland..... 148

List of Tables

Table 1. Aggregate abbreviations and locations.	15
Table 2. Aggregate properties.....	15
Table 3. Coarse (ASTM C1293) and fine (ASTM C33) aggregate gradations.....	17
Table 4. Average compressive strength of concrete used in the CPT.	18
Table 5. Batch quantities for all aggregates used in the CPT.....	19
Table 6. Concrete mixture properties for all aggregates in the CPT.....	19
Table 7. Aggregate gradation for the AMBT.	24
Table 8. AMBT batch quantities.	24
Table 9. Modified CAMBT batch quantities for all aggregate sources.	28
Table 10. Material quantities common to all field specimens.	30
Table 11. Other materials used in field specimens.....	31
Table 12. $Ln(k)$, t_0, and M for eight aggregates analyzed using the Kinetic Method.....	46
Table 13. Visual description of each aggregate.....	53
Table 14. Scale used to determine the severity of ASR.	53
Table 15. AMBT laboratory reactivity classifications versus petrographic classification... 	54
Table 16. CPT laboratory reactivity classifications versus petrographic classification.....	55
Table 17. Measured CPT expansions and failure ratios for each aggregate.....	56
Table 18. Measured AMBT expansions and failure ratios for each aggregate.....	57
Table 19. Measured CAMBT expansions and failure ratios for each aggregate.	58
Table 20. Aggregate classification based on accelerated test methods.	59
Table 21. Expansions after 4-5 years of exposure.....	61
Table 22. Final classification of each aggregate source.....	63

Table 23. Kinetic Method results for Blackrock aggregate.	104
Table 24. Kinetic Method results for Devries Farm aggregate.	109
Table 25. Kinetic Method results for Goton aggregate.	115
Table 26. Kinetic Method results for Harris aggregate.....	121
Table 27. Kinetic Method results for Knife River aggregate.....	127
Table 28. Kinetic Method results for Labarge aggregate.	132
Table 29. Kinetic Method results for Lamax aggregate.....	139
Table 30. Kinetic Method results for Worland aggregate.....	144

Chapter 1 Introduction

Alkali-silica reactivity (ASR) is a global concrete durability problem that caused damage in concrete around Wyoming, particularly in the Cheyenne area. Currently WYDOT evaluates ASR potential in aggregates using the Accelerated Mortar Bar Test (AMBT) before using them in new concrete. This test was selected because of its relatively short duration (16 days). When the AMBT showed an aggregate to be reactive, mitigation involved adding a Class F fly ash or lithium admixture to the concrete mixture containing the reactive aggregate. Because fly ash was inexpensive, this mitigation technique added very little to the cost of a concrete project, and even though the AMBT is known to sometimes classify innocuous aggregates as reactive, the minimal cost of mitigation made these errant classifications irrelevant. Previously the demand for fly ash increased, and the material became less available, forcing the use of costlier mitigation techniques such as the addition of lithium compounds and other specialty supplementary cementitious products. This increase in mitigation cost has made it more important for aggregates to be classified correctly; mitigating an innocuous aggregate would now add a significant cost to a construction project.

A concrete survey was performed in towns in Big Horn Basin. The study revealed that some ASR damage existed but not all concrete was damaged. Therefore, some of the selected sources are expected to be nonreactive. A full report is shown in Appendix A.

Chapter 2 Objectives

Wyoming Department of Transportation provided funding to quantify the ASR potential of aggregate sources throughout the state using accelerated testing methods and long term field exposure sites. After an initial study of existing ASR damage, eight aggregate sources, many concentrated in the Big Horn Basin, were selected for evaluation. Although the AMBT is currently used as the screening test for WYDOT, it has known shortcomings such as false positive and negative classifications. Consequently, the aggregates were also tested using the Concrete Prism Test (CPT), a modified Chinese Accelerated Mortar Bar Test (CAMBT), and an analytical technique referred to as the Kinetic Method which uses the expansion data from the AMBT. Large scale field specimens were also cast and transported to an outdoor exposure site where they will have 4.5 years of expansion data.

In each accelerated test mortar bars or concrete prisms were cast using a specific aggregate, and the specimen expansion was monitored during the course of the test. These expansions resulted in a reactivity classification for each aggregate. The CPT is regarded as the most reliable accelerated test, so it was used as the authoritative test in the case of differing classifications.

A field exposure site was also constructed, and field specimens containing each of the eight aggregates were cast. For each aggregate source at least two specimens were cast with normal alkalinity, and at least one specimen contained an additional amount of NaOH to increase the alkalinity to 1.25 percent in an effort to provide an upper bound on field reactivity and compare results with CPT data. The specimens were cast in the University of Wyoming concrete laboratory and transported to the exposure site and measured periodically to monitor their expansion.

Chapter 3 Background and Literature Review

Alkali-silica reaction (ASR) was first recognized as a distinct concrete durability problem in California in 1940 (Stanton 1940), and it has been identified in countries all over the world since then. Stanton recognized that the reaction was dependent on the interaction of several factors including the type of cement, the aggregate used in the concrete mixture, and the environmental exposure conditions. Soon after the problem was recognized, the need for an accelerated test to evaluate cement-aggregate combinations became apparent. The goal of developing a test method that allowed for the identification of reactive constituents in a short amount of time has given rise to numerous methods over the years, some of which will be discussed in this review.

In this section, the components of the alkali-silica reaction are discussed in some detail. Then the test methods that are most relevant to this research are described with a brief synopsis of their strengths and weaknesses.

3.1 Mechanism of reaction

Although ASR has been studied for many years, there are still some aspects of the reaction mechanism that are not well understood. What is known is that alkali-silica reaction can only proceed when three ingredients are present in the concrete; reactive aggregate, sufficient alkalies and moisture.

The reaction can be described by a two-step process. The alkali hydroxides in the concrete pore solution attack and react with the free silica in the aggregate to produce an alkali-silica gel reaction product. Then this gel absorbs water and expands which leads to the expansion and cracking of the concrete (Rear et al. 1994).

3.1.1 Reactive Aggregate

Reactive aggregate was once thought to include only a few select rock constituents such as opal, chalcedony, and some glassy volcanic rocks (ACI 2008), but it is now understood that a much broader range of constituents can be reactive. In general, a reactive aggregate contains silica (SiO_2) as a major component, and the silica has an open or disturbed microstructure (Chatterji 2005). A smaller aggregate particle size and more microcrystalline quartz in the aggregate tends

to increase reactivity (Fournier and Berube 2000). Aggregates with an amorphous crystal structure or microporous nature also appear to be reactive (Farny et al. 1997).

The process of identifying reactive aggregate is made more challenging by the fact that very small amounts of reactive constituent are required for reaction. In addition, a higher degree of reactivity in the constituent results in a smaller quantity needed for deleterious reaction. Farny and Kosmatka (Farny et al. 1997) compiled the following list of some reactive constituents and the quantities that are required for potential reactivity:

- Opal – more than 0.5 percent by mass.
- Chert or chalcedony – more than 3.0 percent.
- Tridymite or cristobalite – more than 1.0 percent.
- Optically strained or microcrystalline quartz – more than 5.0 percent.
- Natural volcanic glasses – more than 3.0 percent.

While different types of constituents demonstrate varying levels of reactivity, no form of silica can be regarded as completely nonreactive. Reactivity is simply a measure of how much alkali hydroxide is required for deleterious expansion so even the thermodynamically stable silica, quartz, can react if the alkalinity of the pore solution is high enough.

3.1.2 Alkalies

The term “alkalies” generally refers to elements in the alkali metal category of the periodic table such as lithium, sodium, potassium, etc. In the case of ASR, “alkalies” only refers to sodium and potassium; in fact, lithium has a mitigating effect on the reaction. Consequently, the total alkali content of cement, expressed as equivalent sodium oxide, is calculated as

$$Na_2O_e = \% Na_2O + 0.658 \times \% K_2O$$

Figure 2. Equation. Sodium oxide equivalent

The alkali content of the cement has long been understood to play a significant role in ASR expansion (Stanton 1940). Alkalies in concrete are mostly supplied by the cement, but can also come from external sources such as alkali-bearing aggregates, unwashed sea dredged sand, mixture water, and high alkali fly-ash (Fournier and Berube 2000). Despite the name, alkali-silica reaction is not between alkali ions and silica particles. Rather, the concentration of alkali ions have been shown to have a direct relationship with the hydroxide ion concentration in the pore solution (Diamond 1989). It is these hydroxide ions that are responsible for both attacking reactive silica particles, thereby introducing them into the pore solution, and reacting with the silica in the pore solutions to form the reaction gel (ACI 2008).

A form of mitigation that is still used today is limiting the alkali content of the cement (typically <0.6 percent). Type II cement controls the alkalinity, and Type I cement is often replaced with Type I/II. At one time this was thought to be sufficient to inhibit ASR, but it is now understood that this method, by itself, is ineffective. Although the total alkali content of the cement may be low, various processes such as evaporation, electric/magnetic fields or currents, cathodic protection (Fournier and Berube 2000), or repeated cycles of wetting and drying (Farny et al. 1997) can cause alkali migration and create localized areas of high alkalinity. In addition, if a high cement content is specified, even with a low alkali cement, there will be a significant amount of alkalies still introduced into the concrete. Lastly, the quantity of alkali necessary for ASR is dependent on the reactivity of the aggregate. A low alkali cement may still provide the necessary environment for deleterious expansion when a highly reactive aggregate is used.

3.1.3 Moisture

A sufficient amount of moisture is required for ASR to occur because it is the absorption of water by the ASR gel that causes expansion within the concrete. It also serves to transport alkalies and hydroxyl ions to locations where the reaction can take place (ACI 2008). Even if moisture is not introduced by the environment, the water used for the concrete mixture is usually enough to support the reaction. Research suggests that ASR can occur when the internal relative humidity of the concrete is greater than 80 percent (Stark 1991), which is often the case even in dry climates. This is especially true of thicker concrete members as the internal relative humidity in the interior of the concrete is less affected by environmental conditions.

External moisture ingress can be detrimental due to its ability to transport materials into the concrete or cause alkali migration that may enhance the opportunity for reaction. Using supplementary cementing materials (SCM) such as fly ash and lowering the water/cement ratio to limit the permeability of concrete, in conjunction with designing structures to limit the pooling of water on concrete members, can help to control the negative effects of external moisture ingress.

3.2 Test Methods

Because ASR is a problem that exists all over the world, there are numerous test methods to identify potentially deleterious alkali-silica reaction. Additionally, methods exist to test specific properties related to ASR such as the ability of mineral admixtures or slag to mitigate the reaction (ASTM C441) or procedures for examining aggregates (ASTM C295) or hardened concrete (ASTM C856) using petrographic analysis. ASTM test methods that were used directly in this research or were used as the basis for developing these procedures are discussed.

3.2.1 Mortar Bar Method - ASTM C227

ASTM C227, accepted as an ASTM standard in 1950, calls for the casting of 25 x 25 x 285 mm (1 x 1 x 11¼ in.) mortar bars that will be stored at 38°C (100 °F) in containers designed to guarantee an environment with 100 percent relative humidity. Length change measurements are taken at specific time periods for at least 12 months. The aggregate is classified as deleteriously reactive if expansion is greater than 0.05 percent at three months or 0.10 percent at six months (ASTM C33, 2003).

Some deficiencies in this test have been identified. The test does not specify a water to cement ratio or a cement alkali content, and the testing environment can cause the leaching of alkalis that can further obscure test results (Cornell 2002). In addition, the use of this test on slowly reactive aggregates is not advised because it is known to produce overly conservative results (ASTM C33, 2003). The use of ASTM C227 is now less widespread due to the availability of the ASTM C1260 test.

3.2.2 Chemical Method - ASTM C289

The chemical method was developed at the Bureau of Reclamation (Mielenz et al. 1948) and was first accepted as an ASTM standard in 1952. This test requires aggregate to be crushed to a size

fraction between 150 and 300 μm and placed in a 1 N NaOH solution at 80°C (176 °F). The purpose of this high temperature is to dissolve all the soluble silica in the aggregate that is available for reaction (ACI 2008). The aggregate remains in the solution for 24 hours, after which the solution is filtered to determine the amount of dissolved silica and the reduction in alkalinity of the solution. These two quantities are then plotted to determine if the aggregate is innocuous, potentially reactive, or deleterious.

This test can be completed very quickly, but it may not be reliable for slowly reacting aggregates (ASTM C33, 2003) or aggregates containing some carbonates or silicates (ASTM C289, 2002). In addition, the test is sensitive to poor operator technique or judgment, and grinding the aggregate too fine can also produce inaccurate results (ACI 2008). Similar to ASTM C227, ASTM C289 is not used as frequently anymore due to the development of the ASTM C1260 test.

3.2.3 Accelerated Mortar Bar Test (AMBT) - ASTM C1260

The shortcomings of ASTM C227 and ASTM C289 highlighted the need for and led to the development of ASTM C1260 (Lane 1999), also known as the Accelerated Mortar Bar Test or AMBT. In 1986, Oberholster and Davies developed a test in South Africa (Oberholster and Davies 1986) that would eventually result in the ASTM C1260 test, which was formally adopted in 1994. The test uses the mortar bars from ASTM C227 and the soak solution environment from the ASTM C289 test. The mortar bars are stored in 1 N NaOH solution at 80°C (100°F) to accelerate the reaction, and the water/cement ratio is specified at 0.47. After casting, the bars are stored in a moist curing room for 24 hours. Then an initial comparator reading is taken, after which the bars are immersed in tap water at 80°C (100°F) for 24 hours. The mortar bars are then placed in the NaOH solution at 80°C (100°F) and measured periodically over the next 14 days. According to ASTM C1260, 14 day expansion less than 0.10 percent indicates an innocuous aggregate. Expansion greater than 0.20 percent indicates a potentially deleteriously reactive aggregate, and expansion between 0.10 percent and 0.20 percent includes “both aggregates that are known to be innocuous and deleterious in field performance.” (ASTM C1260, 2001)

This test is preferred to other tests because it is reliable, quick, and the severe testing environment helps to identify more slowly reacting aggregates (ACI 2008), an area in which both ASTM C227 and ASTM C289 were deficient. Unfortunately, the AMBT does have some

limitations. The harshness of the testing environment is not representative of actual field conditions. For this reason, some aggregates that perform well in the field actually fail this test. Therefore, ASTM C1260 should not be used for the rejection of aggregates unless other information is gathered to ensure that the expansion is due to ASR (ASTM C33, 2003) or the aggregate is checked with ASTM C1293 (Touma et al. 2001). This test has also been shown, though rarely, to classify an aggregate as nonreactive when it proves to be reactive in the field (Fournier et al. 2006). Another shortcoming of the AMBT is that it is only effective at evaluating the potential reactivity of the aggregate in question, not the cement-aggregate combination, because of its insensitivity to changes in the alkali content of the cement (Hooton and Rogers 1993). The 1 N NaOH solution provides sufficient alkalies for the reaction to take place, rendering the effect of comparatively small changes in cement alkalinity insignificant in the expansion of the mortar bars.

3.2.4 Kinetic Method

Since the adoption of the AMBT as an ASTM test method there has been an interest in employing the expansion data to build a model that would enable more accurate classifications of aggregate, minimizing the prevalence of false negative and false positive results (Johnston 1994). The Kolmogorov-Avrami-Mehl-Johnson (KAMJ) function (Avrami 1939, 1940, 1941) was initially developed to describe nucleation and growth reaction kinetics. A form of the equation was later used to model the effect of water/cement ratio on C_3S hydration kinetics (Berliner et al. 1998), and that equation was selected to model ASR expansion behavior (Johnston and Fournier 2000).

This method has shown promising results in correctly identifying aggregates that the AMBT classified incorrectly (Johnston and Fournier 2000) and has even proved helpful in predicting the onset of cracking in field concrete (Johnston et al. 2004).

3.2.5 Concrete Prism Test (CPT) - ASTM C1293

The development of the Concrete Prism Test began in the 1950s and was motivated by the failure of ASTM C227 to correctly identify both ASR and alkali-carbonate reactivity (ACR) (Thomas et al. 2006). The test was developed from a method that was originally intended to identify ACR, the test on which ASTM C1105 is based (Hooton 1996). The original testing

environment and procedure for the CPT was found to allow some aggregates that were known to react in the field to pass the test, so it was modified by increasing the total alkali loading and calibrated to field performance until it reached the current version which was formally adopted in 1995 as ASTM C1293.

The test uses 75 x 75 x 285 mm (3 x 3 x 11 ¼ in.) prisms with a w/c ratio between 0.42 and 0.45, a specific proportion of coarse and fine aggregate, and a cement content of 420 kg/m³. The cement should have a total alkali content of 0.9 ± 0.1 percent Na₂O equivalent, and this alkali content is boosted by the addition of NaOH to the mixture to yield a total alkali content of 1.25 percent by mass of the cement. Immediately after casting, the prisms are stored in a moist curing room and demolded after 24 hours. An initial length measurement is then taken and the prism is placed in a 100 percent RH environment at 38°C. Subsequent measurements are taken at 7, 28, and 56 days as well as 3, 6, 9, and 12 months. An aggregate is classified as potentially deleteriously reactive if the expansion at one year is equal to or greater than 0.04 percent.

The CPT has the advantage of testing cement-aggregate combinations and also considers the effects of coarse aggregate instead of just fine aggregate like the mortar bar methods. A disadvantage to this test is the long testing period which makes it impractical for testing aggregate conformance to construction specifications (Lane 1999). The test has also been shown to allow a significant amount of alkalis to leach out of the concrete (Rivard et al. 2003) which can decrease the rate, duration, and maximum value of expansion due to ASR. Though not as severe as ASTM C1260, the testing environment is still much more severe than most field exposure situations so even though it has correlated well to field performance, the test may not be representative of actual field behavior. Currently, of the accelerated test methods, ASTM C1293 provides the best correlation with field performance (Cornell 2002) and is therefore regarded as the most authoritative accelerated test for reactivity.

3.2.6 Chinese Accelerated Mortar Bar Test (CAMBT) and Modifications

The CAMBT seeks to combine the strengths of the AMBT and the Chinese Autoclave Test and eliminate their weaknesses. The AMBT is known to classify some nonreactive aggregates as reactive due to its harsh testing environment, and in rare cases it can fail to classify slowly reactive aggregates as reactive. However, the AMBT is very useful because of its short duration

(16 days from casting). The Chinese Autoclave Test, developed in 1983 (Ming-shu et al. 1983), used 1 x 1 x 4cm (0.4 x 0.4 x 1.6 in.) mortar bars with a single aggregate size fraction of 0.15-0.75 mm. These bars were steam cured at 100°C (212°F) for four hours and then cured in 10 percent KOH solution at 150°C (302°F) for six hours. This method yielded reactivity results in two days, but the small size of the specimens and the limited amount of aggregate relegated this test mainly to the field of research.

In order to create a test method that would be usable in the construction industry and specification compliance, the CAMBT was proposed (Xu et al. 1998). It calls for mortar bars with dimensions of 40 x 40 x 160 mm (1.6 x 1.6 x 6.3 in.) and an aggregate size fraction of 0.15-0.80 mm (0.006-0.03 in.). The water/cement ratio is fixed at 0.33, and the cement to aggregate ratios are 10 to 1, 2 to 1, and 1 to 1 to cover the pessimum cement to aggregate ratio. After casting, these mortar bars are stored in 1 N NaOH solution at 80°C (100°F) as in the case of the AMBT. Unlike the AMBT however, the zero length measurement is taken after the bars have been immersed in the NaOH solution for four hours. An aggregate is classified as reactive if the expansion at seven days is greater than 0.1 percent.

Research (Lu et al. 2006) showed that the 0.15-0.80 mm (0.006-0.03 in.) size fraction was not the most sensitive size fraction to ASR expansion. Also, the correlation between the CPT and the CAMBT was still not very good. In response, modifications were proposed to the CAMBT which included using a size fraction of 2.5-5.0 mm (0.1-0.2 in.), only using a cement to aggregate ratio of 1 to 1, and a new acceptance criteria of 0.093 percent at 14 days (Lu et al. 2007). With these modifications, the new test showed better correlation with the CPT and also possessed the ability to identify ACR as well. While more research needs to be done to further confirm the reliability of this modified CAMBT, early results are promising.

3.2.7 Large Scale Field Exposure Testing

Large scale field testing of ASR is much less widespread than the use of accelerated methods to test for ASR. There are a few researchers who have used larger specimens in ASR tests, but they did not subject them to outdoor exposure (Fan and Hanson 1998), (Smaoui et al. 2004), (Zhang et al. 1999). To date, there are only a small number of field exposure sites in the world. In addition to the site at the University of Wyoming in Laramie, WY, there is the site constructed

by the Building Research Establishment in the U.K. and the sites at CANMET in Ottawa, Canada, at the University of Texas in Austin, TX, and in Treat Island, ME (Thomas et al. 2006). A negative aspect of field exposure specimens is that variables are introduced that are absent in controlled tests. The environment can cause thermal gradients and moisture changes in the specimens that may be difficult to quantify. In addition, measurements must be taken with a portable gauge which introduces more variability than when measuring using a comparator stand. Still, these sites most accurately represent field concrete including the mixture to be used and the local exposure environment. This eliminates the extrapolation required when using standard mixes and controlled environments in accelerated laboratory tests. The increased size of the specimens also limits the leaching of alkalis that is sometimes a problem in other tests (Zhang et al. 1999).

3.3 Summary

ASR is a global concrete durability problem with a complexity that demands respect. Even though the fundamental constituents of the reaction were identified when ASR was first recognized, a complete understanding of the mechanisms of reaction appears to be elusive. A simple, expeditious way to identify reactive aggregate and cement-aggregate combinations has also proved difficult to define. While there are several useful accelerated tests currently employed, their results require engineering judgment, and in some cases further analysis, before they become useful. Until a more reliable accelerated test is developed, large scale field exposure of specific concrete mixtures will remain the most reliable method in determining the potential for alkali-silica reactivity.

Chapter 4 Materials and Methods

Aggregates from eight different sources in Wyoming were evaluated in this research. Their names, locations, and abbreviations used in this document are shown in Table 1, and their relative locations are identified on the map in Figure 1. Specific gravity and absorption of each aggregate was measured by the WYDOT Materials Lab and is reported in Table 2. Additionally, coarse aggregate unit weight, used to proportion the concrete mixture in the CPT, was measured at UW and is also presented in Table 2 (ASTM C29). All measurements are based on aggregate as it was received from the source. Researchers sieved representative samples from each source to provide a summary of their gradations (Figure 3). In some cases all the aggregate was sieved and in other cases a representative sample was sieved.

Table 1. Aggregate abbreviations and locations.

<i>Aggregate Name</i>	<i>Abbreviation</i>	<i>Location</i>
Devries Farm	DFP	Thermopolis, WY
Harris	HPC	Cody, WY
Lamax	LX	Basin, WY
Goton	GP	Greybull, WY
Knife River	KR	Cheyenne, WY
Worland	WOR	Worland, WY
Labarge	LBG	Rock Springs, WY
Blackrock	BR	Powell, WY

Table 2. Aggregate properties.

<i>Aggregate Name</i>	COARSE AGGREGATE			FINE AGGREGATE	
	<i>Specific Gravity (SSD)</i>	<i>Absorption</i>	<i>Unit Weight (pcf)</i>	<i>Specific Gravity (SSD)</i>	<i>Absorption</i>
Devries Farm	2.518	2.19%	96.6	2.614	1.56%
Harris	2.601	1.83%	97.2	2.621	2.25%
Lamax	2.540	2.02%	97.7	2.603	1.81%
Goton	2.579	1.07%	99.0	2.627	1.01%
Knife River	2.662	0.67%	98.8	2.629	0.91%
Worland	2.549	1.45%	99.0	2.614	1.56%
Labarge	2.600	0.67%	98.8	2.622	1.05%
Blackrock	2.591	1.80%	97.7	2.600	2.15%

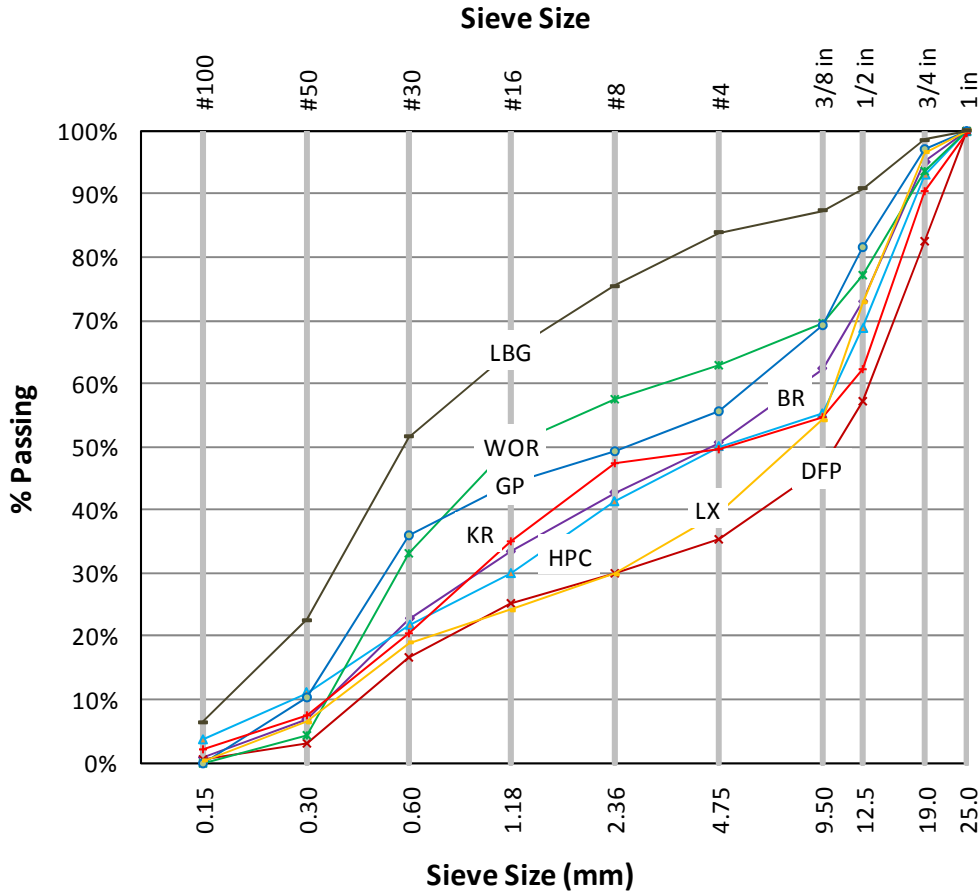


Figure 3. Aggregate gradations.

Holcim Type I/II cement was used for all concrete mixtures in this research. The cement was analyzed in accordance with ASTM C 114, and its alkalinity was measured to be 0.706 percent as Na₂O equivalent.

4.1 Accelerated Testing Methods

Aggregates from eight sources in Wyoming were subjected to the Concrete Prism Test (CPT), the Accelerated Mortar Bar Test (AMBT), the Kinetic Method, a modified Chinese Accelerated Mortar Bar Test (CAMBT), and field exposure. In this section the procedures for each method are discussed.

The CPT and field specimens used tap water for the concrete mixture, and the AMBT and modified CAMBT used distilled water. Holcim Type I/II cement was used for all testing, and NaOH pellets were used to increase alkalinity when required. Technical grade NaOH pellets were purchased from the Chemical Stockroom and used in the solutions in the AMBT and the modified CAMBT and to boost the alkalinity of the field specimens and CPT prisms. Liquid air entrainment composed of a blend of high-grade saponified rosin and organic acid salts was added to the field specimen mixtures, as was a polycarboxylate-based superplasticizer.

4.1.1 Concrete Prism Test (ASTM C1293)

ASTM C1293 provides instructions for testing either a coarse aggregate or a fine aggregate for reactivity, and the standard outlines the gradation requirements for both types of aggregate, depending on which one is being tested for reactivity. Because both fine and coarse aggregate will be used together in the field, they were combined for testing. The individual specified gradations were used for fine and coarse aggregates as defined in ASTM C1293 and ASTM C33 and shown in Table 3.

Table 3. Coarse (ASTM C1293) and fine (ASTM C33) aggregate gradations.

<i>COARSE</i>		<i>FINE</i>	
Retained On	Mass %	SIZE	% PASSING
1/2"	33	#8	80-100
3/8"	33	#16	50-65
#4	33	#30	25-60
		#50	5-10
		#100	0-10

Once the aggregate was obtained it was sieved into the sizes required by the standards. The aggregate with a size greater than a number 30 sieve was then washed and oven dried. After drying, the unit weight of the coarse aggregate was measured and recorded using the procedure described in ASTM C29.

4.1.1.1 Casting

The concrete mixture was proportioned according to ASTM C1293. The aggregates were oven dried before use in the concrete, and the w/c ratio was 0.42. The volume of coarse aggregate per

unit volume of concrete is specified as 0.70 ± 0.2 percent in ASTM C1293. In this research that was taken to mean that 70 percent of the total concrete mixture volume was to be occupied by coarse aggregate.

A NaOH admixture was used to bring the alkalinity of the concrete mixture to 1.25 percent Na_2O equivalent by mass of the cement as specified in ASTM C1293. Because the cement had an alkalinity of 0.706 percent, slightly lower than the 0.9 ± 0.1 percent specified, more NaOH was added to raise the concrete alkalinity to 1.25 percent. More expansion occurs with a high alkali cement than with low alkali cement whose alkalinity has been increased by the addition of alkali hydroxide (Mo et al. 2010). Still, because the difference between the standard and actual alkalinity is less than 0.2 percent, this is not expected to affect the results of this test.

The concrete mixture was proportioned using the absolute volume method described by the Portland Cement Association (Kosmatka et al. 2002) while assuming the aggregate was dry. The specific gravities and absorptions of the aggregates were known, and the specific gravity of the cement was taken as 3.15. The amount of mixing water was adjusted for each aggregate to reflect their different capacities for absorption. Enough concrete was batched so that four 75 x 75 x 285 mm (3 x 3 x 11 ¼ in.) specimens and three 102 x 203 mm (4 x 8 in.) cylinders could be cast. The first mixture confirmed that the theoretical batch quantities were yielding the expected amount of concrete. Table 4 shows the compressive strengths of the cylinders from each batch, and Table 5 summarizes the materials that were used in each concrete mixture.

Table 4. Average compressive strength of concrete used in the CPT.

<i>Aggregate Name</i>	<i>Compressive Strength (psi)</i>	<i>COV</i>
Lamax	4653	9.4%
Harris	3987	8.6%
Goton	4214	9.7%
Devries Farm	4581	4.0%
Worland	4319	4.6%
Knife River	4465	21.3%
Blackrock	4193	19.4%
Labarge	3840	10.8%

The reason for the higher compressive strength COV in the cases of Knife River and Blackrock is unclear, but it may be an indication of variability within the aggregate used in the compressive strength for the CPT testing.

Table 5. Batch quantities for all aggregates used in the CPT.

<i>Aggregate Name</i>	<i>Cement (lb)</i>	<i>Water (lb)</i>	<i>CA (lb)</i>	<i>FA (lb)</i>	<i>NaOH (lb)</i>
Lamax	19.89	9.90	51.87	27.82	0.14
Harris	19.89	9.96	51.58	29.53	0.14
Goton	19.89	9.21	52.54	28.93	0.14
Devries Farm	19.89	9.83	51.28	28.11	0.14
Worland	19.89	9.55	52.58	27.77	0.14
Knife River	19.89	8.98	52.43	30.97	0.14
Blackrock	19.89	9.90	51.89	28.84	0.14
Labarge	19.89	9.01	52.48	29.57	0.14

Slump (ASTM C143) and air content (ASTM C138) were measured and recorded. Because the air content was measured using the gravimetric method, its accuracy was related to the accuracy of the aggregate property measurements such as specific gravity, absorption, and moisture content. Due to this sensitivity, the gravimetric method resulted in dubious air content measurements. Air content measurement using the pressure method is recommended instead.

Table 6 summarizes the measurements that were taken on the concrete mixtures.

Table 6. Concrete mixture properties for all aggregates in the CPT.

<i>Aggregate Name</i>	<i>Slump (in)</i>	<i>Air (%)</i>	<i>Yield (ft³)</i>	<i>Theoretical Yield (ft³)</i>
Lamax	1	-0.09%	0.743	0.758
Harris	1.5	1.10%	0.752	0.758
Goton	1.5	-0.30%	0.741	0.758
Devries Farm	2	-0.44%	0.74	0.758
Worland	1.5	-0.01%	0.743	0.758
Knife River	1.25	0.66%	0.748	0.758
Blackrock	1	1.00%	0.751	0.758
Labarge	1.5	1.11%	0.752	0.758

After the slump and air content were measured the concrete was placed in the ASTM C1293 molds (Figure 4) and in 102 x 203 mm (4 x 8 in.) cylinders for later compression testing. WD-40 was used as the debonding agent and was applied before the measurement gage studs were screwed into place to avoid weakening the bond between the studs and the concrete. Concrete was placed in the molds in two equal layers, and each layer was rodded 33 times. After the concrete was placed, the ends and corners of the molds were tapped with a rubber mallet to aid in the consolidation process. The surface of the mold was struck off flush and finished.



Figure 4. Mold for ASTM C1293 with four measurement pin inserts.

Immediately after the concrete was placed in the molds and cylinders they were taken to a moist curing room for 24 hours. Plastic lids were placed on the cylinders and plastic was placed over the molds to limit moisture loss. ASTM C511 calls for the moist curing room to be $23 \pm 2^{\circ}\text{C}$ ($73.4 \pm 3.6^{\circ}\text{F}$) with a relative humidity not less than 95 percent, but due to a malfunction with the fog sprayer the relative humidity was only 69 percent.

4.1.1.2 Measurement and Storage

When the concrete had cured for 24 hours from the time that water was mixed with the cement, the CPT specimens were removed from their molds and measured using the comparator shown in Figure 5.



Figure 5. Length comparator with reference bar.

The specimen was placed in the comparator and then spun gently, and when the measurement settled on a number it was recorded. Each specimen was labeled with a name and an arrow to ensure that it was measured with the same end up every time. The specimens were measured at 1, 7, 28, and 56 days, and 3, 6, 9, and 12 months. After each measurement the specimens were stored with a different end facing up to limit alkali migration.

The requirements for the storage environment are specified by ASTM C1293. In fulfillment of the standard, 1.01 kg (2.3 lbs) of water was added to each 18.9 liter (5 gallon) bucket to provide slightly less than 25.4 mm (1 inch) of water in the bottom. Wicking material, needed to aid in moving moisture throughout the storage container, was then placed around the edge of the bucket. A rack to elevate the specimens above the water was placed in the bucket which can be seen in Figure 6.

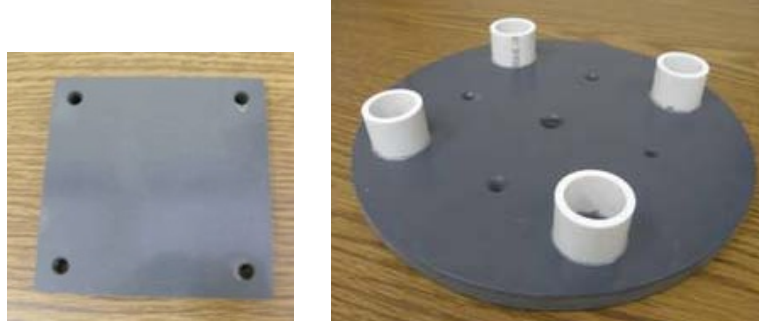


Figure 6. Top portion of rack (left) and bottom portion of rack shown upside-down (right).

Once the specimens were placed on the rack, a top piece was added to ensure separation between them. The storage environment without the lid is shown in Figure 7.

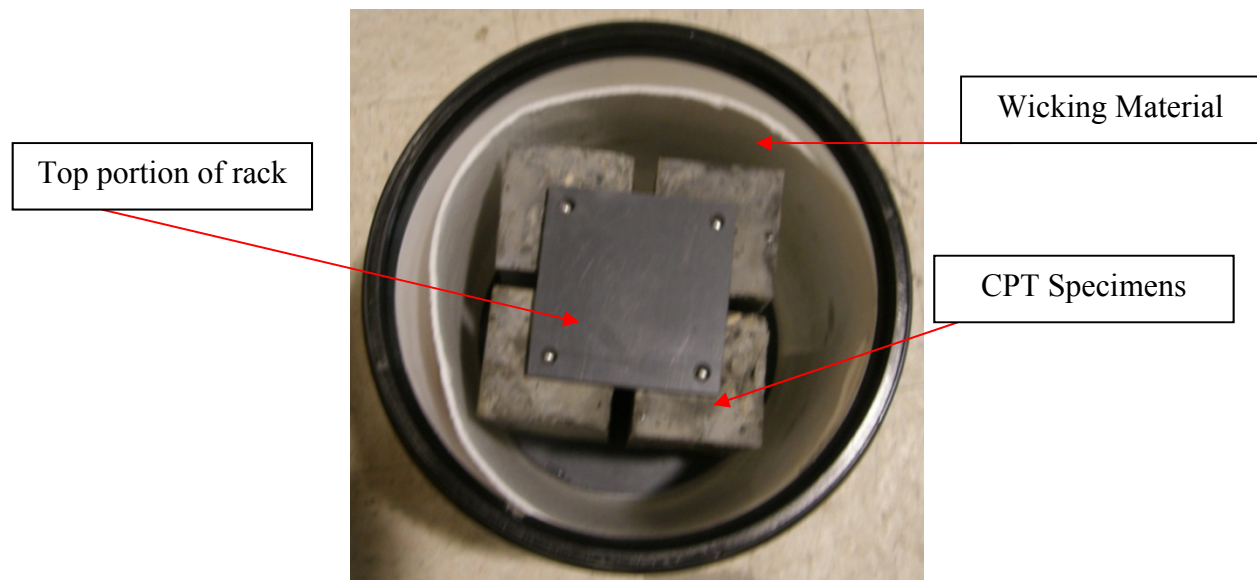


Figure 7. CPT storage environment without lid.

Then a lid that provided an airtight seal was screwed on and the bucket was placed in an oven at 38°C (100°F).

ASTM C1293 states that the specimens should be removed from the storage environment for 16 ± 4 hours to allow them to cool to room temperature before measurement takes place (“cold” measurement), but in this research the specimens were taken out of the storage environment immediately before measuring (“hot” measurement). The difference in one year expansion between “hot” and “cold” measurement techniques is negligible (Cornell 2002; Pugh 2003). In this research, the 1 day measurement was taken at 23°C (73.4°F) and the subsequent

measurements were taken at 38°C (100°F) so there is expansion between the day 1 and day 7 measurements that is due to thermal changes. This was accounted for at the end of the testing process by allowing specimens to cool to 23°C (73.4°F) after the “hot” measurement and taking a “cold” measurement as well. These measurements allow the 1 to 7 day measurement to be scaled accordingly and permit a direct comparison between the first and last measurement. While the total expansion between the first and last measurement will be accurate, the expansion values for the intermediate days, especially early in the test, may be skewed. Research shows that the coefficient of thermal expansion (CTE) for cementitious paste changes significantly at early ages (Choktaweekarn and Tangtermsirikul 2009). In general, the CTE reaches a minimum at day 1 and increases to a stable value at a later age. Because the CTE of the cement paste changes, it is expected that the CTE of the concrete changes as well. Therefore, after the thermal expansion that is calculated from the one year measurements at “hot” and “cold” temperatures is subtracted from the preceding measurements, there may be some error in the early age expansion results which would appear as negative expansions.

At the end of one year, expansion values that exceed 0.04 percent indicate a potentially deleteriously reactive aggregate, while expansions less than 0.04 percent indicate a nonreactive aggregate.

4.1.2 Accelerated Mortar Bar Test (ASTM C1260)

The aggregate gradation used in the AMBT conformed to the gradation outlined in the ASTM standard and is shown in Table 7. To better characterize field concrete, each aggregate portion was composed of 60 percent crushed coarse aggregate and 40 percent natural fine aggregate. First, the natural aggregate was sieved into coarse and fine size fractions. Then the coarse aggregate (retained on number 4 sieve) was crushed and sieved into fine size fractions. To arrive at the appropriate amount of material, 40 percent of each size fraction was taken from the natural fine aggregate and 60 percent was taken from the applicable size fraction of the crushed aggregate. The aggregate was washed and dried before use in the mortar mixture.

Table 7. Aggregate gradation for the AMBT.

<i>Passing</i>	<i>Retained On</i>	<i>Mass (%)</i>
#4	#8	10
#8	#16	25
#16	#30	25
#30	#50	25
#50	#100	15

4.1.2.1 Casting

The ASTM standard specifies a cement to aggregate ratio of 1 to 2.25 and a water to cement ratio of 0.47. This resulted in the quantities of materials shown in Table 8 for each mortar mixture.

Table 8. AMBT batch quantities.

<i>Material</i>	<i>Quantity (g)</i>
Cement	440
Aggregate	990
Water	207

Mixing was then carried out using a Hobart mixer that conformed to ASTM C305. The mixing procedure followed ASTM C1260. After mixing, the mortar was placed into the 25 x 25 x 285 mm (1 x 1 x 11 ¼ in.) molds in two equal layers, and each layer was compacted with a tamping tool. Then the mortar was struck off flat and finished.

4.1.2.2 Measurement and Storage

Measurement and storage procedures followed the ASTM C1260 standard. After casting, the specimens were placed in a fog room conforming to ASTM C511 for 24 ± 2 hours. Then the bars were demolded, and initial length measurements were recorded. The bars were placed in a tap water solution at 80 °C (176°F) for 24 ± 2 hours and measured again before they were placed in a 1 N NaOH solution at 80 °C (176°F). The bars were measured at regular intervals, in accordance with the standard, for 28 days after immersion in the NaOH solution. ASTM C1260 only requires the bars to be measured for 14 days, but this research extended the duration of the test to allow for the use of a kinetic method of analysis. An aggregate is considered innocuous if the 14 day expansion is less than 0.10 percent and potentially deleteriously reactive if the expansion exceeds 0.20 percent. An area exists between 0.10 percent and 0.20 percent expansion where the

aggregate cannot be classified. However, it should be noted that some agencies use different expansion limits. For example, the FHWA uses a limit of 0.08 percent and WYDOT uses a limit of 0.10 percent to indicate reactive aggregate.

To measure the length of a specimen, a single bar was removed from the soak solution container and towed dry. Then it was placed in the length comparator and gently spun. The reading displayed on the indicator during the spinning process was recorded. Then the bar was set aside, out of the container, while the other specimens were measured. A gage length of 254 mm (10 in.) was used for the expansion calculation, which is shown in the equation below.

$$\% \text{ Expansion at Day}_i = \frac{\text{Day}_i \text{ measurement} - \text{Day}_0 \text{ measurement}}{\text{Gage length}}$$

Figure 8. Equation. Percent expansion at day i.

4.1.2.3 Kinetic Method

This analysis method fitted a curve to the AMBT expansion data and used the points on the curve as input into a function for modeling ASR. Linear regression was performed to yield values that were used to delineate reactive and nonreactive aggregates. The MMF equation, a sigmoidal growth curve developed by Morgan, Mercer, and Flodin (Morgan et al. 1975) was fitted to the actual expansion data using a computer program called CurveExpert. The equation has the form illustrated in Figure 9 where t is time and a , b , c , and d are curve fitting constants.

$$\text{Percent Expansion} = \frac{(a * b + c * t^d)}{(b * t^d)}$$

Figure 9. Equation. Percent expansion.

The form of the Kolmogorov-Avrami-Mehl-Johnson (KAMJ) equation that is described in (Johnston and Fournier 2000) and used to model ASR is expressed in Figure 10 where α is the

expansion at time t , α_0 is the expansion at time t_0 , k is the expansion rate constant, and M is the Avrami exponent.

$$\alpha = 1 + \alpha_0 - e^{-k(t-t_0)^M}$$

Figure 10. Equation. Alpha.

Linear regression of Figure 10 yields Figure 11.

$$M \ln(t - t_0) = \ln \left(\left[\ln \left(\frac{1}{1 + \alpha_0 - \alpha} \right) \right] \right) - \ln(k)$$

Figure 11. Equation. Linear regression of alpha.

The value of t_0 depends on the induction period before ASR begins (Johnston et al. 2004), which varies with each aggregate type. A technique to consistently select the appropriate value of t_0 was recently proposed (Stokes 2006). An algorithm is used to calculate $\ln(k)$ and M for all possible values of t_0 and return the maximum value of $\ln(k)$ along with the corresponding M and t_0 .

Because the MMF equation was fitted to the expansion data, intermediate expansion values could be calculated. An algorithm was used to calculate $\ln(k)$ and M for 100 values of t_0 (0.28 day intervals) and return the maximum value of $\ln(k)$ along with the corresponding values of M and t_0 . The value of t_0 refers to the time at which nucleation and growth reaction kinetics begin to dominate the reaction (Berliner et al. 1998) and is intended to correlate to the time at which ASR begins. The value of M depends on the form and growth of the reaction products, and k is influenced by the effects of nucleation, multidimensional growth, the geometry of the reaction site, and diffusion. An aggregate is classified as nonreactive if $\ln(k) < -6$ and as reactive if $\ln(k) > -6$ (Johnston and Fournier 2000).

4.1.3 Modified CAMBT

Because the CAMBT is still in development, several test variations were possible. A modified CAMBT test was proposed that seems to provide better correlation with the CPT than the standard CAMBT as well as the AMBT. This modified test calls for an aggregate size fraction of 2.5 – 5.0 mm (0.1-0.2 in.), so this research used aggregate that passed the number 4 sieve and were retained on the number 8 sieve giving an aggregate size range of 2.36 – 4.75 mm (0.09-0.18 in.) (Lu et al. 2007).

NaOH was added to increase the cement alkalinity of the mortar bars to 1.5 percent Na₂O equivalent. The test procedure calls for the alkalinity to be boosted by the addition of KOH to the mortar, but in an effort to remain consistent with all the ASR tests conducted in this research the alkalinity was boosted using NaOH. Compared to KOH, NaOH was found to have the most detrimental effect on ASR and ACR aggregates (Lu et al. 2006) so the substitution of NaOH for KOH will yield conservative conclusions on reactivity. The effect of boosting the mortar alkalinity with NaOH instead of KOH will also be muted because the specimens will already be soaking in a 1 N NaOH solution. This substitution of NaOH for KOH is consistent with the RILEM AAR-5 test method, which is similar to this test (Sommer et al. 2005).

4.1.3.1 Casting

The modified CAMBT procedure specifies a 1 to 1 cement to aggregate ratio and a water to cement ratio of 0.33. The specific gravity of cement was taken as 3.15, and the specific gravities of the aggregate and water were measured and used to calculate the theoretical volume of mortar. As in the CPT, the quantity of mixing water was adjusted for each aggregate depending on their absorption capacities. Enough mortar was proportioned for three specimens plus 30 percent, which yielded an adequate amount of mortar. Once the required material quantities were measured and set aside (Table 9), a debonding agent was applied to the specimen molds prior to installing the gage studs to ensure an uninhibited bond between the stud and the mortar. In this test the distance between gage studs was set as close as possible to 127 mm (5 in.) to guarantee that the length comparator would have enough displacement capacity to measure the total expansion of the bar. Mixing was performed using a Hobart mixer that conformed to ASTM C305. The mixing procedure was the same as that given in ASTM C1260.

Table 9. Modified CAMBT batch quantities for all aggregate sources.

Aggregate Name	Cement (g)	Water (g)	FA (g)	NaOH (g)
Lamax	961.3	317.2	961.3	7.69
Harris Pit	962.2	317.5	962.2	7.70
Goton Pit	967.5	319.3	967.5	7.74
Devries Farm Pit	964.3	318.2	964.3	7.71
Worland BLM	963.7	318.0	963.7	7.71
Knife River	968.1	319.5	968.1	7.74
Black Rock	959.7	316.7	959.7	7.68
Labarge	966.6	319.0	966.6	7.73

After mixing, the mortar was placed into the 40 x 40 x 160 mm (1.6 x 1.6 x 6.3 in.) molds in two equal layers. Each layer was compacted by tamping with special attention given to the areas around the gage studs and in the corners of the mold to eliminate voids. Then the mortar was struck off flat and finished.

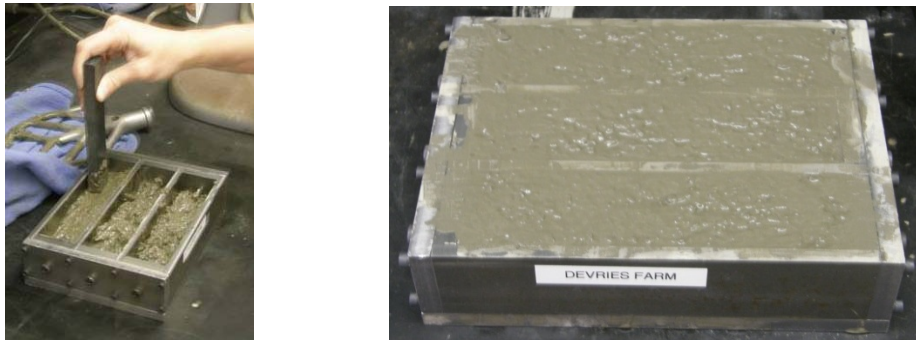


Figure 12. Compacting mortar (left), finished CAMBT specimen (right).

4.1.3.2 Measurement and Storage

Measurement and storage procedures followed the recommendations of (Lu et al. 2007) which were similar to the ASTM C1260 procedures. After casting, the specimens were placed in a fog room conforming to ASTM C511 for 24 ± 2 hours. The bars were demolded and initial length measurements were recorded. The bars were placed in a tap water solution at $80 \text{ }^\circ\text{C}$ (176°F) for 24 ± 2 hours and measured again before they were placed in a 1 N NaOH solution at $80 \text{ }^\circ\text{C}$ (176°F). The bars were measured at 1, 4, 7, 11, 14, 21, and 28 days after immersion in the NaOH solution. Although it is only required to measure the bars for 14 days, this research extended the duration of the test for observational purposes.

To measure the length of a specimen, a single bar was removed from the container with silicone tipped tongs and toweled dry. Then it was placed in the length comparator (Figure 13) and spun gently.

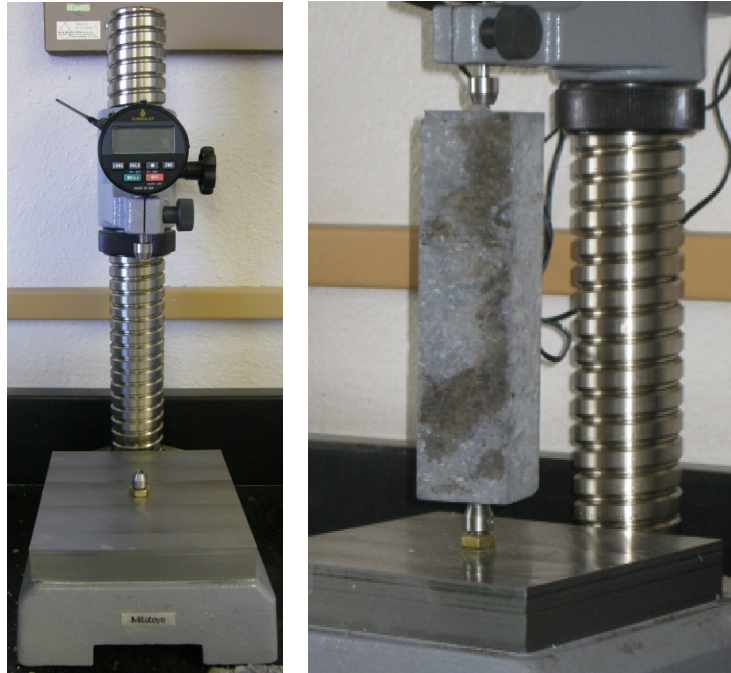


Figure 13. Length comparator setup (left) and specimen in measurement position (right).

The lowest number displayed on the indicator during the spinning process was recorded. Care was exercised to ensure that each specimen was measured within 15 seconds of being removed from the solution. Then the bar was set aside, out of the container, while the other specimens were measured. For quality control, the temperature of the NaOH solution was also measured when the container of specimens was taken out of the oven. A gage length of 127 mm (5 in.) was used for expansion calculations.

To measure the mass, the bar was wiped again with a towel to remove any excess materials that had adhered to the bar in the solution and then weighed on a nearby scale.

An expansion less than 0.093 percent on the 14 day measurement indicates an innocuous aggregate, and a potentially deleteriously reactive aggregate is indicated by expansion greater than 0.093 percent. An advantage of the modified CAMBT is its ability to identify ACR as well

as ASR. RILEM's AAR-5 test contains recommendations for identifying ACR. First, AAR-2 (similar to the AMBT) is conducted on the aggregate. Depending on those results, further testing may be required with AAR-5 and AAR-3 (similar to the CPT). In general, an aggregate is considered to have ACR potential if the expansion in AAR-5 exceeds the expansion in AAR-2. This generality cannot be directly applied to this research because this comparison should be done using the same size bars in both tests. However, any expansion in the modified CAMBT that exceeds the AMBT expansion should be given further consideration.

4.2 Large Scale Field Exposure

The aggregate gradation used in the field specimens was the same as the gradation of each aggregate source, which was determined by sieving material from each pit. Each field specimen was cast using the same amounts, by weight, of coarse aggregate, fine aggregate, cement, and air entrainment admixture. The amount of water added to each mixture varied by a small amount depending on the workability of the concrete. Superplasticizer was added to many of the mixtures in order to improve workability and to further represent field mixtures. The effect of superplasticizer on ASR expansion was studied recently (Leemann et al. 2010), and it was concluded that polycarboxylate superplasticizers had a negligible effect on concrete expansion due to ASR.

To represent an upper bound estimate of an aggregate's reactive potential, at least one field specimen from each aggregate source contained a cement alkalinity that was boosted to 1.25 percent Na₂O equivalent by the addition of NaOH to the mixing water.

Table 10 shows the materials whose quantities were the same in all the field specimens, and Table 11 shows the materials specific to each specimen. In Table 11 the BHP and BHC specimens refer to the Blackrock aggregate.

Table 10. Material quantities common to all field specimens.

<i>Material</i>	<i>Quantity (lb)</i>
Coarse Aggregate	305
Fine Aggregate	196
Cement	124

Table 11. Other materials used in field specimens.

Specimen	Water (lb)	NaOH (lb)	Air Ent. (lb)	Superplasticizer (lb)	Slump (in)	Air Content (%)
BHC-1	57.5	0	0.2	2.2	3	4.5
BHC-2	57.5	0	0.2	2.32	5.5	6
BHC-3	53.1	0.68	0.15	2.8	7.5	4.1
BHP-1	61.25	0	0.25	0	5	7
BHP-2	58	0	0.25	0	6	6
BHP-3	56.5	0.68	0.16	2.18	6.5	4.2
DFP-1	57.5	0	0.25	0	3.5	5
DFP-2	58	0	0.25	0	4.5	7
DFP-3	57.5	0.68	0.24	2.74	4.5	5
GP-1	57.5	0	0.24	2.2	6.5	7.5
GP-2	53.4	0	0.2	2.2	4.5	4.5
GP-3	55.2	0.68	0.19	2.3	7	5.2
HPC-1	57.5	0	0.25	0	2.5	5
HPC-2	57.5	0	0.25	2.3	5.5	7
HPC-3	57.5	0.68	0.24	2.44	3.5	5
KR-1	57.5	0	0.2	2.26	7.5	6.6
KR-2	49	0	0.2	2.3	5	4.7
KR-3	55	0	0.25	2.1	3.5	5
KR-4	55	0.68	0.25	2.3	4	8
LBG-1	60.4	0	0.25	0	0.5	4
LBG-2	65	0	0.25	0	2	4
LBG-3	65	0.68	0.25	0	6	6
LX-1	57.5	0	0.25	3	6	8
LX-2	53.9	0	0.25	2.4	8.5	9
LX-3	57.5	0.68	0.24	2.47	7.5	7.4
WOR-1	63	0	0.25	0	5.5	4.5
WOR-2	60.2	0	0.25	0	5	6
WOR-3	57.5	0.68	0.15	2.3	5.5	5.8

Measurement studs, cast into the specimens, were fabricated first by cutting galvanized threaded rod and then grinding off the burrs on the edges. Later, it proved more efficient to buy galvanized carriage screws for the measurement studs. The heads of the screws were cut off with a chop saw and the burrs were ground. Two advantages of this method were that the screws were readily available and eliminated the need for a length measurement. To allow for variation in the field when locating the studs, two holes were drilled; one in the center and one offset

approximately 0.1 inch using a milling machine. This allowed approximately 10.2 mm (0.4 in.) of tolerance, depending on the orientation of the measurement stud as shown in Figure 14.

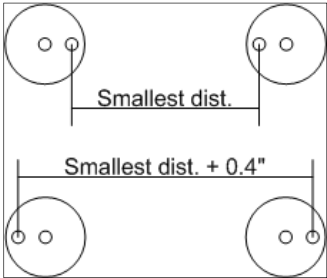


Figure 14. Tolerance gained from offset orientation.

4.2.1 Exposure Site

An outdoor exposure site, shown in Figure 15, was constructed on a bed of 4 in. minus rock to coarsely level the area and ensure proper drainage, and 3/4 in. minus angular gravel was then placed on top of the rock for fine leveling. To date, a total of 28 field specimens have been transported to the site for outdoor exposure.



Figure 15. Outdoor exposure site.

Weather data was logged daily to monitor temperature, relative humidity, and precipitation. This weather data may make future comparisons to other exposure site data more meaningful. Graphs of the average daily maximum and minimum temperature, average daily relative humidity, and total monthly precipitation are included in Appendix B.

4.2.2 Casting

Forms for the 380 x 380 x 660 mm (15 x 15 x 26 in.) specimens were constructed using standard lumber and plywood. The bottom, sides, and ends were all constructed separately to be assembled at the time of casting which allowed for efficient construction and stripping of the forms. Both inside corners and edges of the formwork were caulked to prevent moisture loss during curing, and a debonding agent was sprayed on the inside of the form. To secure the measurement studs into the concrete block, a threaded steel insert assembly was bolted to the inside of the form after the debonding agent was applied to ensure a good bond between the insert and the concrete. This assembly (Figure 16) consisted of the steel insert, a threaded rod, a wooden spacer, and a nut. The insert and the wooden spacer were placed on the inside of the forms and the nut was placed on the outside as shown in Figure 17. Ten of these assemblies were installed in the forms: three on each side and two on each end.

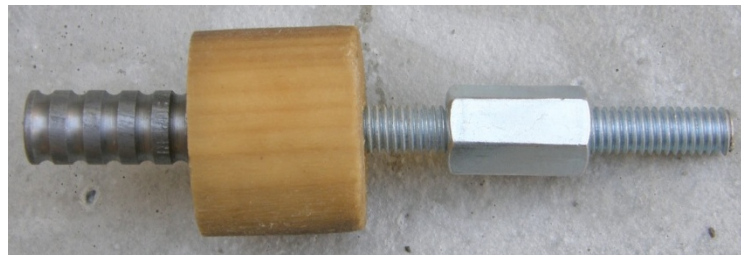


Figure 16. Threaded steel insert assembly.



Figure 17. Portion of the insert assembly on the inside of the form (left) and the outside of the form (right).

Before casting, all the required quantities of materials were measured and set aside. A gas powered concrete mixer was used to mix the concrete. After measuring the slump (ASTM C143) and air content (ASTM C231) the concrete was placed in the form in two layers. Each layer was

consolidated using an internal concrete vibrator, paying special attention to ensure that the concrete was completely consolidated near the corners of the form and around the insert assemblies. When enough concrete had been placed in the form the top was struck off flat and then finished with a magnesium float. An aluminum name plate, a steel lifting insert, and the top measurement pins (except for pins that were installed by drilling after the concrete cured) were installed in the concrete. The specimens were then covered with plastic to limit the moisture loss during curing. A field specimen after casting is shown in Figure 18 before measurement pins are installed and before the block is covered with plastic for curing.



Figure 18. Field specimen immediately after casting.

4.2.3 Measurement Stud Installation

To install the measurement studs on the top of the specimen, the merits of several different methods were analyzed. On the first group of blocks that were cast, holes were drilled in the top of the cured specimen and the measurement pins were installed with epoxy. A problem with this method was that it was very difficult to drill the holes in the exact location that was needed and in a plane that was exactly perpendicular to the surface of the block. In later specimens the top pins were cast into the wet concrete after measuring and marking out the appropriate locations for the studs. The setting out bar (Figure 19) included with the Demec mechanical strain gauge was used to confirm the accuracy of the measurement pin locations in the wet concrete. This method provided much better precision and ultimately made it easier to obtain reliable measurements.

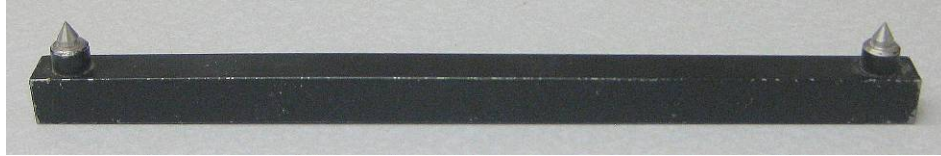


Figure 19. Setting out bar.

To install the side measurement studs into the field specimens the studs were screwed into the threaded steel inserts that were cast into the block. The orientation of the stud was critical due to its effect on the location of the drilled offset hole. To control this orientation, a hex nut was screwed onto the stud before the stud was installed in the block. Once the stud was screwed into the threaded insert and the orientation of the offset hole was chosen, the hex nut was tightened against the block to lock the stud orientation in place. It was helpful to use a hollow socket when tightening the hex nut so the location of the offset hole could be monitored. An example of the installed measurement stud can be seen in Figure 20.



Figure 20. Side of field specimen (left) and close up of installed measurement stud (right).

After the measurement studs were installed, pliable vinyl caps with pull tabs were placed over the studs to protect the measurement holes from corrosion. The pull tab made these caps easy to remove during measurement.

4.2.4 Measurement

Because each measurement was recorded to the nearest 0.001 mm (0.00004 in.), the effect of variations in exposure conditions during the time of measurement was significant. Factors that would be negligible in less precise measurements, such as thermal expansion or thermal gradients, had to be accounted for in this process. Ideally, these factors would be eliminated by

measuring each field specimen at the same ambient temperature and under constant cloud cover to avoid direct sunlight. However, due to the erratic weather that is common in Laramie, WY it was not feasible to wait for these ideal conditions. To account for thermal expansion effects, the surface temperature was taken at the time of measurement, and the recorded measurements were then scaled to obtain an equivalent value at 21°C (70°F). For preliminary results, the coefficient of thermal expansion used to scale the measurements was $11.7 \times 10^{-6}/^{\circ}\text{C}$ ($5.5 \times 10^{-6}/^{\circ}\text{F}$).

In addition to the challenges that were introduced by measuring at different temperatures, measuring in direct sunlight instead of cloud cover introduced thermal gradients into the specimens. The difference in temperature between direct sunlight and shade on the blocks could be significant at times and could interfere with the comparison of measurements from different locations on the same block. This issue was addressed by shading the block with a 2.7 m (9 ft) patio umbrella for at least 20 minutes prior to measuring which allowed the difference in temperature at different locations in the specimen to be more consistent.

In many cases the expansion measurements did not begin for some time after the specimens were cast. This was due to a combination of factors including the challenges stated above, the need to learn how to take reliable measurements using the Demec gauge, and the extra time that was required to retrofit some specimens to allow for more precise measurement. Even though there was a delay in initial measurement, the field specimens are not expected to display reactive behavior in the early phases of exposure. In addition, the visual signs of ASR will be apparent as exposure continues.

To monitor the expansion, twelve locations on each block were measured. There were four longitudinal measurements on the top, and two longitudinal measurements along each side. In addition, there were two transverse measurements on top and one vertical measurement on each end. All measurements had an approximate gage length of 203.2 mm (8 in.). Figure 21 shows the typical measurement location layout for each field specimen where 9 of the 12 measurements are shown.

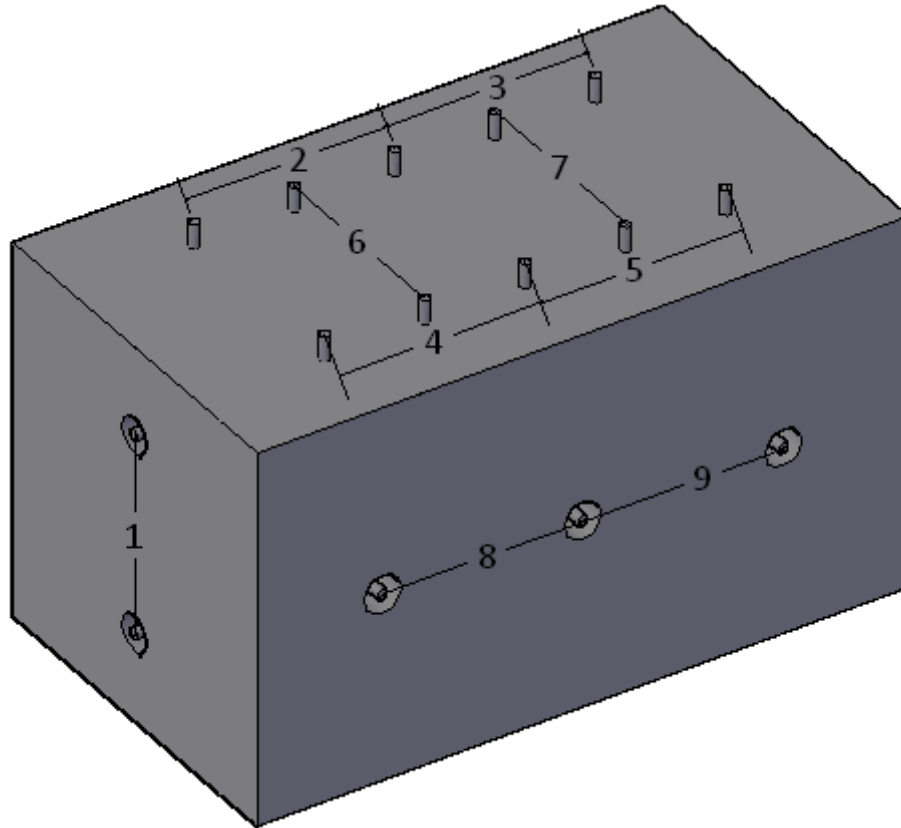


Figure 21. Field specimen diagram showing the layout of the measurement locations.

4.2.5 Labeling

Because of the offset hole, there are four possible measurements between any two pins. To document which measurement holes to use, a labeling method was developed using three letters. “M” stands for the middle hole, “O” refers to the outside hole, and “I” stands for the inside hole. A given measurement was described by a combination of two letters, which were written on the block in permanent marker as well as on the template for recording measurements. Figure 22 shows two example measurements using the labeling system where the left measurement is designated OM and the right measurement is designated IM.

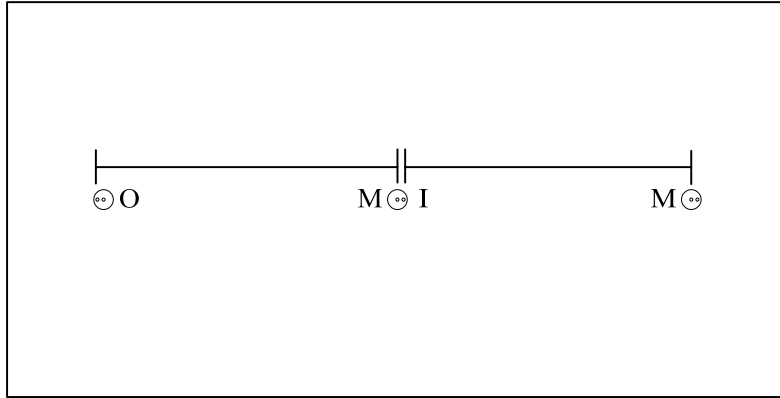


Figure 22. Using labeling system to measure side of block.

It was also important that the pivot point and fixed point of the measurement gauge were located in the same position for each respective measurement. For this reason, the orientation of the gauge was specified on the measurement recording sheet by the vertical line and an indicator arrow shown in Figure 23. The vertical line indicates placement of the pivot point of the strain gauge, and the arrow points toward the fixed point of the gauge.

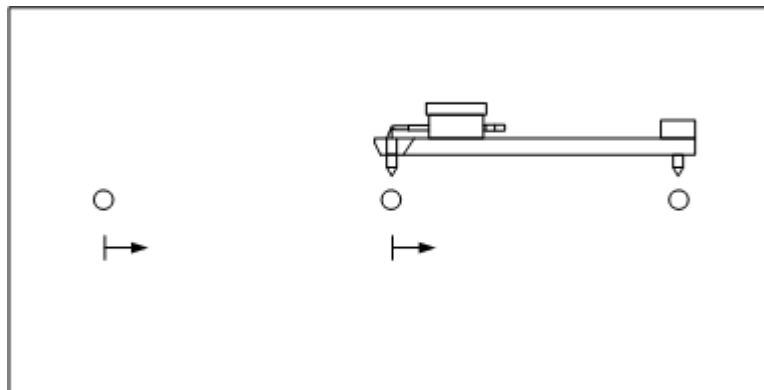


Figure 23. Orientation of strain gauge based on indicator arrow.

4.2.6 Demec Measurement Technique

To obtain consistent results with the Demec system, several guidelines are provided. The points on the Demec gauge must be placed in exactly the same location in the studs every time a measurement is taken, so care must be taken to make sure the gauge points are securely seated in the drilled holes. The angle of the gauge with respect to the block affects the measurement significantly, and rotation of the gauge may result in an incorrect measurement.

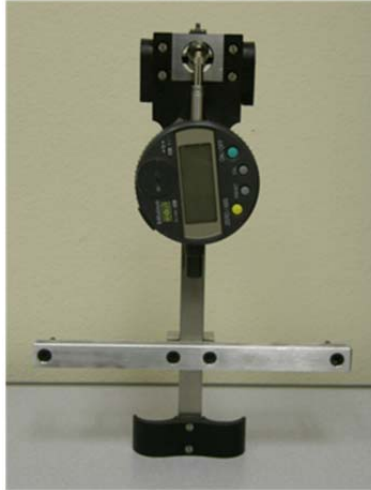


Figure 24. Photo of Demec instrument.

The amount of pressure that is applied to the gauge in any direction when measuring will also affect the measurement obtained. When measuring the top of the block the gauge can be balanced on the studs with minimal force. However, on the four vertical sides of the block it can be difficult to feel how much pressure is being applied. A method that proved effective was to hold the gauge normally but to resist the weight of the gauge by one finger and push the points into the holes in the studs until it could be seen that they were securely seated.

A standard measurement procedure was developed to ensure that all field specimen measurements in the future are consistent with past measurements.

1. Expose the gauge and the reference bar (Figure 25) to field conditions to avoid errors due to thermal changes in the measurement equipment.



Figure 25. Invar reference bar.

2. After the gauge and reference bar have normalized to the outdoor temperature turn on the gauge and measure the reference bar (Figure 25) to obtain the reference measurement.

3. On the block, measure each distance between studs at least three times, and confirm that the difference in measurements is less than 0.005 mm (0.0002 in.) each time.
4. Record the average of these three measurements.
5. Repeat steps 2 through 4. The second series of measurements should be completely independent of the first measurement series.
6. If the difference between related measurements in the two series is more than 0.015 mm (0.0006 in.) (equivalent to 0.0075 percent expansion) then that location on the specimen should be measured again.

Chapter 5 Results

Overall reactivity is based on accelerated testing methods, field specimen results and a detailed petrography study. Each of these categories is presented below and followed by Section 0 Discussion of Results.

5.1 Accelerated Test Methods

Researchers classified each aggregate on the basis on standardized and state-of-the art methods. Despite the length of time to complete CPT testing, it is still considered an accelerated test method.

5.1.1 Concrete Prism Test (ASTM C1293)

The average measured expansions of the concrete prisms cast with each aggregate are presented in Figure 26. Figure 27 illustrates the average one year expansion with error bars showing \pm one standard deviation. Complete coefficient of variation data is given in Appendix C.

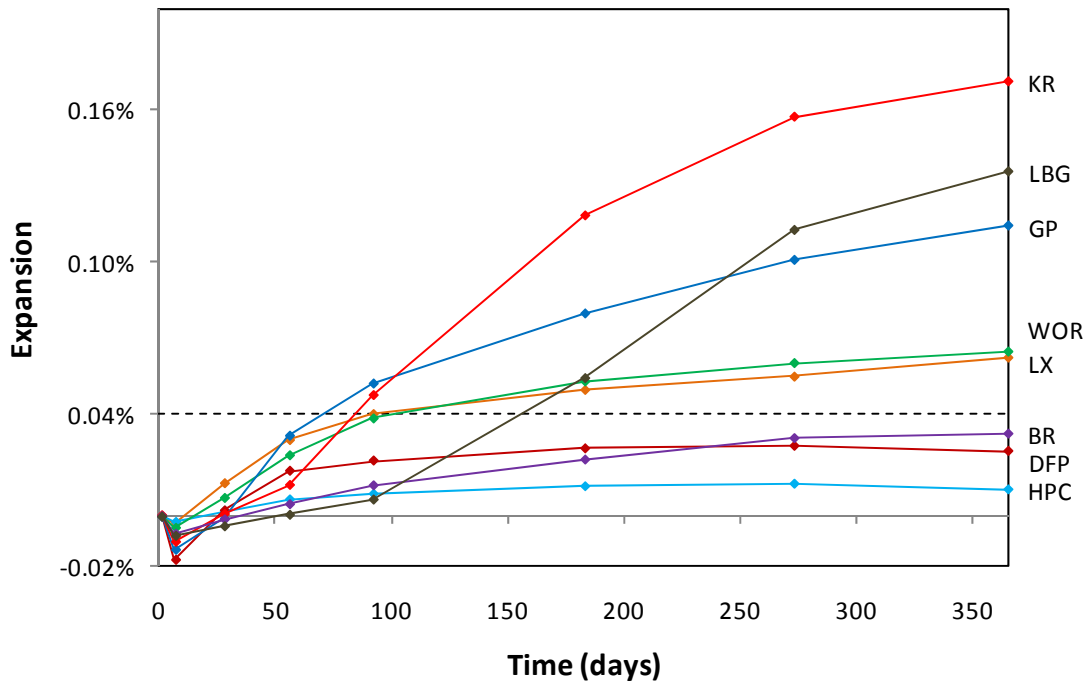


Figure 26. Average expansion for eight aggregates subjected to the CPT.

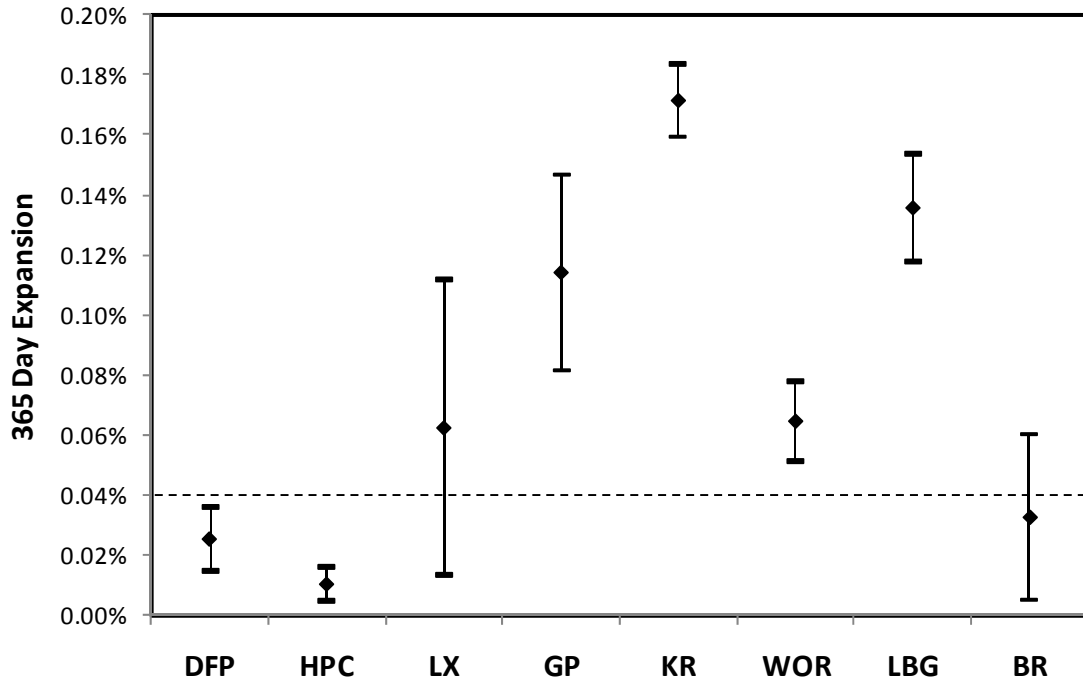


Figure 27. Average one year expansion in the CPT with error bars showing standard deviation.

Negative expansion values at early ages in the test are likely due to differences in coefficient of thermal expansion (CTE) of the concrete during the course of testing. CPT measurements should be taken after the specimen has cooled to room temperature. During this study intermediate expansions were measured before the concrete was completely cooled. As a result, corresponding measurements were scaled down based on the difference between hot and room temperature expansions. Because the first and last measurements were evaluated at the same temperature, the total expansion value is accurate and was not affected by the correction.

Four specimens were cast for each pit and classifications were generally straightforward. Knife River, Labarge, and Goton exhibited the highest expansions and exceeded the critical expansion limit by factors of 4.3, 3.4 and 2.9, respectively. Harris and Devries Farm experienced the least expansion and were classified as nonreactive. Blackrock, Worland and Lamax proved to be moderately expansive in relation to the other aggregates but are still considered potentially

deleteriously reactive. A summary of expansion data for each aggregate is presented in Appendix C.

A summary of the original Black Rock data is illustrated in Figure 28 and the average is indicated by a solid blue line without markers. Although, the average expansion of all four Black Rock specimens was below the ASTM limit, one specimen had over twice the measured expansion of the other three specimens cast at the same time. Because this one specimen exceeded the ASTM limit by a factor of 1.8, additional testing was conducted.

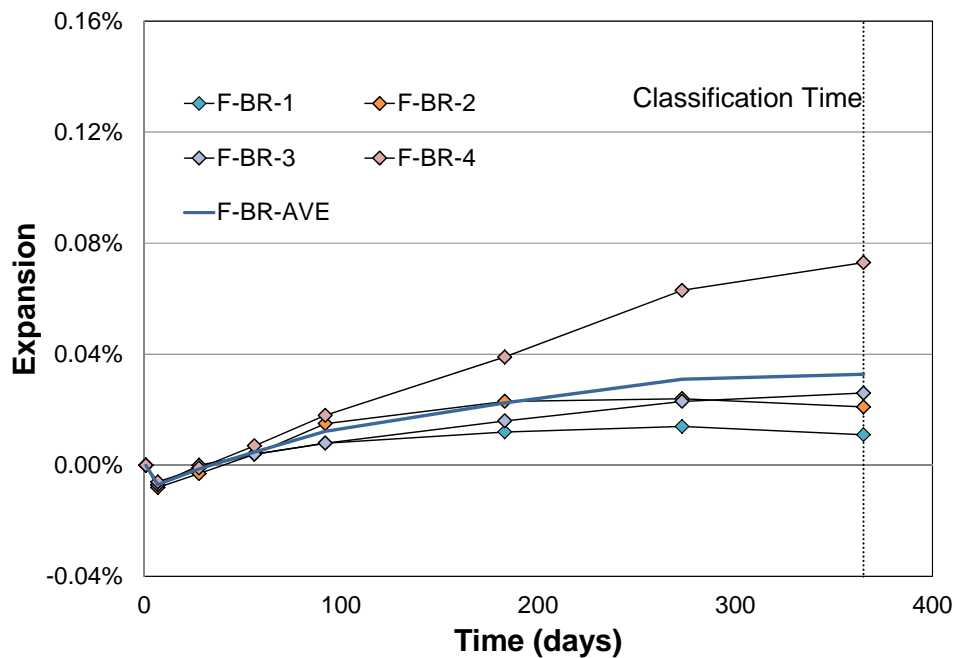


Figure 28. ASTM C 1293 Black Rock Test Results (Fertig 2008).

Due to the outlying data point, an additional eight Black Rock specimens were cast in August 2012. A single concrete mix was produced and specimens were stored in two buckets during the exposure period. All eight results are illustrated in Figure 29, and results of each bucket are distinguished by different line styles. Both groups of four specimens followed the same trend as that obtained by Fertig (2008). Average results obtained by Fertig and the additional eight specimens are shown by distinct colored lines in Figure 29. Although the averages are different, it is worth noting that a 0.04 percent expansion corresponds to a measured displacement of 0.1 mm (0.004 in.). The variation is partly attributed to the difficulty in measuring such small

expansions. Out of all 12 specimens, 6 exceeded the ASTM limit of 0.04 percent expansion. This justifies a moderately reactive classification of the Black Rock aggregate.

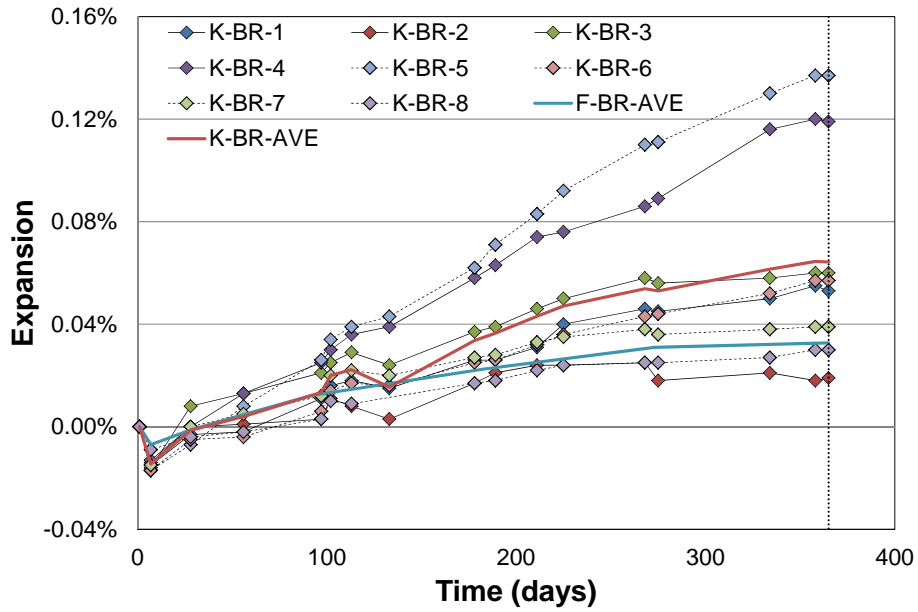


Figure 29. ASTM C 1293 Black Rock Test Results.

5.1.2 Accelerated Mortar Bar Test (ASTM C1260)

The average expansions of all the mortar bars cast with each aggregate are shown in Figure 30. The average expansion at 14 days is shown in Figure 31 with error bars designating \pm one standard deviation.

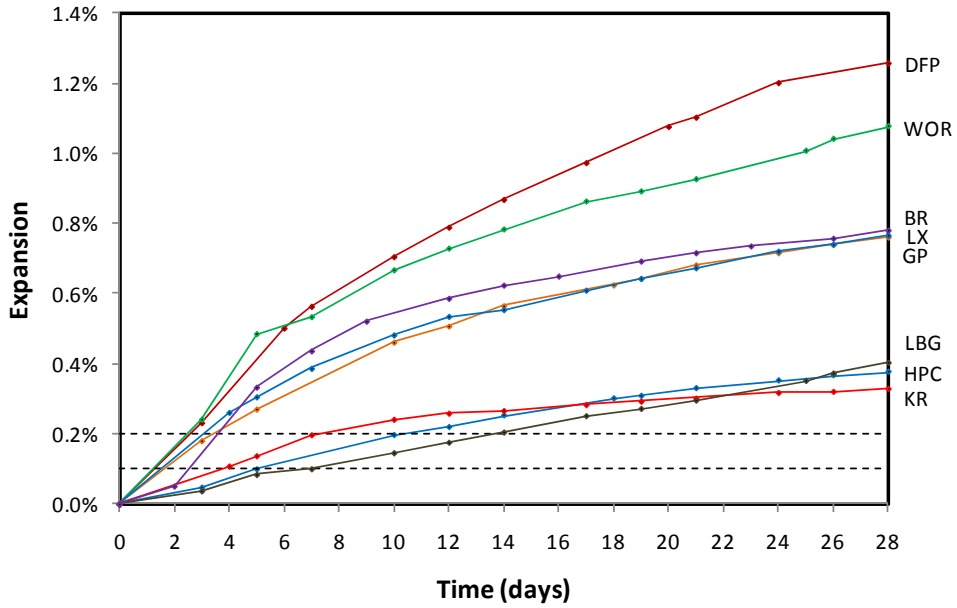


Figure 30. Average expansions for eight aggregates subjected to AMBT.

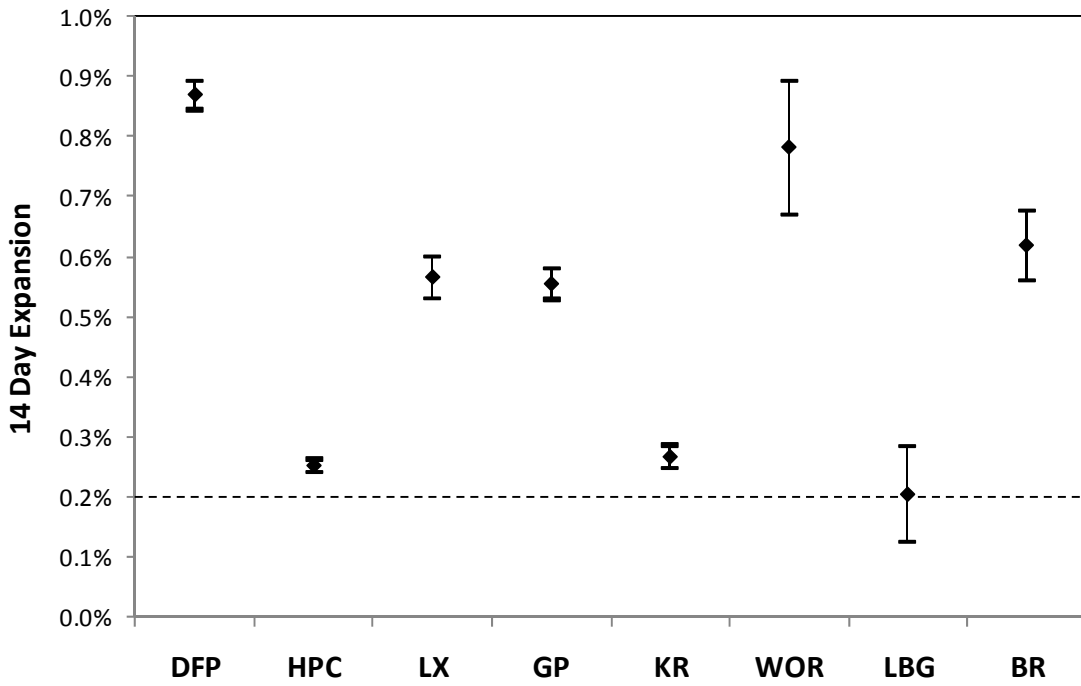


Figure 31. Average 14 day expansion in the AMBT with error bars showing standard deviation.

All the aggregates exhibited relatively smooth, growth curve type expansion behavior throughout the test. Five of the aggregates exceeded the expansion limit by day 4, very early in the test. The expansions of the other three aggregates exceeded the limit later, between 7 and 14 days. These more slowly reacting aggregates included Knife River and Labarge which exhibited delayed reaction in the CPT as well. This test classified all the aggregates tested as potentially deleteriously reactive.

5.1.3 Kinetic Method

The values obtained using the Kinetic Method of analysis are presented in Table 12 and Figure 32 below.

Table 12. $\ln(k)$, t_0 , and M for eight aggregates analyzed using the Kinetic Method.

Aggregate	t_0	M	$\ln(k)$
DFP	0.28	1.197	-2.465
HPC	3.08	0.903	-3.728
LX	0.28	0.913	-2.665
GP	0.00	0.801	-2.304
KR	1.68	0.698	-3.160
WOR	0.00	1.041	-2.204
LBG	6.16	1.036	-4.227
BR	2.24	0.781	-2.343

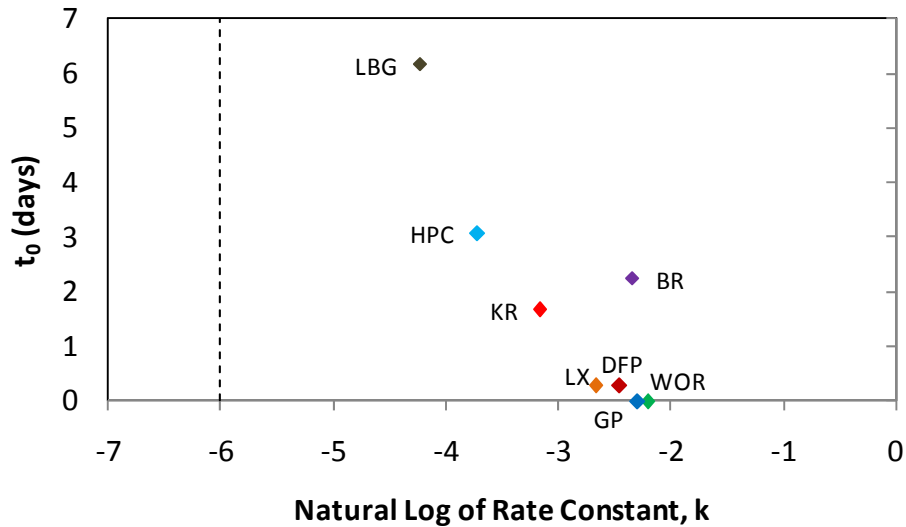


Figure 32. t_0 versus $\ln(k)$ for eight aggregates analyzed using the Kinetic Method.

The results of the Kinetic Method are very similar to the results of the AMBT. Labarge, Harris, and Knife River are together in a group, and the remaining aggregates exhibit higher reactivity. Still, the $\ln(k)$ value for each of the aggregates was greater than -6 so this method classifies all the aggregates as reactive.

Four of the t_0 values were very close to zero and represent a very short induction period. The other four values of t_0 are slightly larger, and with the exception of Blackrock, seem to correlate with lower levels of reactivity. The trend of increasing reactivity with decreasing induction period is evident in Figure 32. This could be a true relationship between t_0 and ASR potential, or it could be an indication of the ineffectiveness with which the AMBT identifies slowly reacting aggregates.

5.1.4 Modified CAMBT

The average expansions of all the mortar bars cast with each aggregate are shown in Figure 33. The average 14 day expansion is shown in Figure 34 with error bars designating plus or minus one standard deviation.

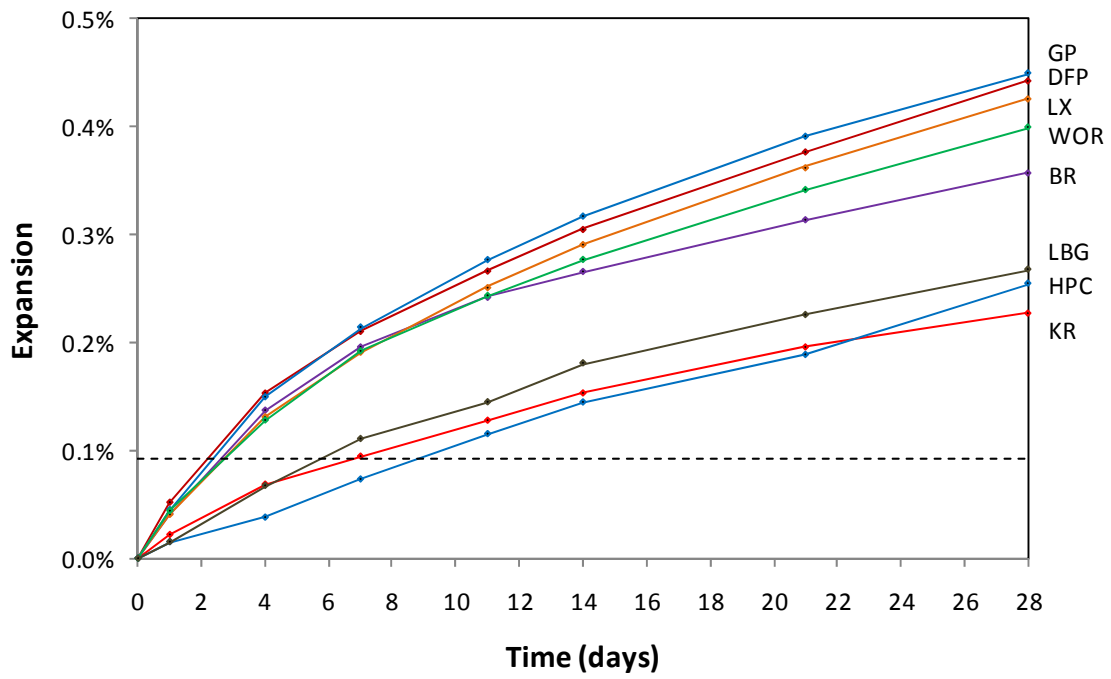


Figure 33. Average expansions for eight aggregates subjected to the modified CAMBT.

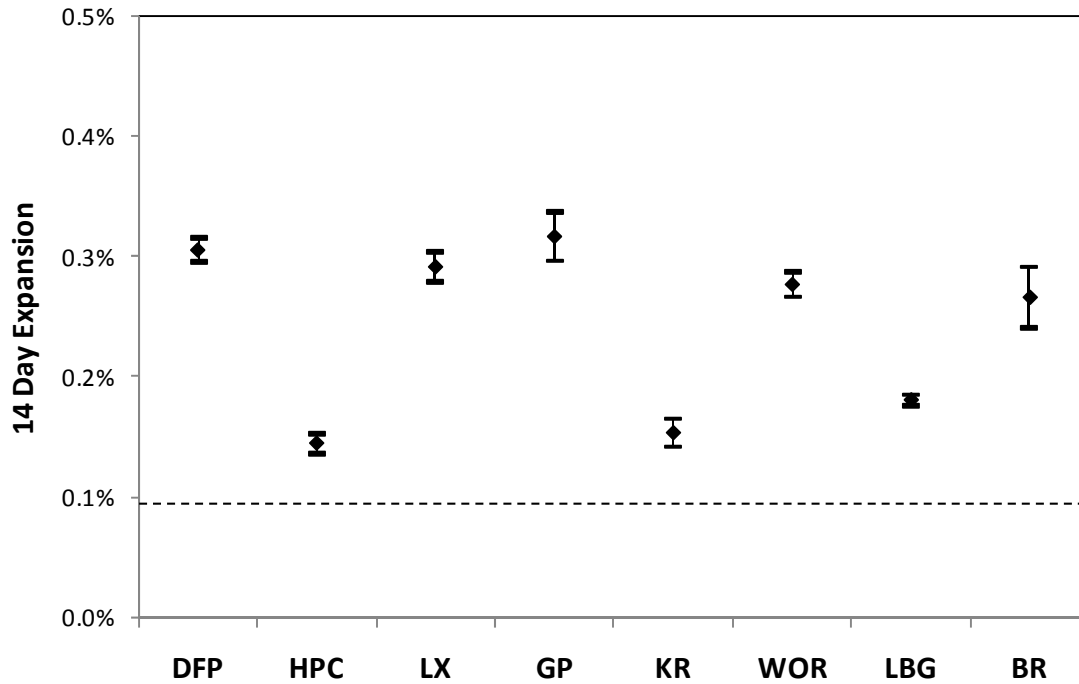


Figure 34. Average 14 day expansion in the CAMBT with error bars showing standard deviation.

Five of the aggregates exceeded the expansion limit by day 3 in the test. The expansions of the other three aggregates exceeded the limit later, between 5 and 9 days. These more slowly reacting aggregates included Knife River and Labarge which exhibited delayed reaction in the CPT as well. This test classified all the aggregates tested as potentially deleteriously reactive.

The mass change data is presented in Figure 35, and although the curves are slightly more erratic than the expansion data, there are two distinct mass signatures.

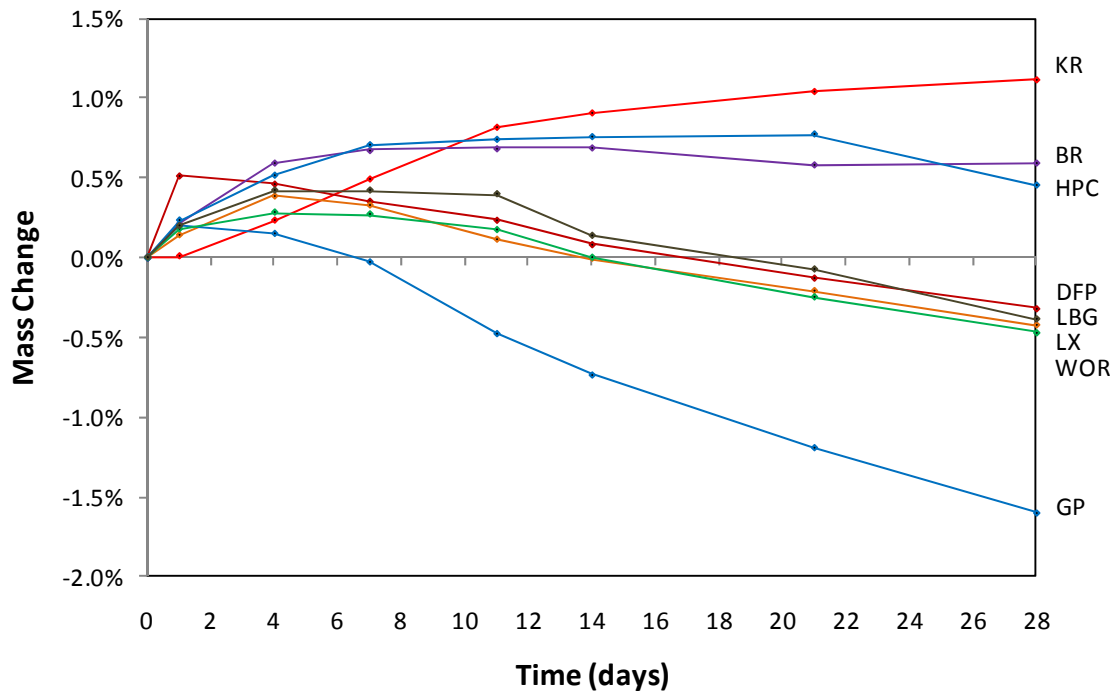


Figure 35. Average mass changes for eight aggregates subjected to the modified CAMBT.

Knife River, Blackrock, and Harris gained mass for the majority of the test. Most of this mass gain occurred in the early phases, and minimal mass loss was seen for the remainder of the test. Another group of specimens gained mass initially but then lost more than was gained over the remaining days. This group included Devries Farm, Labarge, Lamax, and Worland. Goton's mass signature was similar to the first group, but less mass was gained at the beginning and more was lost at the end.

Typically, the mass signatures are related to the type of aggregate being tested (Grattan-Bellew et al. 2004). There was similarity in both the mass signatures and expansion paths of Goton, Devries Farm, Lamax, and Worland. This group lost the most mass and exhibited the highest expansion. Knife River and Harris gained mass during the test and expanded the least amount. No correlation seemed to exist for Blackrock or Labarge because the group their expansion value placed them in was different than the grouping from their mass change signature.

5.2 Field Specimens

A total of 28 large-scale field specimens comprise an ASR field site in Laramie. These blocks represent the eight Wyoming aggregates tested and a control nonreactive aggregate used to test environmental conditions. Each pit is represented by a minimum of two unboosted and one boosted specimen. Results are taken as the average of the unboosted and boosted specimens separately. Each individual data point is developed as the average of 12 measurement locations on the given specimen as shown in Figure 21.

Based on field performance, the eight Wyoming aggregates are classified as nonreactive and potentially reactive. Harris Pit and Devries Farm are classified as nonreactive, while Black Rock, Goton, Knife River, Labarge, Lamax and Worland are potentially reactive. Test results to date are represented as a function of time in Figure 36 and Figure 37. These graphs are by reactivity and boosting condition.

Potentially reactive aggregates have greater expansions. In Figure 36, boosted expansions are consistently higher than unboosted. Classifications are based on the unboosted state. All specimens will continue to be monitored.

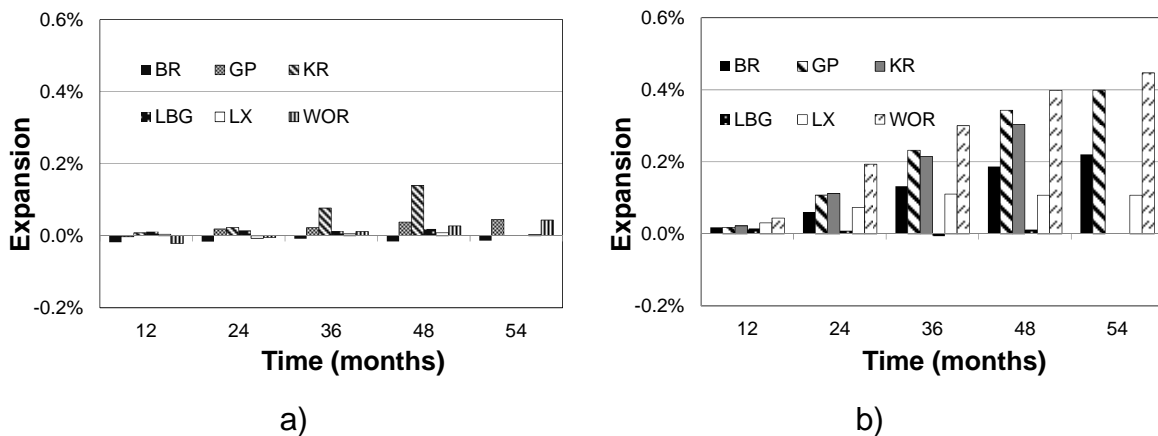


Figure 36. Potentially Reactive Aggregates – a) Unboosted b) Boosted.

Unboosted nonreactive aggregates show an average initial compression. While the control field block is two years old, it has been included for comparison purposes only.

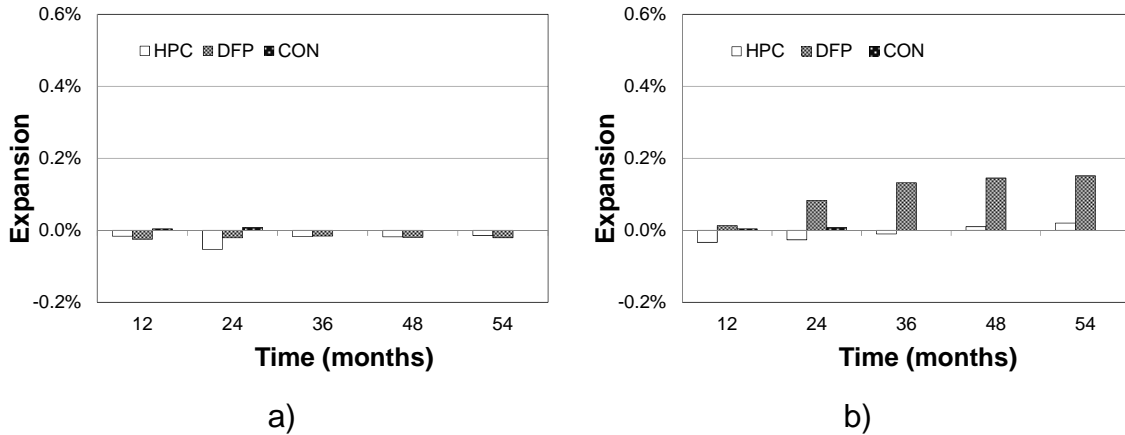


Figure 37. Nonreactive Aggregates – a) Unboosted b) Boosted.

5.3 Petrography Results

Selected specimens from accelerated laboratory tests and cores from outdoor field specimens were sent to DRP Consulting Inc. for examination. Each specimen was analyzed according to ASTM C 856 to evaluate the presence and severity of ASR. The visual description and reactive components of each aggregate are summarized in Table 13. Table 14 summarizes the rankings that describe each ASR level. Appendix D contains a summary of the petrographic report.

Table 13. Visual description of each aggregate.

Aggregate	Reactive Components (decreasing reactivity)	Other Components (decreasing abundance)
BR	Rhyolite, Granitic Rocks	Rhyolite, Andesite, Quartzite, Limestone, Basalt, Granitic to Dioritic Rocks
DFP	Rhyolite, Granitic Rocks, Quartzite	Rhyolite, Andesite, Quartzite, Quartz*, Feldspar*, Minor Granitic Rocks*, Chert*, Limestone*
GP	Rhyolite, Granitic Rocks, Quartzite	Rhyolite, Granite, Quartzite, Andesite, Chert, Quartz*, Feldspar*, Limestone*
HPC	Granite, Rhyolite, Quartzite	Limestone, Granitic Rocks, Andesite, Quartzite, Rhyolite, Basalt
KR	Granite, Rhyolite, Quartzite	Granitic Rocks, Rhyolite
LBG	Granite, Quartzite	Granitic Rocks, Quartzite
LX	Rhyolite, Granite, Quartzite	Rhyolite, Andesite, Quartzite, Granite, Limestone, Dioritic
WOR	Rhyolite, Quartzite, Granite	Rhyolite, Quartzite, Andesite, Granite, Limestone

* Fine Aggregate Only

Table 14. Scale used to determine the severity of ASR.

ASR Presence Ranking	Description
None	No evidence of ASR.
Negligible	Reaction rims abundant; no micro cracking linked to ASR observed.
Minor	Reaction rims observed, rare microcracks associated with ASR; gel deposits occasionally present.
Moderate	Microcracks filled with ASR commonly cut paste; deposits of gel commonly observed in voids.
Severe	Macroscopic cracks and microcracks filled with ASR gel commonly observed; abundant reaction rims and gel deposits in voids commonly observed.

A comparison of CPT, AMBT, and petrographic analysis is shown in Figure 38 with corresponding error bars for each accelerated test method. Table 15 and 16 summarize the petrographic conclusions for AMBT and CPT specimens, respectively. For the AMBT, all eight aggregates were classified as reactive by laboratory methods and these results were validated by

petrographic analysis. For the CPT, only half of the laboratory results agreed with the petrographic classification. Those aggregates that did not agree include: BR, GP, KR and WOR.

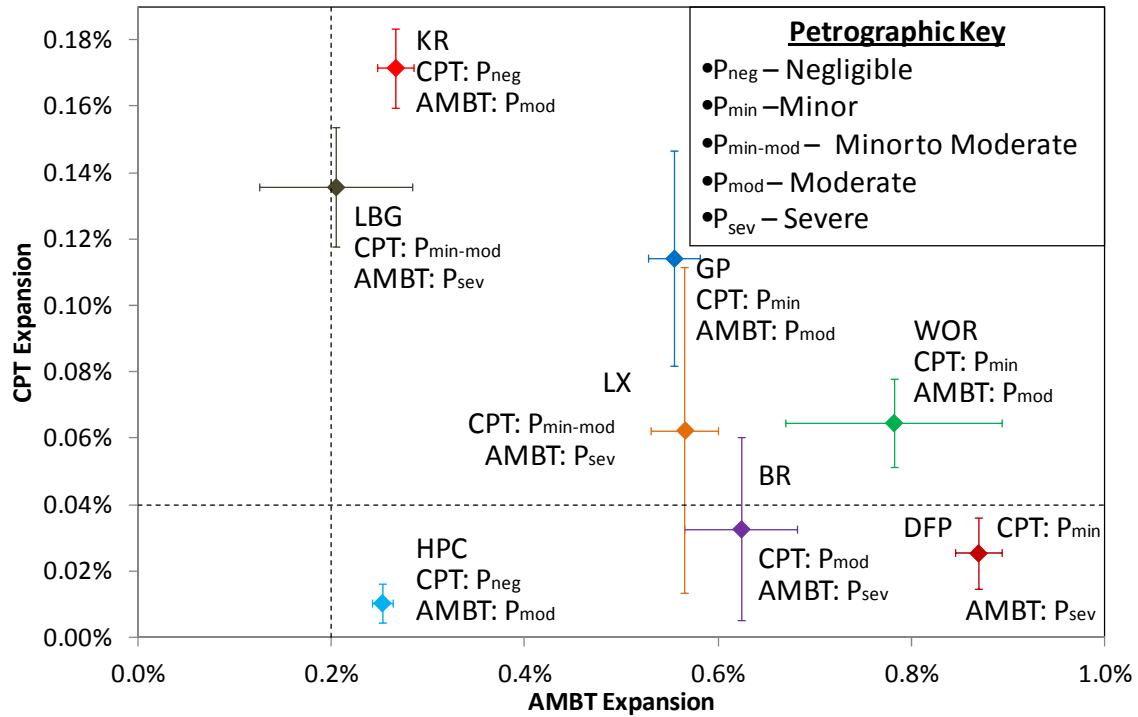


Figure 38. Comparison of the CPT and the AMBT expansions with error bars for each aggregate.

Table 15. AMBT laboratory reactivity classifications versus petrographic classification.

Aggregate Source	Laboratory Classification	Petrographic Classification
BR	reactive	severe
DFP	reactive	severe
GP	reactive	moderate
HPC	reactive	moderate
KR	reactive	moderate
LBG	reactive	severe
LX	reactive	severe
WOR	reactive	moderate

Table 16. CPT laboratory reactivity classifications versus petrographic classification.

Aggregate Source	Laboratory Classification	Petrographic Classification
BR	nonreactive	moderate
DFP	nonreactive	minor
GP	reactive	minor
HPC	nonreactive	negligible
KR	reactive	negligible
LBG	reactive	minor to moderate
LX	reactive	minor to moderate
WOR	reactive	minor

Petrographic analysis of two year old cores extracted from unboosted field specimens revealed little ASR expansion. This is attributed to the early age and location of the core. Cores were extracted after two years of exposure. Field specimen expansion starts at the top of each block and moves downward. This is corroborated by the fact that top expansions are routinely larger than side or bottom expansions. Because the cores were extracted from the bottom of one side, it is logical that there was no evidence of gel formation.

An additional set of cores were removed from BR, GP, KR, LBG, LX and WOR field specimens after five years of exposure. Extraction occurred in top side of unboosted field blocks. BR cores had no evidence of ASR and the remaining five had reaction rims present around the coarse aggregate. Next the specimens were exposed to a moderate temperature of 40°C (105°F) and 100 percent relative humidity for 72 hours. At this time, white exudations consistent with ASR gel appeared in all six cores. Thus, continued ASR expansion is expected as time progresses.

5.4 Discussion of Results

Aggregates from eight different sources in Wyoming were subjected to the Concrete Prism Test (CPT), the Accelerated Mortar Bar Test (AMBT), the Kinetic Method, and a modified Chinese Accelerated Mortar Bar Test (CAMBT). Large scale field specimens were cast as real-time expansion measurement or the most accurate indicator of reactivity.

5.4.1 Accelerated test methods

Each accelerated test method has advantages and disadvantages. Because ASTM classifications are based on a single limit, when aggregates are close to this limit results can be difficult to interpret. The research team followed the Canadian standard for CPT testing and used a moderately reactive classification. For example, when CPT test data was between 0.04 and 0.12 percent aggregates are moderately reactive (Ideker et al. 2010). Likewise, ASTM C1260 defines an intermediate category when ABMT expansions are between 0.1 and 0.2 percent. A failure ratio was calculated to compare measured expansions with limits of the appropriate ASTM standards. When the ratio is less than one, an aggregate passes a particular test. When CPT failure ratios exceed three, an aggregate clearly fails the test. Ratios between one and three correspond to a moderately reactive aggregate. In the same sense a failure ratio of two or greater indicates a reactive aggregate for the AMBT.

Table 17. Measured CPT expansions and failure ratios for each aggregate.

Pit	Expansion				Average	Standard Deviation	Average Failure Ratio
	Specimen						
	1	2	3	4			
BR	0.011%	0.021%	0.026%	0.073%	0.033%	0.00024	0.82
DFP	0.026%	0.021%	0.015%	0.040%	0.026%	0.00009	0.64
GP	0.081%	0.110%	0.159%	0.107%	0.114%	0.00028	2.86
HPC	0.013%	0.012%	0.015%	0.002%	0.011%	0.00005	0.26
KR	0.184%	0.165%	0.158%	0.179%	0.172%	0.00010	4.29
LBG	0.153%	0.148%	0.115%	0.127%	0.136%	0.00015	3.39
LX	0.046%	0.043%	0.135%	0.026%	0.063%	0.00043	1.56
WOR	0.045%	0.070%	0.071%	0.073%	0.065%	0.00011	1.62

Table 18. Measured AMBT expansions and failure ratios for each aggregate.

Pit	Casting	Expansion					Average Failure Ratio
		Specimen			Average	Standard Deviation	
		1	2	3			
BR	1	0.551%	0.591%	0.584%	0.575%	0.00017	6.18
	2	0.591%	0.597%	0.561%	0.583%	0.00016	
	3	0.699%	0.730%	0.709%	0.713%	0.00013	
	4	0.621%	0.665%	0.579%	0.622%	0.00035	
	5	0.651%	0.550%	0.553%	0.585%	0.00047	
	6	0.645%	0.585%	0.669%	0.633%	0.00035	
DFP	1	0.887%	0.907%	0.855%	0.883%	0.00021	8.69
	2	0.861%	0.879%	0.849%	0.863%	0.00012	
	3	0.888%	0.888%	0.869%	0.882%	0.00009	
	4	0.854%	0.816%	0.873%	0.848%	0.00024	
GP	1	0.554%	0.539%	0.538%	0.544%	0.00007	5.54
	2	0.521%	0.545%	0.561%	0.542%	0.00016	
	3	0.538%	0.599%	0.594%	0.577%	0.00028	
HPC	1	0.253%	0.240%	0.231%	0.241%	0.00009	2.52
	2	0.256%	0.258%	0.256%	0.257%	0.00001	
	3	0.258%	0.251%	0.267%	0.259%	0.00007	
KR	1	0.280%	0.285%	0.292%	0.286%	0.00005	2.67
	2	0.259%	0.257%	0.283%	0.266%	0.00012	
	3	0.260%	0.246%	0.239%	0.248%	0.00009	
LBG	1	0.225%	0.242%	0.227%	0.231%	0.00008	2.04
	2	0.280%	0.277%	0.282%	0.280%	0.00002	
	3	0.106%	0.106%	0.095%	0.102%	0.00005	
LX	1	0.545%	0.523%	0.524%	0.531%	0.00010	5.66
	2	0.563%	0.623%	0.581%	0.589%	0.00025	
	3	0.591%	0.597%	0.543%	0.577%	0.00024	
WOR	1	0.832%	0.882%	0.923%	0.879%	0.00037	7.81
	2	0.813%	0.869%	0.777%	0.820%	0.00038	
	3	0.605%	0.647%	0.685%	0.646%	0.00033	

Table 19. Measured CAMBT expansions and failure ratios for each aggregate.

Pit	Expansion				Average Failure Ratio	
	Specimen			Average		Standard Deviation
	1	2	3			
BR	0.242%	0.264%	0.292%	0.266%	0.00020	2.86
DFP	0.312%	0.294%	0.310%	0.305%	0.00008	3.28
GP	0.335%	0.295%	0.321%	0.317%	0.00017	3.40
HPC	0.154%	0.138%	0.142%	0.145%	0.00007	1.56
KR	0.158%	0.140%	0.162%	0.153%	0.00010	1.65
LBG	0.178%	0.178%	0.186%	0.181%	0.00004	1.94
LX	0.294%	0.278%	0.302%	0.291%	0.00010	3.13
WOR	0.288%	0.274%	0.268%	0.277%	0.00008	2.97

Because both ABMT and CAMBT provide an unlimited supply of alkalis, all eight aggregate sources failed those tests. Aggregates performed quite differently in the CPT test and the preliminary classification is based on this test. While average expansions for BR, DFP and HPC meet the 0.04 percent limit, one of the BR specimens exhibited expansion of 0.073 percent which corresponds to an individual failure ratio of 1.8. As a result this aggregate is classified as potentially reactive based on accelerated test methods. Additional testing of BR is underway to determine if this is an isolated incident. Data at 11.5 months indicates this aggregate is moderately reactive. LX and WOR are also moderately reactive. GP, KR and LBG are clearly reactive based on all three accelerated test methods.

Table 20. Aggregate classification based on accelerated test methods.

Aggregate	Classification based on CPT	Classification based on ABMT and CABMT	Accelerated methods classification
BR	NR/MR	R	MR
DFP	NR	R	NR
GP	R	R	MR
HPC	NR	R	NR
KR	R	R	R
LBG	R	R	R
LX	MR	R	MR
WOR	MR	R	R

NR=Nonreactive; MR=Moderately reactive; PR=Potentially reactive; R=Reactive
 NR* - Average test results were below the expansion limit but one data point fell above the limit. Additional studies are ongoing to further evaluate this aggregate source.

Standard deviations for each test vary based on aggregate and test method as illustrated in Figure 27, Figure 31 and Figure 34. Summaries of these values are recorded in Table 17-Table 19. CPT data is the standard deviation of four specimens; ABMT values are based on 9-12 specimens; and CAMBT values are based on three specimens. Also, the deviations are higher than typically expected because the deflections are very small. A plot of standard deviations for expansions of each aggregate is shown in Figure 39. Clearly mortar bars have the largest variation and the CAMBT test has the least variation. This may be attributed to the limited aggregate size used in the CAMBT test. It is interesting to note that the smallest variations occurred in HPC (nonreactive) and KR aggregates (highly reactive). Using five or more specimens for each calculation would be better than using either three or four as specified by the respective ASTM standards.

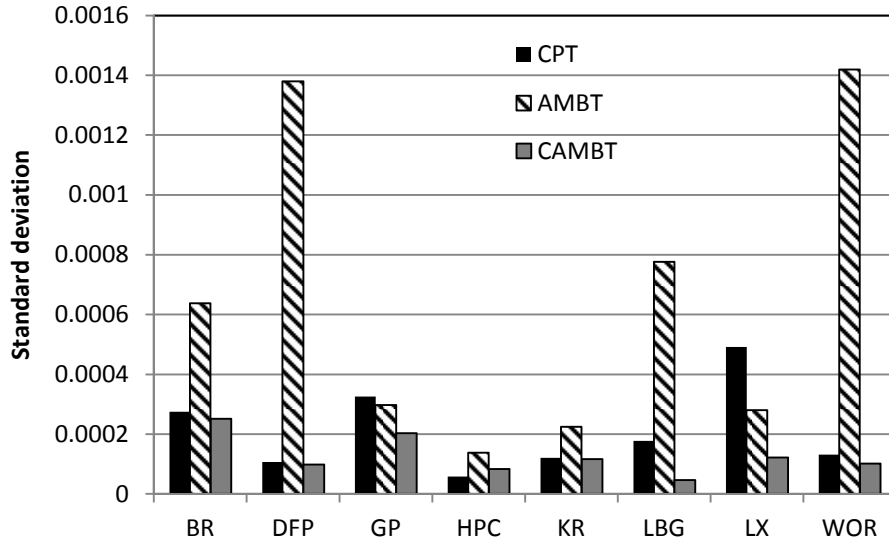


Figure 39. Standard deviation values versus accelerated test method.

5.4.2 Field specimen results

Field specimen results are available through the first 4.5 years (54 months). Data is presented in terms of boosted and unboosted; as expected, boosted specimens exhibit higher expansions. Measured field expansions are summarized in Table 21 and plotted in Figure 40. Preliminary limits have been applied to both figures in an attempt to better classify the aggregates reactivity using categories of nonreactive, moderately reactive, and reactive. Due to the magnitude of expansions, classifications will be based on boosted limits which accelerate expansion. Final classification should be based on unboosted specimens, however this requires sufficient time. At five years, limits of 0.1 percent between nonreactive and moderately reactive and 0.3 percent between moderately reactive and reactive are applied to boosted specimens as shown by solid black lines in Figure 38b.

Using these proposed limits for boosted specimens, Goton, Knife River and Worland aggregates are reactive; Black Rock, Devries Farm, and Lamax are moderately reactive; and Labarge and Harris Pit are nonreactive. One half of the boosted limits were applied to unboosted specimens for limits of 0.05 percent and 0.15 percent at five years, Figure 38a. Unboosted Knife River is reactive, while the others remain nonreactive. Goton Pit and Worland specimens approach

moderate reactivity and may be exceed this limit after five years. These preliminary limits should be verified with other field specimen data.

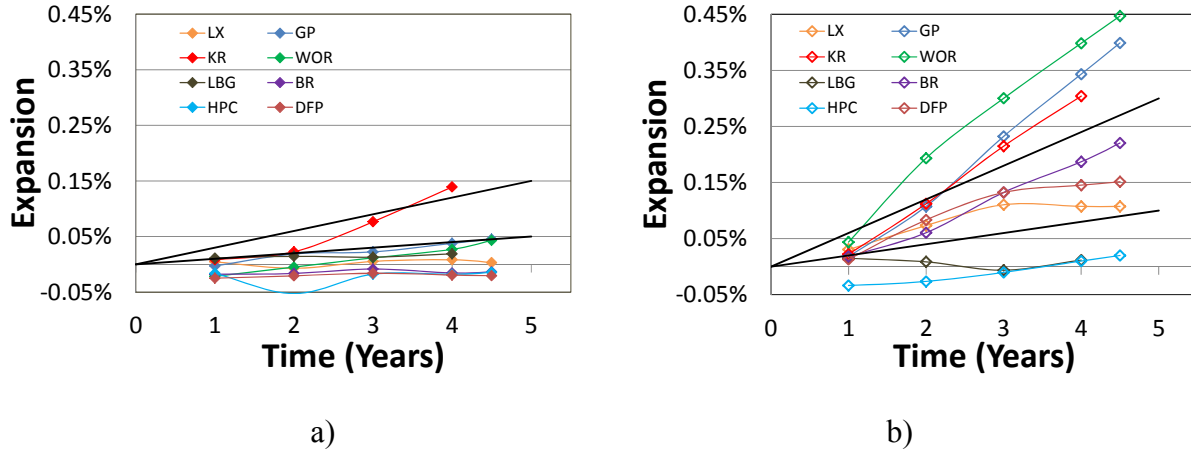


Figure 40. Expansion Limits for Field Specimens – a) Unboosted and b) Boosted.

A minimum of two replicates exist for all unboosted specimens. In most cases, both specimens have similar expansions. This is not the case for KR and WOR. Two KR specimens exceed 0.25 percent while the third is 0.054 percent. One WOR specimen has approximately 4 times the expansion of an identical specimen as shown in Figure 41. Future expansions will be closely monitored to better classify these inconsistencies in the field specimens.

Table 21. Expansions after 4-5 years of exposure.

Aggregate	Time (months)	Unboosted field specimen 1 or 3	Unboosted field specimen 2 or 5	Boosted field specimen
BR	56	-0.0103% -0.0239%	-0.0034% -0.0144%	0.3367% (54) 0.1044% (54)
DFP	56	-0.0319%	-0.0097%	0.1514%
GP	54	0.0419%	0.0472%	0.3989% (54)
HPC	56	-0.0042%	-0.0223%	0.0199% (54)
KR	56	0.0540% 0.2513%	0.2420% (52)	0.3353% (52)
LBG	44	0.0179%	0.0157%	0.0055%
LX	56	0.0114%	-0.0037%	0.1074% (54)
WOR	56	0.0188%	0.0782%	0.4468% (54)

NR=Nonreactive; MR=Moderately reactive; R=Reactive; PR=Potentially reactive.

*All time intervals are that of column 2 unless noted within parenthesis following expansion results.

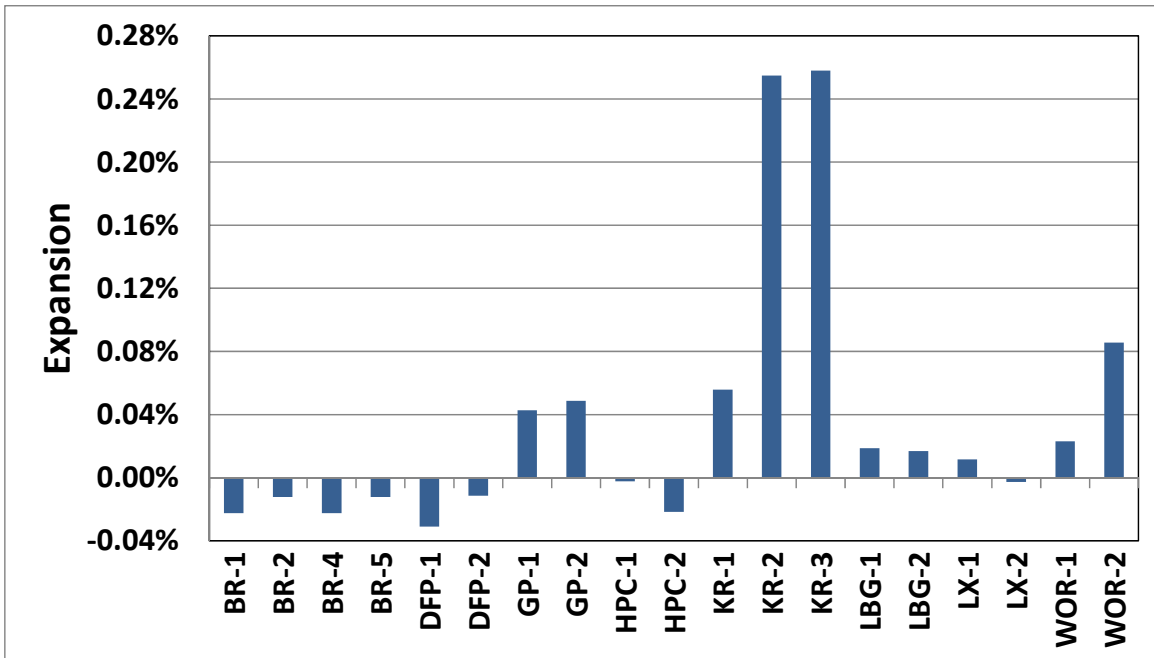


Figure 41. Expansion to date of unboosted field specimens.

5.4.3 Final classifications

As expected, results do not always agree. Because the CPT and field specimen expansions are the closest to field performance a summary is provided in **Error! Reference source not found.** When the average or maximum unboosted field specimen expansion is less than 0.01 percent at five years the source is labeled nonreactive. By the same token when either of these values exceeds 0.04 percent the source is deemed reactive. All other cases are moderately reactive. In the event of differing classification between CPT and field specimen results, the more severe classification becomes the final classification. The two indicators were in agreement for the following five aggregate sources: DFP; HPC; KR; LX; and WOR.

Table 22. Final classification of each aggregate source.

Aggregate	Average unboosted field specimen expansion	Maximum unboosted field specimen expansion	Field specimen classification	CPT classification	Final classification
BR	-0.013%	-0.0034%	MR	MR	MR
DFP	-0.0208%	-0.0097%	MR	NR	NR
GP	-0.0456%	0.0472%	R	MR	R
HPC	-0.0133%	-0.0042%	NR	NR	NR
KR	0.181%	0.251%	R	R	R
LBG	0.0168%	0.0179%	NR	R	R
LX	0.00385%	0.0114%	MR	MR	MR
WOR	0.0485%	0.0782%	R	R	R

5.4.4 Rate of Reaction

The research team knows of few studies related to rate of reaction. As a result, rate calculations and comments are presented herein. Although the CPT reactivity classification is based solely on the total expansion at one year, the behavior of the aggregates during the course of the test can also offer valuable information. Figure 42 shows the expansion rates for the tested aggregates, neglecting the expansion behavior before day 28 because of the variability associated with the CTE that resulted in negative expansion values for this period. Smooth lines were used in the plot to aid in readability, but they are not meant to represent any assumptions made about the data. The vertical axis represents the instantaneous expansion rate, given in units of relative expansion times 10^6 per day.

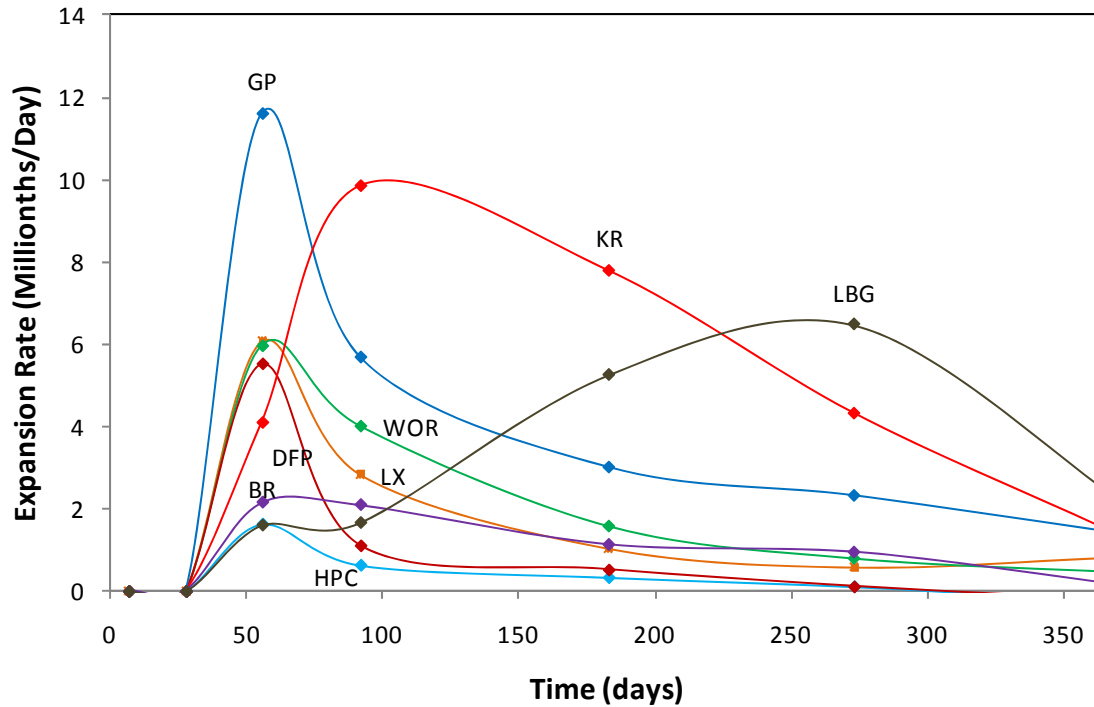


Figure 42. Expansion rates for eight aggregates subjected to the CPT.

Magnitudes of the expansion rates are vastly different. Goton reaches a maximum rate of nearly 12 millionths of expansion per day, and Harris does not even reach two millionths per day. The areas under the curves are also vastly different. Some of the expansion rates drop off sharply after reaching their maximum values. Others, like Knife River and Labarge, maintain an elevated expansion rate for an extended period, which is the key factor in their higher total expansion. Also of interest is the time at which the maximum expansion rate is attained. For most of the aggregates this occurs around day 56, but Knife River and Labarge reach their maximum rates around day 92 and 273 respectively. This delay of peak expansion rate suggests that Knife River and Labarge might be slowly reacting aggregates.

Because GP, KR and LBG may be slowly reacting aggregates based on CPT expansions, a similar analysis was performed for field specimen expansions. The rate of change of expansion is illustrated in Figure 43. Positive trend lines indicate that the specimens are continuing to expand. The research team will continue to monitor this data.

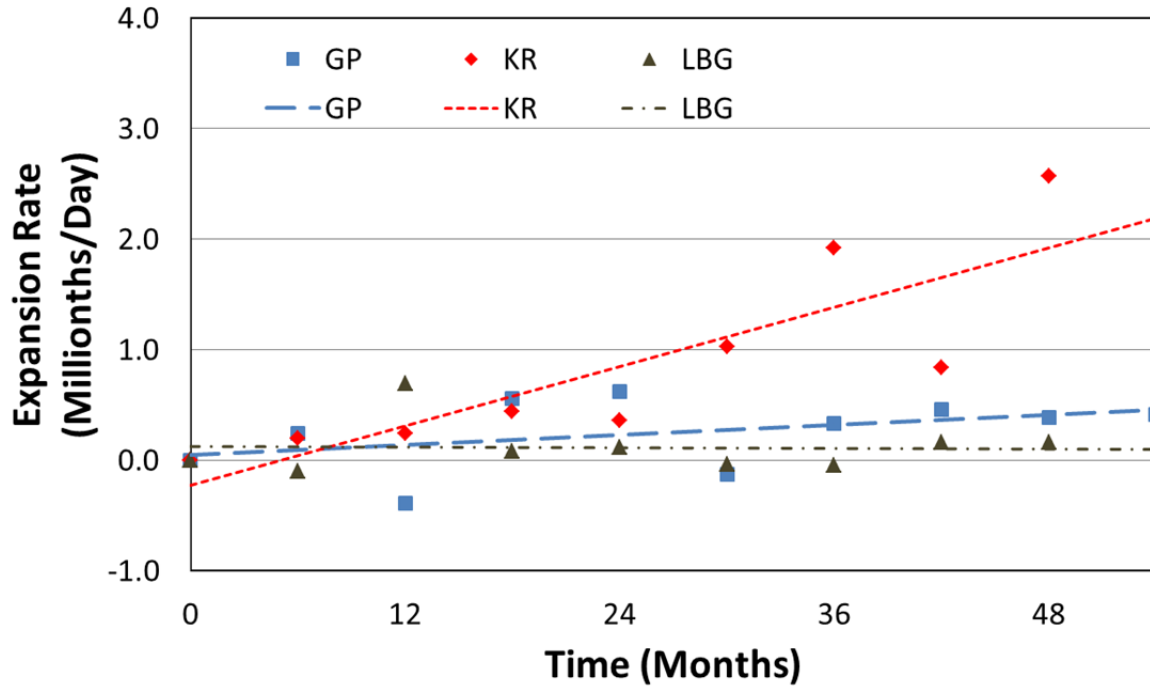


Figure 43. Rate of expansion for unboosted field specimens.

Chapter 6 Conclusions and Recommendations

A comprehensive study was performed to evaluate multiple accelerated test methods and real-time field specimens to determine the ASR potential in eight Wyoming aggregates. Because each test method has unique advantages and disadvantages, results do not always agree. It is not surprising that all eight aggregates failed both the AMBT and CAMBT tests because these methods provide an unlimited supply of alkalis during the test. The CPT is the most reliable accelerated test method and it considers the combined effect of coarse and fine aggregates. A clear disadvantage to this test method is the one-year duration for unmitigated concrete. While field specimen results are the closest to real-life performance, the testing duration can be up to 10 years.

A final classification of aggregates is based on combined CPT and real-time field block specimens because they are the two most accurate methods to predict expansion. Three levels of reactivity exist: reactive (R); moderately reactive (MR); and nonreactive (NR). Goton, Knife River and Worland are classified as reactive in the accelerated test methods and field specimen results. Labarge is also reactive based on the CPT results. Lamax is moderately reactive based on both indicators. Blackrock is conservatively classified as moderately reactive. Harris Pit was always among the least reactive aggregates in each test and is nonreactive. Although, Devries Farm showed relatively high reactivity in the other tests, it is classified as nonreactive because of the consistent behavior in CPT expansions. The severity of AMBT and CAMBT methods further justifies this conclusion.

No mitigation is recommended when using Harris Pit Cody or Devries Farm aggregates. WYDOT should continue CPT testing for Wyoming aggregates used in highway construction projects. A study using fly ash to mitigate ASR in moderate and highly reactive aggregates is currently underway at UW. Presently Goton, Knife River and Worland aggregates should be used with caution. If other options are limited, mitigation using supplementary cementitious materials (SCMs) or lithium treatments is recommended. It must be noted that lithium is a more costly mitigation strategy. Fly ashes used in WYDOT projects should undergo testing to ensure

effective mitigation. This can be in the form of testing the fly ash or testing the concrete mixture including fly ash using ASTM C1567.

When mitigating using SCMs, a minimum level is required to reduce expansion. Above this level, expansions decrease with increasing levels of SCMs (ACI 2008, Fournier 2000, Malvar 2002, Thomas). Additionally, there is a maximum level of SCMs that can be used to provide functional concrete. Preliminary results of C1567 testing at UW indicate that Knife River aggregates can be mitigated using a 25 percent fly ash replacement using Craig fly ash supplied by WYDOT. A data base of field performance that quantifies the aggregate, age, cement type and mitigation methods should be developed.

A more rapid test method should be sought to replace ASTM C1293. Although other investigators have worked on a 60 day replacement for this test method, there are still cases of misidentified aggregates (Fournier et al. 2004, Touma et al. 2001). Current work at UW focuses on a promising method using an autoclave for accelerating the CPT testing process.

References

Cited and Referenced Standards

1. ASTM C1260, Standard Test Method for Potential Alkali Reactivity of Aggregates (Mortar-Bar Method). *ASTM International*, 2007
2. ASTM C1293, Standard Test Method for Determination of Length Change of Concrete Due to Alkali-Silica Reaction. *ASTM International*, 2008
3. ASTM C289, Standard Test Method for Potential Alkali-Silica Reactivity of Aggregates (Chemical Method). *ASTM International*, 2008
4. ASTM C33, Standard Specifications for Concrete Aggregates. *ASTM International*, 2013
5. ASTM C856, Standard Practice for Petrographic Examination of Hardened Concrete. *ASTM International*, 2011

Cited References

1. ACI (2008). State-of-the-Art Report on Alkali-Aggregate Reactivity-ACI 221.1R-98(2008). *ACI manual of concrete practice*. Detroit, Mich.: 221.
2. Avrami, M. (1939). "Kinetics of Phase Change. I General Theory." *The Journal of Chemical Physics* 7(12): 1103-1112.
3. Avrami, M. (1940). "Kinetics of Phase Change. II Transformation-Time Relations for Random Distribution of Nuclei." *The Journal of Chemical Physics* 8(2): 212-224.
4. Avrami, M. (1941). "Granulation, Phase Change, and Microstructure - Kinetics of Phase Change III." *The Journal of Chemical Physics* 9(2): 177-184.
5. Berliner, R., Popovici, M., Herwig, K. W., Berliner, M., Jennings, H. M. and Thomas, J. J. (1998). "Quasielastic Neutron Scattering Study of the Effect of Water-to-Cement Ratio on the Hydration Kinetics of Tricalcium Silicate." *Cement and Concrete Research* 28(2): 231-243.
6. Chatterji, S. (2005). "Chemistry of alkali-silica reaction and testing of aggregates." *Cement and Concrete Composites* 27(7-8): 788-795.
7. Choktaweekarn, P. and Tangtermsirikul, S. (2009). "A model for predicting the coefficient of thermal expansion of cementitious paste." *ScienceAsia* 35(5): 57-63.
8. Cornell, B. D. (2002). "Laboratory investigations of alkali silica reaction using the concrete prism test and its modifications". Austin, Texas, University of Texas at Austin.
9. Diamond, S. (1989). ASR - Another look at mechanisms. *8th International Conference on Alkali-Aggregate Reaction in Concrete*, Kyoto, Japan.
10. Fan, S. and Hanson, J. M. (1998). "Length Expansion and Cracking of Plain and Reinforced Concrete Prisms due to Alkali-Silica Reaction." *ACI Materials Journal* 95(4): 480-487.
11. Farny, J. A., Kosmatka, S. H. and Association, P. C. (1997). Diagnosis and control of alkali-aggregate reactions in concrete. Skokie, Ill., Portland Cement Association.
12. Fournier, B. and Berube, M. A. (2000). "Alkali-aggregate reaction in concrete: a review of basic concepts and engineering implications." *Canadian Journal of Civil Engineering* 27(2): 167-191.
13. Fournier, B., Chevrier, R., de Grosbois, M., Lisella, R., Folliard, K., Ideker, J., Shehatad, M., Thomas, M. and Baxter, S. (2004). The Accelerated Concrete Prism Test (60°C):

- Variability of the Test Method and Proposed Expansion Limits. *12th International Conference on Alkali-Aggregate Reaction in Concrete*, Beijing, China.
14. Fournier, B., Nkinamubanzi, P.-C., Lu, D., Thomas, M. D. A., Folliard, K. J. and Ideker, J. H. (2006). Evaluating potential alkali-reactivity of concrete aggregates, how reliable are the current and new test methods. Marc-Andre Berube *Symposium on Alkali-Aggregate Reactivity in Concrete*, CANMET, Ottawa.
 15. Grattan-Bellew, P. E., Lu, D., Fournier, B. and Mitchell, L. (2004). Mass Change, Petrography and Damage Ratings of Bars at the Completion of the Concrete Microbar Test. *12th International Conference on Alkali-Aggregate Reaction in Concrete*, Beijing, China.
 16. Hooton, R. D. (1996). Recent developments in testing for ASR in North America. *10th International Conference on Alkali-Aggregate Reaction in Concrete*.
 17. Hooton, R. D. and Rogers, C. A. (1993). "Development of the NBRI rapid mortar bar test leading to its use in North America." *Construction and Building Materials* 7(3): 145-148.
 18. Ideker, J., East, B., Folliard, K., Thomas, M. and Fournier, B. (2010). "The Current State of the Accelerated Concrete Prism Test." *Cement and Concrete Research* 40: 550-555.
 19. Johnston, D. (1994). Interpretation of Accelerated Test Method ASTM P124 Test Results. Transportation Research Record. Washington, D.C., National Research Council: 129-134.
 20. Johnston, D. and Fournier, B. (2000). A kinetic-based method for interpreting accelerated mortar bar test (ASTM C1260) data. *11th International Conference on Alkali-Aggregate Reaction*, Quebec.
 21. Johnston, D. P., Stokes, D. B., Fournier, B. and Surdahl, R. W. (2004). Kinetic Characteristics of ASTM C1260 Testing and ASR-induced Concrete Damage. *12th International Conference on Alkali-Aggregate Reactivity*, Beijing, China.
 22. Kosmatka, S. H., Kerkhoff, B. and Panarese, W. (2002). *Design and Control of Concrete Mixtures*. Skokie, IL, Portland Cement Association.
 23. Lane, D. S. (1999). "Comparison of Results from C441 and C1293 with Implications for Establishing Criteria for ASR-Resistant Concrete." *Cement, Concrete, and Aggregates, CCAGDP* 21(2): 149-156.
 24. Leemann, A., Lothenbach, B. and Thalmann, C. (2010). "Influence of superplasticizers on pore solution composition and on expansion of concrete due to alkali-silica reaction." *Construction and Building Materials*.
 25. Lu, D., Fournier, B. and Grattan-Bellew, P. E. (2006). "Evaluation of accelerated test methods for determining alkali-silica reactivity of concrete aggregates." *Cement and Concrete Composites* 28(6): 546-554.
 26. Lu, D., Fournier, B., Grattan-Bellew, P. E., Xu, Z. and Tang, M. (2007). "Development of a universal accelerated test for alkali-silica and alkali-carbonate reactivity of concrete aggregates." *Materials and Structures* 41(2).
 27. Lu, D., Mei, L., Xu, Z., Tang, M. and Fournier, B. (2006). "Alteration of alkali reactive aggregates autoclaved in different alkali solutions and application to alkali-aggregate reaction in concrete: (I) Alteration of alkali reactive aggregates in alkali solutions." *Cement and Concrete Research* 36(6): 1176-1190.
 28. Malvar, L. J., Cline, G. D., Burke, D. F., Rollings, R., Sherman, T. W., Greene, J. L. (2002). "Alkali-Silica Reaction Mitigation: State of the Art and Recommendations." *ACI Materials Journal*: 480-489.

29. Mielenz, R. C., Greene, K. T. and Benton, E. J. (1948). "Chemical Test for Reactivity of Aggregates with Cement Alkalies: Chemical Processes in Cement-Aggregate Reaction." *ACI Proceedings* 44: 193-219.
30. Ming-shu, T., Su-fen, H. and Shi-hua, Z. (1983). "A rapid method for identification of alkali reactivity of aggregate." *Cement and Concrete Research* 13(3): 417-422.
31. Mo, X., Zhang, Y., Yu, C., Deng, M., Tang, M., Hunger, K. J. and Fournier, B. (2010). "Investigation of Alkali-Silica Reaction Inhibited by New Lithium Compound." *ACI Materials Journal* 107(1): 37-41.
32. Morgan, P. H., Mercer, P. L. and Flodin, N. W. (1975). "General model for nutritional responses of higher organisms." *Proceedings of the National Academy of Sciences of the United States of America* 72(11): 4327-4331.
33. Oberholster, R. E. and Davies, G. (1986). "An accelerated method for testing the potential alkali reactivity of siliceous aggregates." *Cement and Concrete Research* 16(2): 181-189.
34. Pugh, J. S. (2003). On the ability of accelerated test methods to assess potential for alkali-silica reaction. Austin, Texas, University of Texas at Austin.
35. Rear, K., Meinheit, D. F., Chrest, A. P., Brown, R., Breeze, P. C., Clarke, J. L. F., D'Arcy, T. J., Durning, T., Eddy, D. B., Gami, S. S., Iverson, P. J., Magnesio, C., Nadeau, F. A., Peterson, C. A., Schupack, M. and Walker, H. C. (1994). "Alkali-Aggregate Reactivity: A Summary." *PCI Journal* (Nov-Dec): 26-35.
36. Rivard, P., Bérubé, M.-A., Ollivier, J.-P. and Ballivy, G. (2003). "Alkali mass balance during the accelerated concrete prism test for alkali-aggregate reactivity." *Cement and Concrete Research* 33(8): 1147-1153.
37. Smaoui, N., Berube, M.-A., Fournier, B. and Bissonnette, B. (2004). "Influence of Specimen Geometry, Orientation of Casting Plane, and Mode of Concrete Consolidation on Expansion Due to ASR." *Cement, Concrete, and Aggregates* 26(2): 58-70.
38. Sommer, H., Nixon, P. J. and Sims, I. (2005). "AAR-5: Rapid preliminary screening test for carbonate aggregates." *MATERIALS AND STRUCTURES* 38(8): 787-792.
39. Stanton, T. E. (1940). "Expansion of concrete through reaction between cement and aggregates." *Proceedings of the American Society of Civil Engineers* 66(10): 1781-1811.
40. Stark, D. (1991). The Moisture Condition of Field Concrete Exhibiting Alkali-Silica Reactivity. *CANMET/ACI 2nd International Conference on Durability of Concrete*, Montreal, Canada.
41. Stokes, D. (2006). Concerning the Use of Expansion Data from ASR Testing. *8th CANMET/ACI International Conference on Recent Advances in Concrete Technology*, Montreal, Canada.
42. Thomas, M., Fournier, B., Folliard, K., Ideker, J. and Shehata, M. (2006). "Test methods for evaluating preventive measures for controlling expansion due to alkali-silica reaction in concrete." *Cement and Concrete Research* 36(10): 1842-1856.
43. Thomas, M. "Optimizing the Use of Fly Ash in Concrete." PCA.
44. Touma, W. E., Fowler, D. W., Carrasquillo, R. L., Folliard, K. J. and Nelson, N. R. (2001). "Characterizing Alkali-Silica Reactivity of Aggregates using ASTM C 1293, ASTM C 1260, and Their Modifications." *Transportation Research Record* (1757): 157-165.
45. Xu, Z., Shen, Y. and Lu, D. (1998). "Main parameters in the new test method for alkali-silica reactivity." *Journal of Nanjing University of Chemical Technology* 20(2): 1-7.

46. Zhang, C., Wang, A., Tang, M. and Zhang, N. (1999). "Influence of Dimension on Test Specimen on Alkali-Aggregate Reactive Expansion." *ACI Materials Journal* 96(2): 204-207.

Acknowledgements

Many individuals participated in a six-year study to evaluate the alkali silica reactivity (ASR) of eight Wyoming aggregates. The research team consisted of four graduate students and one post-doctoral researcher working under the supervision of Dr. Jennifer Tanner, Principle Investigator (PI). Ryan Fertig and Angela Jones wrote their theses based on this work and graduated in 2008 and 2011, respectively. Margaret Kimble and Darby Hacker are currently completing MS degrees on the topic of ASR. Dr. Saadet Toker helped to construct field specimens and calibrate our instrumentation system. Numerous undergraduate students worked diligently to create the field exposure site presented in this study.

The Wyoming Department of Transportation (WYDOT) Materials Lab provided support for this project in numerous ways. Mike Reyes and Basil Brookhouser brought countless bags of Wyoming aggregates back to the University of Wyoming (UW). Tracy Quinn and Chris Foster supplied information and trained UW students to use equipment to crush and sieve aggregate. Finally, Rick Harvey and Bob Rothwell made numerous efforts to keep the project moving forward. Without WYDOT support this project would not have been possible.

Appendix A Field Study

From June 15th to August 26th, 2007 the ASR research team visited eight towns in Wyoming to evaluate concrete field conditions related to ASR. The objective was to inspect all concrete roadways and rigorously document all cracking damage. The following towns were inspected:

- Cody (8-2007).
- Greybull (7-2007).
- Lovell (8-2007).
- Powell (8-2007).
- Riverton (6-2007).
- Rock Springs (8-2007).
- Thermopolis (7-2007).
- Worland (7-2007).

To classify the data, an extent-of-damage system was created. Damage ratings vary from 1 to 7.

The damage classifications are designated as follows:

- 1 Very faint lines.
- 2 Faint lines.
- 3 Easily visible lines.
- 4 Cracking (less than 0.03 inches wide).
- 5 Wide cracking (greater than 0.03 inches wide).
- 6 Chipping (small pieces of concrete missing).
- 7 Spalling (pieces of concrete missing greater than 2 inches across).

Blank entries indicate no damage. The sections we investigated are indicated with initials listed in a table at the top of each information sheet. They are as follows:

- G Gutter.
- SW Sidewalk.
- S Street.
- I Intersection.
- C Curb.

A.1 Data Collection

An approximate percentage of damage for each section is listed in each respective damage category. Due to heavy traffic in Riverton, damage listings for Federal Street do not include percentages. The percentages, ranging from “less than 10%” to “100%”, approximate the surface area affected. In addition, the type of cracking is specified. The existing cracks were classified as one of the following: pattern, longitudinal, transverse, and random.

To ensure a complete inspection, all cracks found were documented, whether or not they appeared to be caused by ASR. A street map of each town locates the roadways inspected (Appendix A). A spreadsheet of the recorded damage observations is attached (Appendix B). Over 300 photographs were taken and recorded with their locations (town, street location) to visually document the damage. A summary of 58 of those photos have been burned to a CD. The list of the photos for each town is included (Appendix C).

A.2 Data Analysis

In Riverton, the concrete along Main Street appears to be in very good shape. The lines and cracking observed are only detectable upon very close observation. Federal Street, on the other hand, has been heavily damaged. Classic signs of ASR are visible down the entire length of the road. The majority of the damage is pattern cracking, often with the orientation of predominate cracks being longitudinal. Chipping and spalling is occurring at locations of concentrated cracking, and is especially bad at gutters, drains, and sewer manholes. Portions of the sidewalks along Federal are also displaying signs of ASR, though at an earlier development stage.

In both Greybull and Worland, the majority of the concrete roadways are in good shape. Large cracks present appear to primarily be the result of settling. Chipping and spalling occurs in gutters, most likely as a result of freeze-thaw cycles where large amounts of water collect. Some road surface area, especially in the intersections, displays faint pattern cracking. This is possibly ASR, but if it is it is certainly not well developed. The oldest portions of the road (assumed older because of large amount of wearing) also contain pattern and random lines which appear to be non-detrimental to the surface.

Although the concrete road surfaces in Lowell are quite worn, they do not display signs of ASR damage. Existing cracks are primarily large in size, singular, and appear to be caused by settling and expansion. Cracking around sewer manholes, for example, was documented. Certain sections of sidewalks within the town appear to be damaged by ASR, however, as they display classic pattern cracking. Some cracking is at an accelerated stage and has been extremely destructive to the sidewalk.

Concrete within the town of Powell is in good shape overall. Large street cracks that exist appear to have formed because of large distances between contraction joints (a construction issue rather than a materials issue). It can be concluded that the majority of other cracks have been caused by several other non-ASR related issues. Stress concentrations from traffic lights have created random cracking in sidewalk sections; this is apparent by observing that the cracks radiate from the base of the pole. Settling is also another large source of damage; this is apparent by observing cracked sidewalk slabs that have sunk below the level of the curb. The final major source of damage is caused by freeze-thaw cycles. This predominately occurs at gutter locations, where large amounts of water are collected.

In Rock Springs, the majority of the concrete appears to be in good condition. The concrete roads documented are in fact one road that changes names every so often. Observations were begun at 9th Street, which became Pilot Butte, then Bridger, then Center, and finally Dewar. On Dewar, there is a bridge that spans from Hancock to Black streets. Large transverse and longitudinal cracks were documented on this stretch of road, and are assumed to be caused by deformation of the bridge. The concrete most heavily damaged in this town is in the gutter area. Because this is an area of heavy water collection, it is assumed that the destruction is caused by multiple freeze-thaw cycles.

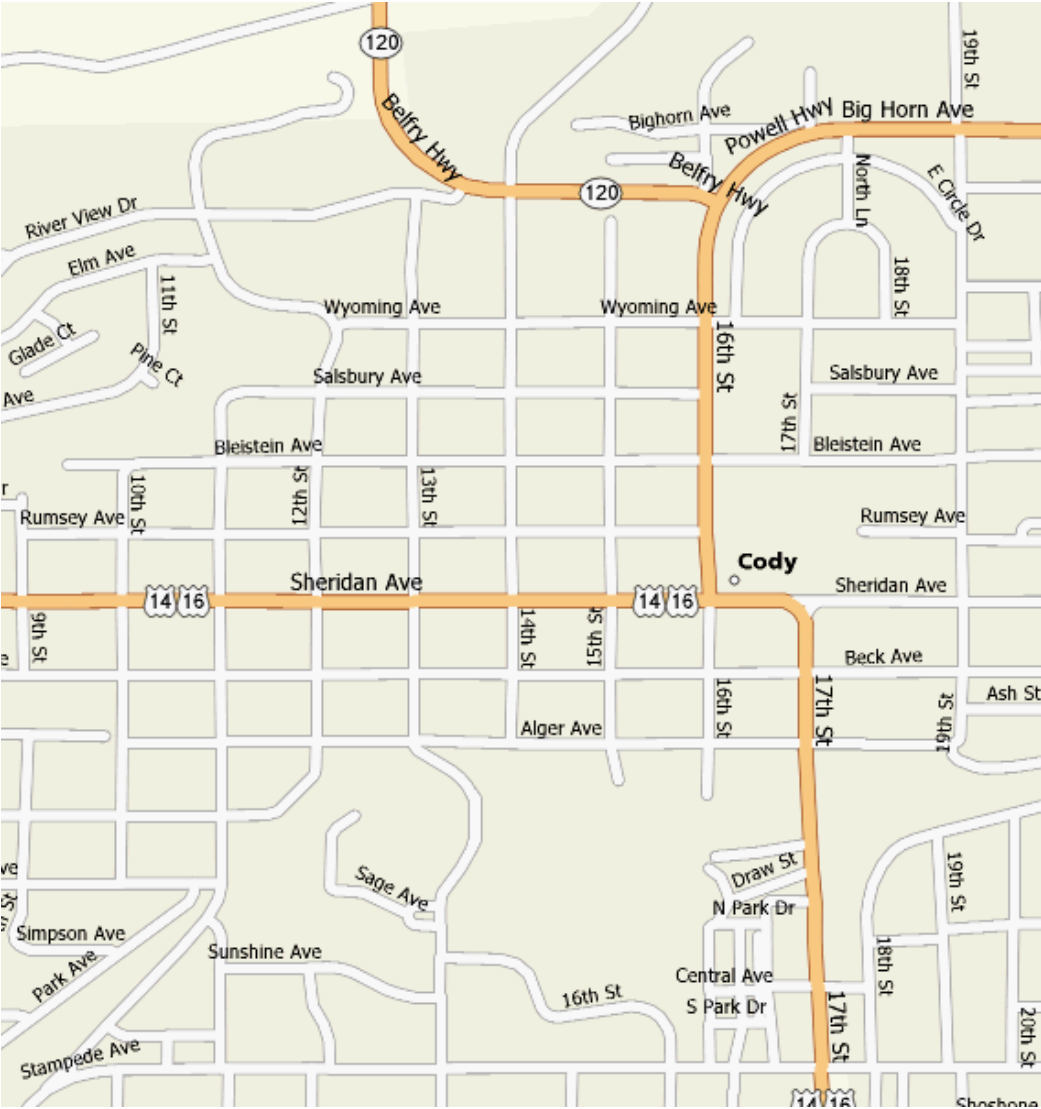
In the town of Thermopolis, US Highway 20 and 789 meet at a concrete intersection. The intersection is in excellent shape, with only faint lines being found on only a small percentage of the surface area. This concrete appears to be fairly new. However, the other concrete road in Thermopolis, which leads into the Hot Springs State Park, is in poor shape. The road appears to be fairly old, and contains large sections marked with pattern and random cracking, possibly

caused by ASR. Transverse cracks on the bridge deck and bridge barriers are assumed to be caused by deformation of the bridge.

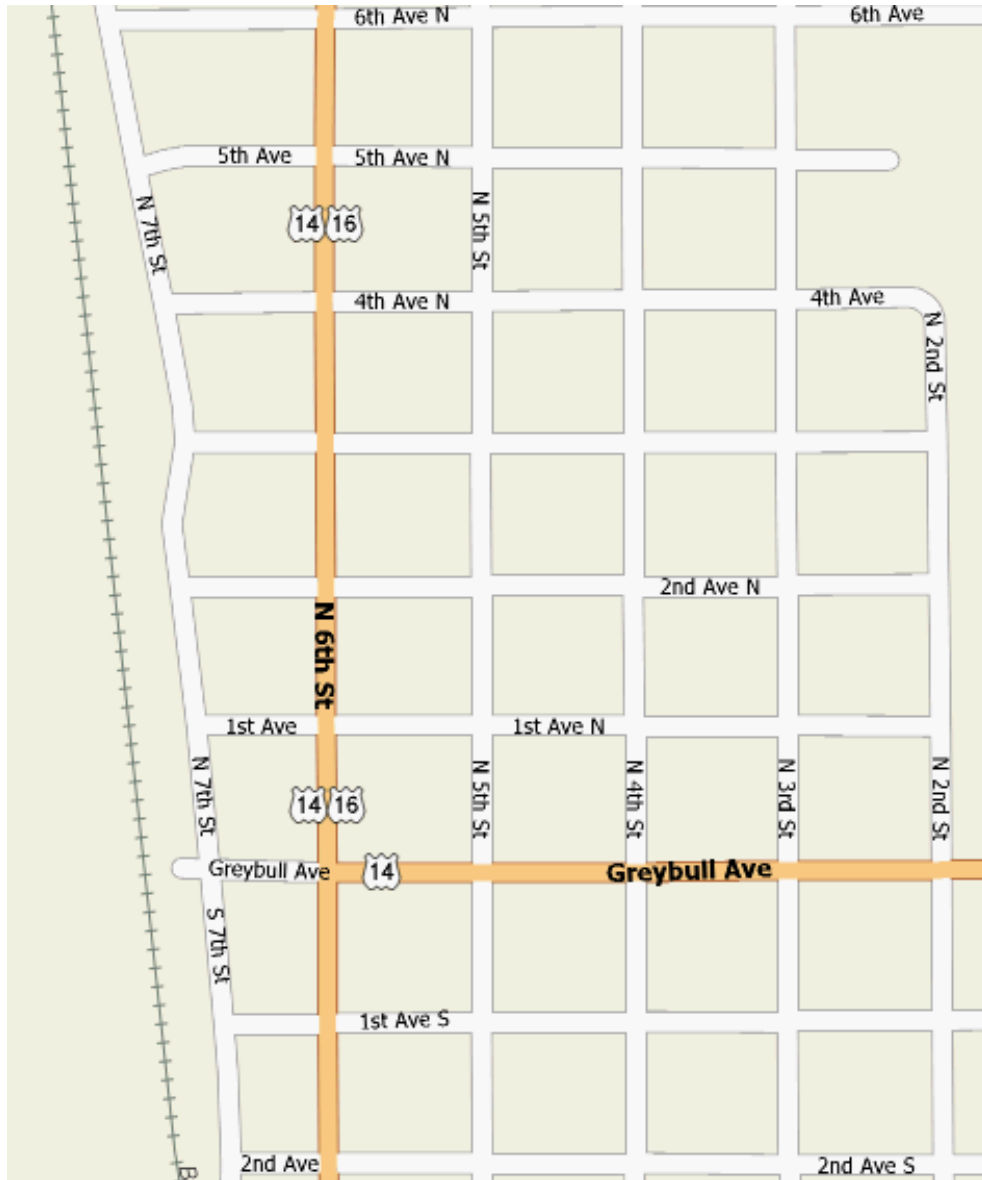
In Cody, large transverse cracks were observed in many open sections of the streets. It is assumed that these cracks are the result of insufficient contraction joints. The large transverse cracks are spaced in the center of each slab. This conclusion is supported by the fact that these cracks do not exist in areas where the road is divided into smaller sections. The majority of the surface area is in good shape, with only small portions of the streets and sidewalks displaying faint surface lines.

MAPS OF WYOMING TOWNS INSPECTED

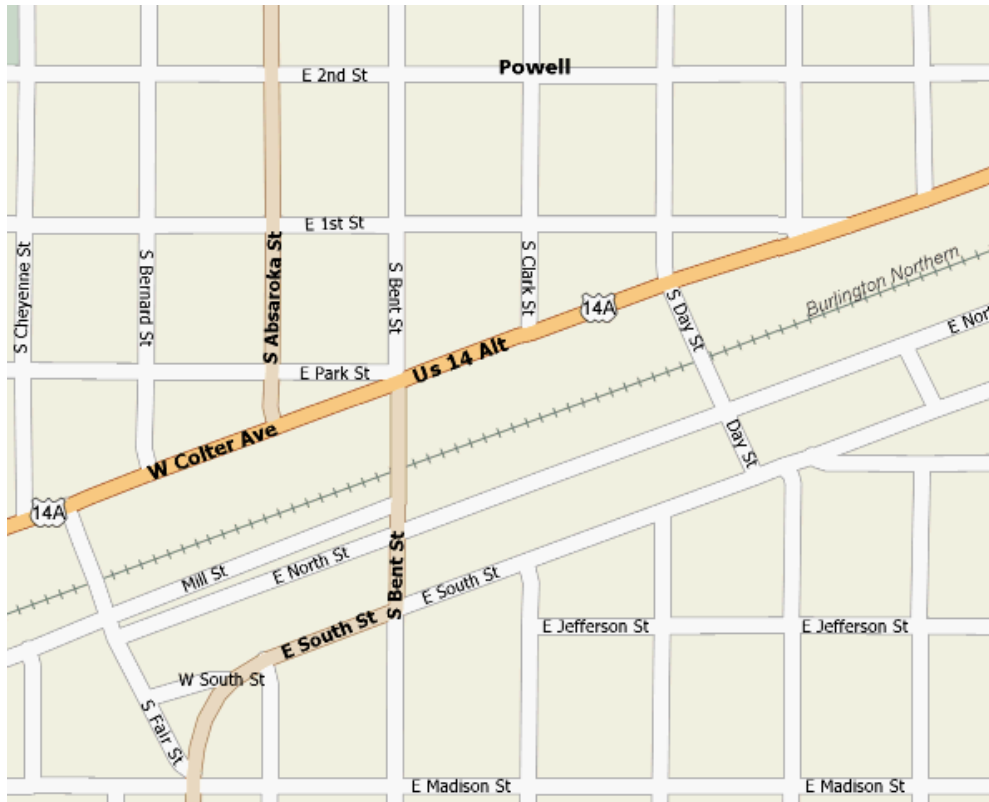
Cody



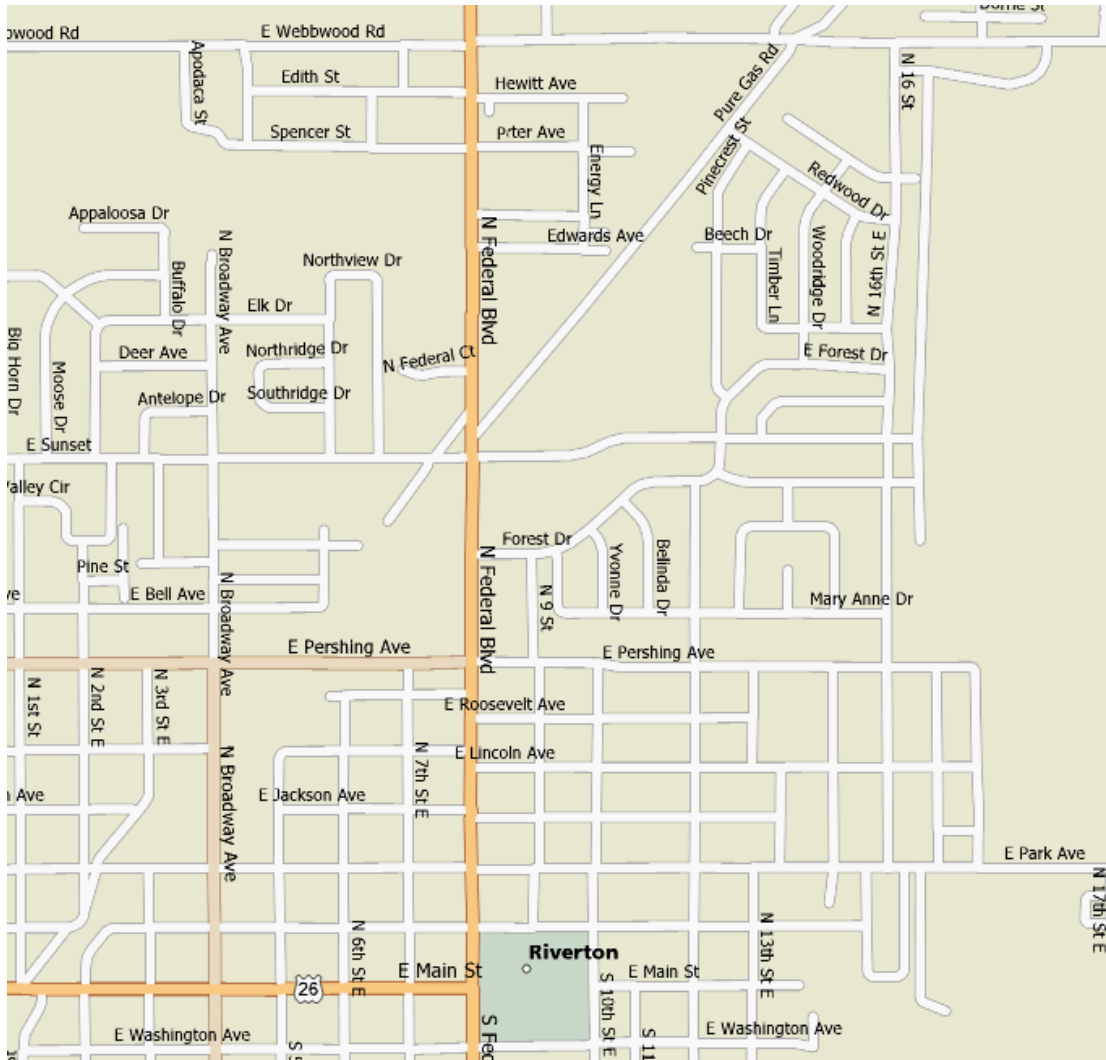
Greybull



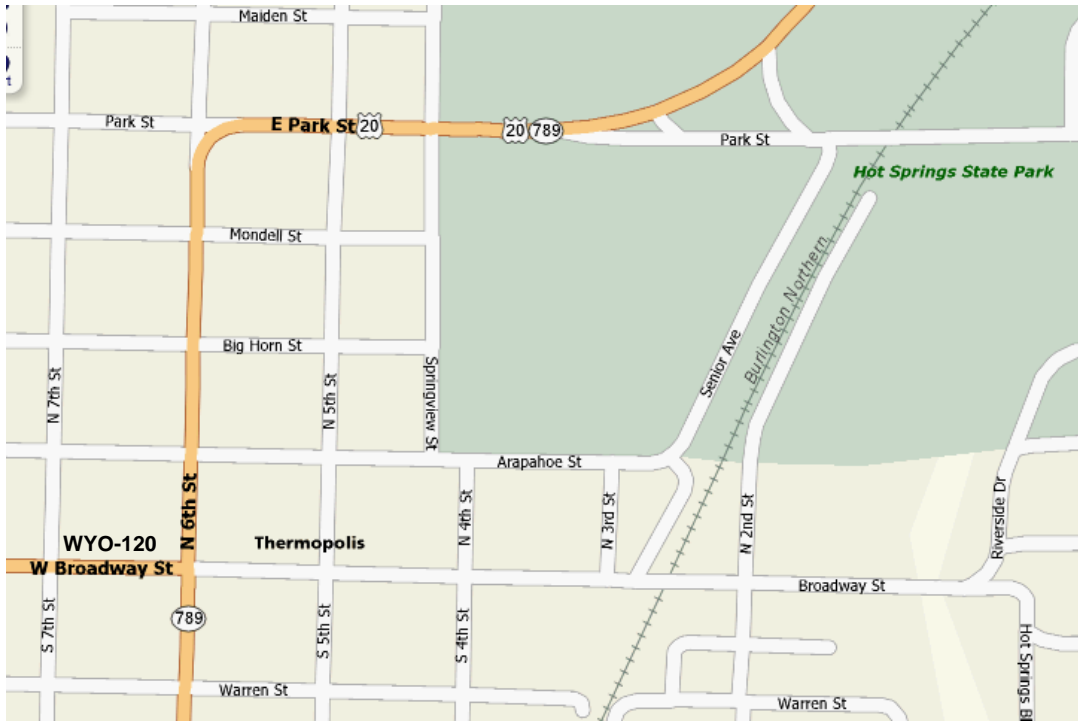
Powell



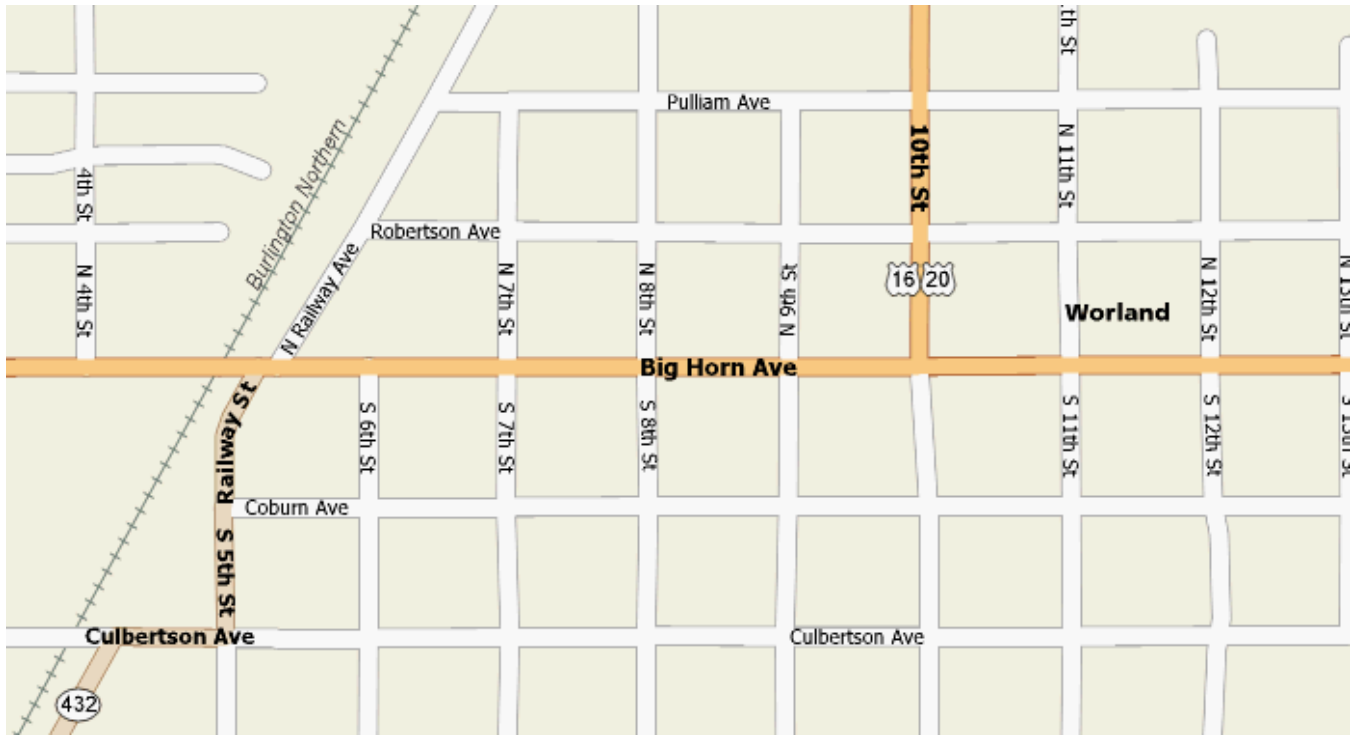
Riverton



Thermopolis



Worland



CODY: DAMAGE OBSERVATIONS OF CONCRETE ROADS

Inspected 8-26-07

Damage Classification

very faint lines	1
faint lines	2
easily visible lines	3
cracking	4
wide cracking	5
chipping	6
spalling	7

Section Classification

P	patch
G	gutter
SW	sidewalk
S	street
I	Intersection
C	curb

16th Street

Location	Section	Damage 1	Damage 2	Damage 3	Damage 4	Damage 5	Damage 6	Damage 7
Sheridan Intersection	I							
Sheridan to Rumsey	SW					Yes, transverse, 25%	Yes, transverse, 25%	
Rumsey Intersection	I	Yes, pattern, 75%	Yes, pattern, 75%	Yes, pattern, 75%				
Rumsey to Bleistein								
Bleistein Intersection	I					Yes, longitudinal, <10%	Yes, longitudinal, <10%	Yes, longitudinal, <10%
Bleistein to Salsbury	SW	Yes, pattern, 25%	Yes, pattern, 25%	Yes, pattern, 25%				
	S	Yes, pattern, 50%	Yes, pattern, 50%					
Salsbury Intersection	I	Yes, pattern, 25%	Yes, pattern, 25%					
Salsbury to Wyoming								
Wyoming Intersection	I	Yes, random, 25%	Yes, random, 25%					
Wyoming to Hwy 120	SW				Yes, random, <10%	Yes, random, <10%	Yes, random, <10%	
	S					Yes, transverse, <10%		
Hwy 120 Intersection	I					Yes, transverse, 10%	Yes, transverse, 10%	
Hwy 120 to 17th	S					Yes, transverse, <10%		
17th Intersection								
17th to North Lane								
North Intersection	I					Yes, longitudinal, <10%		
North to 19th	S				Yes, random, <10%	Yes, random, <10%		
19th Intersection	I	Yes, pattern, 25%	Yes, pattern, 25%	Yes, pattern, 25%				

Highway 120

Location	Section	Damage 1	Damage 2	Damage 3	Damage 4	Damage 5	Damage 6	Damage 7
16th to end	S					Yes, transverse, 10%		

17th Street

Location	Section	Damage 1	Damage 2	Damage 3	Damage 4	Damage 5	Damage 6	Damage 7
Stampede Intersection								
Stampede to Central	S					Yes, transverse, 10%	Yes, transverse, 10%	Yes, transverse, 10%
	SW					Yes, random, <10%	Yes, random, <10%	
	G					Yes, random, <10%	Yes, random, <10%	
Central Intersection	I					Yes, transverse, 10%	Yes, transverse, 10%	

Central to Draw	C				Yes, transverse, <10%	Yes, transverse, <10%	Yes, transverse, <10%	
	G				Yes, transverse, <10%	Yes, transverse, <10%	Yes, transverse, <10%	
	S					Yes, trans. & long., 50%	Yes, trans. & long., 50%	
	SW					Yes, transverse, 50%	Yes, longitudinal, 50%	
Draw Intersection	I					Yes, transverse, 25%	Yes, transverse, 25%	
Draw to Alger	S					Yes, transverse, 50%	Yes, longitudinal, 50%	
	C				Yes, transverse, <10%	Yes, transverse, <10%	Yes, transverse, <10%	
	G				Yes, transverse, <10%	Yes, transverse, <10%	Yes, transverse, <10%	
Alger Intersection	I							
Alger to Beck	SW						Yes, longitudinal, <10%	
	S					Yes, transverse, 25%	Yes, transverse, 25%	
Beck Intersection	I					Yes, transverse, 10%	Yes, transverse, 10%	
Beck to Sheridan	SW				Yes, random, <10%	Yes, random, <10%	Yes, random, <10%	
	G				Yes, transverse, <10%	Yes, transverse, <10%	Yes, transverse, <10%	
	S					Yes, transverse, 10%		

Sheridan Street

Location	Section	Damage 1	Damage 2	Damage 3	Damage 4	Damage 5	Damage 6	Damage 7
17th Intersection								
17th to 16th	S					Yes, transverse, 25%		
	G					Yes, random, <10%	Yes, random, <10%	Yes, random, <10%
16th Intersection								
16th to 15th	S					Yes, transverse, 25%		
15th Intersection								
15th to 14th	S					Yes, transverse, 10%		
	SW	Yes, random, 25%	Yes, random, 25%					
14th Intersection								
14th to 13th	SW	Yes, random, 50%	Yes, random, 50%		Yes, random, <10%	Yes, random, <10%	Yes, random, <10%	
13th Intersection								
13th to 12th	SW	Yes, random, 50%	Yes, random, 50%					
	S					Yes, transverse, <10%		
12th Intersection								
12th to 11th	SW	Yes, random, 25%	Yes, random, 25%					
	S					Yes, transverse, <10%		
11th Intersection	I				Yes, transverse, <10%	Yes, transverse, <10%		
11th to 10th	S					Yes, transverse, <10%		
	SW				Yes, random, <10%	Yes, random, <10%	Yes, random, <10%	
10th Intersection	I					Yes, transverse, 25%		

GREYBULL: DAMAGE OBSERVATIONS OF CONCRETE ROADS

Inspected 7-17-07

Damage Classification

very faint lines	1
faint lines	2
easily visible lines	3
cracking	4
wide cracking	5
chipping	6
spalling	7

Section Classification

P	patch
G	gutter
SW	sidewalk
S	street
I	Intersection
C	curb

6th Street - west side

Location	Section	Damage 1	Damage 2	Damage 3	Damage 4	Damage 5	Damage 6	Damage 7
2nd Intersection	I		Yes, random, 25%	Yes, random, 25%	Yes, random, 25%	Yes, transverse, 25%		
2nd to 1st	S			Yes, random, 10%	Yes, random, 10%	Yes, random, 10%		
1st Intersection	I			Yes, random, <10%	Yes, random, <10%			
1st To Greybull	S			Yes, random, 10%	Yes, random, 10%			
	G			Yes, random, 50%	Yes, random, 50%			
Greybull Intersection								
Greybull to 1st Ave. North	S			Yes, longitudinal, <10%	Yes, longitudinal, <10%	Yes, longitudinal, <10%		
1st Ave. North Intersection								

6th Street - east side

Location	Section	Damage 1	Damage 2	Damage 3	Damage 4	Damage 5	Damage 6	Damage 7
2nd Intersection	I			Yes, random, <10%	Yes, random, <10%			
2nd to 1st								
1st Intersection	I			Yes, random, <10%	Yes, random, <10%			
1st To Greybull	SW			Yes, random, <10%	Yes, random, <10%	Yes, random, <10%	Yes, random, <10%	Yes, random, <10%
Greybull Intersection								
Greybull to 1st Ave. North	S			Yes, transverse, <10%	Yes, transverse, <10%	Yes, transverse, <10%		
	G			Yes, random, <10%	Yes, random, <10%	Yes, random, <10%	Yes, random, <10%	
1st Ave. North Intersection								

Greybull Avenue - north side

Location	Section	Damage 1	Damage 2	Damage 3	Damage 4	Damage 5	Damage 6	Damage 7
7th Intersection	I							
7th to 6th	S				Yes, longitudinal, 25%	Yes, longitudinal, 25%	Yes, transverse, 25%	Yes, transverse, 10%
6th Intersection								
6th to 5th	SW			Yes, random, <10%	Yes, random, <10%	Yes, random, <10%	Yes, random, <10%	
5th Intersection	I			Yes, random, <25%	Yes, random, <25%			
5th to 4th	SW				Yes, random, <10%	Yes, random, <10%	Yes, random, <10%	
4th Intersection								
4th to 3rd								
3rd Intersection								

3rd to 2nd								
2nd Intersection	I			Yes, random, 50%				

Greybull Avenue - south side

Location	Section	Damage 1	Damage 2	Damage 3	Damage 4	Damage 5	Damage 6	Damage 7
7th Intersection	I						Yes, transverse, 10%	Yes, transverse, 10%
7th to 6th	C					Yes, random, <10%	Yes, random, <10%	Yes, random, <10%
	S					Yes, random, <10%	Yes, random, <10%	Yes, random, <10%
6th Intersection	I					Yes, transverse, 10%	Yes, transverse, 10%	Yes, transverse, 10%
6th to 5th								
5th Intersection	I					Yes, random, 25%		
5th to 4th	SW			Yes, random, <10%	Yes, random, <10%	Yes, random, <10%	Yes, random, <10%	Yes, random, <10%
4th Intersection	I				Yes, transverse, <10%			
4th to 3rd	SW				Yes, random, <10%	Yes, random, <10%	Yes, random, <10%	
3rd Intersection	I					Yes, transverse, <10%	Yes, transverse, <10%	Yes, transverse, <10%
3rd to 2nd	SW					Yes, transverse, <10%	Yes, transverse, <10%	
2nd Intersection	I			Yes, random, 50%				

LOVELL: DAMAGE OBSERVATIONS OF CONCRETE ROADS

Inspected 8-26-07

Damage Classification

very faint lines	1
faint lines	2
easily visible lines	3
cracking	4
wide cracking	5
chipping	6
spalling	7

Section Classification

P	patch
G	gutter
SW	sidewalk
S	street
I	Intersection
C	curb

Main Street

Location	Section	Damage 1	Damage 2	Damage 3	Damage 4	Damage 5	Damage 6	Damage 7
Mile marker 237 to Great Western	S					Yes, transverse, <10%	Yes, transverse, <10%	Yes, transverse, <10%
Great Western Intersection	I				Yes, longitudinal, 50%	Yes, random, 25%	Yes, random, 25%	
Great Western to Hampshire	S		Yes, random, 25%	Yes, random, 25%				
	G					Yes, pattern, <10%		
	SW			Yes, pattern, 10%	Yes, pattern, 10%	Yes, pattern, 10%	Yes, pattern, 10%	
Hampshire Intersection	I					Yes, longitudinal, <10%	Yes, longitudinal, <10%	
Hampshire to Idaho	SW			Yes, pattern, 75%	Yes, pattern, 75%	Yes, pattern, 75%		
	S					Yes, transverse, <10%	Yes, transverse, <10%	Yes, transverse, <10%
Idaho Intersection								
Idaho to Jersey	SW		Yes, pattern, 25%	Yes, pattern, 25%	Yes, pattern, 25%			
Jersey Intersection								
Jersey to Kansas	SW			Yes, pattern, 50%	Yes, pattern, 50%	Yes, pattern, 50%	Yes, pattern, 50%	Yes, pattern, 50%
Kansas Intersection								
Kansas to Shoshone	G				Yes, transverse, <10%	Yes, transverse, <10%	Yes, transverse, <10%	
Shoshone Intersection								
Shoshone to Montana	S					Yes, longitudinal, <10%	Yes, longitudinal, <10%	Yes, longitudinal, <10%
Montana Intersection								
Montana to Nevada	S					Yes, longitudinal, <10%	Yes, longitudinal, <10%	Yes, longitudinal, <10%
	G				Yes, longitudinal, <10%	Yes, longitudinal, <10%	Yes, longitudinal, <10%	
Nevada Intersection	I					Yes, longitudinal, 10%	Yes, longitudinal, 10%	Yes, longitudinal, 10%
Nevada to Oregon								
Oregon Intersection								
Oregon to Pennsylvania	G						Yes, longitudinal, <10%	
Pennsylvania Intersection	I					Yes, random, <10%	Yes, random, <10%	Yes, random, <10%
Pennsylvania to McKinley								
McKinley Insection								
McKinley to Quebec	G					Yes, transverse, <10%		

06

POWELL: DAMAGE OBSERVATIONS OF CONCRETE ROADS

Inspected 8-26-07

Damage Classification

very faint lines	1
faint lines	2
easily visible lines	3
cracking	4
wide cracking	5
chipping	6
spalling	7

Section Classification

P	patch
G	gutter
SW	sidewalk
S	street
I	Intersection
C	curb

Coulter Ave.

Location	Section	Damage 1	Damage 2	Damage 3	Damage 4	Damage 5	Damage 6	Damage 7
Blairs store to Cheyenne	G					Yes, transverse, <10%	Yes, transverse, <10%	
Cheyenne & Coulter	I							Yes, <10%
Cheyenne to Fair	G						Yes, transverse, <10%	
Fair & Coulter	I				Yes, transverse, <10%	Yes, transverse, <10%	Yes, transverse, <10%	Yes, transverse, <10%
Fair to Bernard	G						Yes, transverse, <10%	
	C					Yes, transverse, <10%		
Bernard & Coulter	I				Yes, random, <10%	Yes, random, <10%	Yes, random, <10%	
Bernard to Absaroka	SW				Yes, pattern, 10%	Yes, pattern, 10%	Yes, pattern, 10%	Yes, pattern, 10%
	G					Yes, transverse, 10%	Yes, transverse, 10%	
	C					Yes, transverse, 10%	Yes, transverse, 10%	
Absaroka & Coulter	I							
Absaroka to Bent	SW				Yes, random, <10%	Yes, random, <10%	Yes, random, <10%	
	G					Yes, transverse, <10%	Yes, transverse, <10%	
	C					Yes, transverse, <10%	Yes, transverse, <10%	
Bent & Coulter	I					Yes, longitudinal, <10%	Yes, longitudinal, <10%	
Bent to Clark	SW	Yes, random, 75%	Yes, random, 75%	Yes, random, 75%	Yes, random, 50%	Yes, random, 50%	Yes, random, 50%	
	G					Yes, transverse, <10%	Yes, transverse, <10%	
	C					Yes, transverse, <10%	Yes, transverse, <10%	
Clark & Coulter	I				Yes, random, <10%	Yes, random, <10%	Yes, random, <10%	

RIVERTON: DAMAGE OBSERVATIONS OF CONCRETE ROADS

Inspected 6-15-07

Damage Classification

very faint lines	1
faint lines	2
easily visible lines	3
cracking	4
wide cracking	5
chipping	6
spalling	7

Section Classification

P	patch
G	gutter
SW	sidewalk
S	street
I	Intersection
C	curb

Main Street, North Side

Location	Section	Damage 1	Damage 2	Damage 3	Damage 4	Damage 5	Damage 6	Damage 7
7th & Main	I	Yes, 10%						
6th & Main	I	Yes, 50%	Yes, 10%					
5th & Main	I	Yes, 10%	Yes, 10%	Yes, 10%				
Broadway & Main	I	Yes, 10%	Yes, 10%	Yes, 25%				
3rd & Main	I		Yes, 10%	Yes, 10%				
2nd & Main	I	Yes, 10%		Yes, 10%				
1st to 2nd	S	Yes, 10%	Yes, 10%	Yes, 10%				
1st & Main	I		Yes, 10%					

92

Main Street, South Side

Location	Section	Damage 1	Damage 2	Damage 3	Damage 4	Damage 5	Damage 6	Damage 7
7th & Main	I	Yes, 10%						
6th & Main	I	Yes, 25%						
5th & Main	I	Yes, 10%						
	SW	Yes, 10%						
Broadway & Main	I	Yes, 50%	Yes, 10%					
3rd & Main	I	Yes, 10%	Yes, 25%					
2nd & Main	I	Yes, 25%						
1st to 2nd	SW	Yes, 10%	Yes, 10%	Yes, 10%				
1st & Main	I	Yes, 25%	Yes, 50%					

Federal Street, West Side

Location	Section	Damage 1	Damage 2	Damage 3	Damage 4	Damage 5	Damage 6	Damage 7
Washington to Main	P				Yes	Yes	Yes	
Main & Federal	I			Yes	Yes	Yes		
Main to Fremont	P				Yes	Yes	Yes	
Fremont & Federal	I			Yes	Yes	Yes		
Fremont to Park	C			Yes	Yes	Yes		Yes
	S			Yes	Yes	Yes		

	SW			Yes	Yes	Yes		
Park & Federal	I		Yes	Yes	Yes	Yes		
Park to Jackson	SW		Yes	Yes				
	S				Yes			
Jackson & Federal	I			Yes	Yes	Yes		
Jackson to Lincoln	SW				Yes			
	S				Yes			
Lincoln & Federal	I			Yes				
Lincoln to Roosevelt	SW				Yes	Yes	Yes	
	S				Yes	Yes	Yes	
Roosevelt & Federal	I		Yes	Yes	Yes	Yes		
Roosevelt to Pershing	SW		Yes	Yes	Yes			
	S				Yes	Yes	Yes	
Safeway Entrance	SW				Yes			
Radioshack Entrance	SW				Yes			
KFC Entrance	SW				Yes	Yes		
Pershing to Sunset	G						Yes	Yes
	S				Yes	Yes	Yes	Yes
	SW				Yes			
Sunset & Federal	I		Yes	Yes	Yes	Yes		
Sunset to Federal Court	G		Yes					
	S				Yes	Yes		
Super 8 Motel Entrance	S						Yes	Yes
Federal Court & Federal	I		Yes	Yes	Yes	Yes		
Federal Court to Edith	S		Yes	Yes	Yes	Yes	Yes	
Edith & Federal	I		Yes	Yes	Yes	Yes		
Edith to Webbwood	S		Yes	Yes	Yes	Yes		
Webbwood & Federal	I				Yes	Yes		

93

Federal Street, East Side

Location	Section	Damage 1	Damage 2	Damage 3	Damage 4	Damage 5	Damage 6	Damage 7
Webbwood & Federal	C				Yes			
Webbwood to Hewitt	S			Yes	Yes	Yes		
Hewitt to Porter	S				Yes	Yes		
	C				Yes	Yes		
Porter to Miniweb	S			Yes	Yes	Yes		
Miniweb to Sunset	G				Yes	Yes	Yes	Yes
	S			Yes	Yes	Yes	Yes	
Sears Entrance	S		Yes	Yes				
Sunset to Pershing	S			Yes	Yes			
Pershing to Roosevelt	S			Yes	Yes			
Roosevelt to Lincoln	S			Yes	Yes	Yes		
Lincoln to Jackson	S			Yes	Yes	Yes	Yes	
Jackson to Park	S			Yes	Yes	Yes	Yes	
Park to Fremont	S			Yes	Yes	Yes		
Fremont to Main	S			Yes	Yes			
	P			Yes	Yes	Yes	Yes	Yes
Main & Federal	P			Yes	Yes	Yes	Yes	Yes
Main to Washington	P			Yes				

Park Street, North Side

Location	Section	Damage 1	Damage 2	Damage 3	Damage 4	Damage 5	Damage 6	Damage 7
Federal & Park	I			Yes	Yes	Yes		
Federal to 9th	S							
9th to 10th	S							
10th to 12th	S							
12th & Park	G			Yes	Yes			

Park Street, South Side

Location	Section	Damage 1	Damage 2	Damage 3	Damage 4	Damage 5	Damage 6	Damage 7
Federal & Park	I			Yes	Yes			
Federal to 9th	S							
9th to 10th	S							
10th to 12th	S							
12th & Park	G			Yes	Yes	Yes	Yes	Yes

ROCK SPRINGS: DAMAGE OBSERVATIONS OF CONCRETE ROADS

Inspected 8-1-07

Damage Classification

very faint lines	1
faint lines	2
easily visible lines	3
cracking	4
wide cracking	5
chipping	6
spalling	7

Section Classification

P	patch
G	gutter
SW	sidewalk
S	street
I	Intersection
C	curb

9th Street

Location	Section	Damage 1	Damage 2	Damage 3	Damage 4	Damage 5	Damage 6	Damage 7
Phillips 66 to Swanson	S						Yes, random, <10%	Yes, random, <10%
	SW					Yes, random, 10%	Yes, random, 10%	Yes, random, 10%
Swanson Intersection	I					Yes, random, 10%	Yes, random, 10%	Yes, random, 10%
Swanson to 376 Junction	SW				Yes, random, <10%	Yes, random, <10%		
	G					Yes, random, <10%	Yes, random, <10%	Yes, random, <10%
	S					Yes, random, <10%	Yes, random, <10%	Yes, random, <10%
376 Junction Intersection								
376 Junction to Powerhouse	SW		Yes, random, <10%		Yes, pattern, <10%	Yes, transverse, <10%	Yes, transverse, <10%	
	S			Yes, random, <10%	Yes, random, <10%			
Powerhouse Intersection	I				Yes, random, 10%	Yes, random, 10%	Yes, random, 10%	
Powerhouse to X St. (10th)								
X St. (10th) Intersection	I					Yes, random, <10%	Yes, random, <10%	Yes, random, <10%
X St. (10th) to Perry	SW				Yes, random, <10%	Yes, random, <10%	Yes, random, <10%	
	G						Yes, transverse, <10%	Yes, transverse, <10%
	S					Yes, transverse, <10%	Yes, transverse, <10%	Yes, transverse, <10%
Perry Intersection	I			Yes, pattern, <10%	Yes, pattern, <10%	Yes, pattern, <10%	Yes, pattern, <10%	
Perry to Paulson	G					Yes, transverse, <10%	Yes, transverse, <10%	Yes, transverse, <10%
Paulson Intersection	I				Yes, longitudinal, <10%	Yes, longitudinal, <10%	Yes, longitudinal, <10%	
Paulson to Arapahoe					Yes, transverse, <10%	Yes, transverse, <10%	Yes, transverse, <10%	Yes, transverse, <10%
Arapahoe Intersection	I				Yes, random, <10%	Yes, random, <10%	Yes, random, <10%	Yes, random, <10%
Pilot Butte Intersection	I			Yes, random, 25%	Yes, random, 25%	Yes, random, 25%	Yes, random, 25%	

Pilot Butte

Location	Section	Damage 1	Damage 2	Damage 3	Damage 4	Damage 5	Damage 6	Damage 7
Arapahoe to Clark	C				Yes, transverse, <10%	Yes, transverse, <10%		
	G						Yes, transverse, <10%	Yes, transverse, <10%
Clark Intersection								
Clark to Pearl	G					Yes, transverse, <10%	Yes, transverse, <10%	Yes, transverse, <10%
Pearl Intersection	I					Yes, transverse, <10%	Yes, transverse, <10%	Yes, transverse, <10%
Pearl to N. St.	SW		Yes, random, 10%	Yes, random, 10%	Yes, random, 10%			
	G						Yes, transverse, <10%	Yes, transverse, <10%
N St. Intersection								
N St. to M St.	G				Yes, random, <10%	Yes, random, <10%	Yes, random, <10%	Yes, random, <10%

	SW				Yes, random, <10%	Yes, random, <10%	Yes, random, <10%	Yes, random, <10%
M St. Intersection	I			Yes, transverse, <10%	Yes, transverse, <10%			
M St. to Bridger								
Bridger Intersection	I						Yes, transverse, <10%	Yes, transverse, <10%

Bridger

Location	Section	Damage 1	Damage 2	Damage 3	Damage 4	Damage 5	Damage 6	Damage 7
Pilot Butte to Tisdel	G						Yes, random, 10%	Yes, random, 10%
Tisdel Intersection								
Tisdel to Solsby								
Solsby Intersection								
Solsby to Business 80	G				Yes, random, <10%	Yes, random, <10%	Yes, random, <10%	Yes, random, <10%
	C						Yes, random, <10%	Yes, random, <10%
Business 80 Intersection	I					Yes, random, <10%	Yes, random, <10%	Yes, random, <10%
Business 80 to Grant	SW				Yes, random, <10%	Yes, random, <10%	Yes, random, <10%	Yes, random, <10%
	G				Yes, random, <10%	Yes, random, <10%	Yes, random, <10%	Yes, random, <10%
Grant & Center						Yes, random, <10%	Yes, random, <10%	Yes, random, <10%

Center

Location	Section	Damage 1	Damage 2	Damage 3	Damage 4	Damage 5	Damage 6	Damage 7
Grant to Sherman								
Sherman Intersection								
Sherman to Sheridan								
Sheridan Intersection	I					Yes, transverse, <10%	Yes, transverse, <10%	Yes, transverse, <10%
Sheridan to Thomas								
Thomas Intersection	I					Yes, transverse, <10%	Yes, transverse, <10%	
Thomas to Hancock								

Dewar

Location	Section	Damage 1	Damage 2	Damage 3	Damage 4	Damage 5	Damage 6	Damage 7
Hancock to Black	S				Yes, transverse, 25%	Yes, transverse, 25%	Yes, longitudinal, 10%	Yes, longitudinal, 10%
Black Intersection								
Black to Griffith								
Griffith Intersection	I					Yes, random, 10%	Yes, random, 10%	
Griffith to Sidney								
Sidney Intersection	I					Yes, transverse, <10%	Yes, transverse, <10%	Yes, transverse, <10%
Sidney to Swan	S				Yes, pattern, <10%	Yes, transverse, 10%	Yes, transverse, 10%	
Swan Intersection	I					Yes, random, 10%	Yes, random, 10%	
Swan to Smith								
Smith Intersection								
Smith to Blockbuster								

THERMOPOLIS: DAMAGE OBSERVATIONS OF CONCRETE ROADS

Inspected 7-17-07

Damage Classification

very faint lines	1
faint lines	2
easily visible lines	3
cracking	4
wide cracking	5
chipping	6
spalling	7

Section Classification

P	patch
G	gutter
SW	sidewalk
S	street
I	Intersection
C	curb

Wyoming 120

Location	Section	Damage 1	Damage 2	Damage 3	Damage 4	Damage 5	Damage 6	Damage 7
"One-Eyed Jacks to 789 789 Intersection	SW	Yes, random, 25%						

Wyoming 789

Location	Section	Damage 1	Damage 2	Damage 3	Damage 4	Damage 5	Damage 6	Damage 7
halfway to Warren to 120	SW	Yes, random, 25%						
120 Intersection	I				Yes, random, <10%			
120 to halfway to next st.	SW	Yes, random, 25%						

Hot Springs State Park road

Location	Section	Damage 1	Damage 2	Damage 3	Damage 4	Damage 5	Damage 6	Damage 7
"Best Western" Intersection	I	Yes, random, 50%	Yes, random, 50%	Yes, random, 50%		Yes, transverse, <10%	Yes, transverse, <10%	Yes, transverse, <10%
Best Western front entrance walkway	SW			Yes, pattern, 25%	Yes, pattern, 25%			
Best Western to Big Horn River Bridge	G			Yes, random, 25%				
	C			Yes, random, 25%				
Bridge Pedestrian Barrier				Yes, vertical, 100%				
Bridge Deck	S				Yes, random, 10%			
End of bridge to end on concrete street	S				Yes, transverse, 50%	Yes, transverse, 50%	Yes, longitudinal, 25%	Yes, longitudinal, 25%

WORLAND: DAMAGE OBSERVATIONS OF CONCRETE ROADS

Inspected 7-17-07

Damage Classification

very faint lines	1
faint lines	2
easily visible lines	3
cracking	4
wide cracking	5
chipping	6
spalling	7

Section Classification

P	patch
G	gutter
SW	sidewalk
S	street
I	Intersection
C	curb

N. 10th - west side

Location	Section	Damage 1	Damage 2	Damage 3	Damage 4	Damage 5	Damage 6	Damage 7
Robertson Intersection								
Robertson to Bighorn	SW				Yes, transverse, <10%	Yes, transverse, <10%	Yes, transverse, <10%	
	C				Yes, random, <10%	Yes, random, <10%	Yes, random, <10%	Yes, random, <10%
Bighorn Intersection	I			Yes, pattern, 25%	Yes, pattern, 25%	Yes, pattern, 25%	Yes, pattern, 25%	

N. 10th - east side

Location	Section	Damage 1	Damage 2	Damage 3	Damage 4	Damage 5	Damage 6	Damage 7
Robertson Intersection								
Robertson to Bighorn	SW			Yes, random, <10%	Yes, random, <10%	Yes, random, <10%	Yes, random, <10%	
Bighorn Intersection	I			Yes, pattern, 25%	Yes, pattern, 25%	Yes, pattern, 25%	Yes, pattern, 25%	

Bighorn Avenue - north side

Location	Section	Damage 1	Damage 2	Damage 3	Damage 4	Damage 5	Damage 6	Damage 7
4th Intersection	I			Yes, random, <10%				
4th to Railway	SW			Yes, random, <10%				
	S			Yes, random, 50%				Yes, transverse, <10%
	G		Yes, random, 25%					
Railway Intersection								
Railway to 6th	G					Yes, transverse, <10%	Yes, transverse, <10%	
6th Intersection								
6th to 7th	G		Yes, random, 50%					
7th Intersection	I				Yes, transverse, <10%	Yes, transverse, <10%	Yes, transverse, <10%	Yes, transverse, <10%
7th to 8th	S				Yes, transverse, <10%	Yes, transverse, <10%	Yes, transverse, <10%	
	G					Yes, transverse, <10%	Yes, transverse, <10%	Yes, transverse, <10%
8th Intersection	I				Yes, random, <10%	Yes, random, <10%	Yes, random, <10%	Yes, random, <10%
8th to 9th								
9th Intersection								
9th to 10th	S				Yes, transverse, <10%	Yes, transverse, <10%	Yes, transverse, <10%	

10th Intersection	I			Yes, random, <10%	Yes, random, <10%	Yes, random, <10%	Yes, random, <10%	Yes, random, <10%
10th to 11th	SW		Yes, random, <10%	Yes, random, <10%	Yes, random, <10%	Yes, random, <10%		
11th Intersection	I						Yes, transverse, 10%	Yes, transverse, 10%

Bighorn Avenue - south side

Location	Section	Damage 1	Damage 2	Damage 3	Damage 4	Damage 5	Damage 6	Damage 7
4th Intersection	I			Yes, random, <10%	Yes, random, <10%	Yes, random, <10%	Yes, random, <10%	
4th to Railway								
Railway Intersection	I	Yes, pattern, 25%	Yes, pattern, 25%	Yes, random, <10%	Yes, random, <10%	Yes, random, <10%	Yes, random, <10%	Yes, random, <10%
Railway to 6th	G				Yes, random, <10%	Yes, random, <10%	Yes, random, <10%	Yes, random, <10%
	C				Yes, random, <10%	Yes, random, <10%	Yes, random, <10%	Yes, random, <10%
6th Intersection								
6th to 7th	G				Yes, longitudinal, <10%	Yes, longitudinal, <10%	Yes, longitudinal, <10%	Yes, longitudinal, <10%
	C				Yes, random, <10%	Yes, random, <10%	Yes, random, <10%	Yes, random, <10%
7th Intersection	I					Yes, longitudinal, <10%	Yes, longitudinal, <10%	
7th to 8th	G						Yes, random, <10%	Yes, random, <10%
	S						Yes, random, <10%	Yes, random, <10%
8th Intersection								
8th to 9th								
9th Intersection								
9th to 10th	SW			Yes, random, 10%				
10th Intersection	I			Yes, random, 50%	Yes, random, 50%	Yes, transverse, 25%	Yes, transverse, 25%	
10th to 11th	SW			Yes, pattern, 10%	Yes, pattern, 10%	Yes, longitudinal, <10%	Yes, longitudinal, <10%	
	S					Yes, transverse, <10%	Yes, transverse, <10%	Yes, transverse, <10%
11th Intersection	I						Yes, transverse, 10%	Yes, transverse, 10%

Appendix B Weather Data

A summary of weather data from the 100 block of 10th street in Laramie is presented below.

B.1 Average Daily Temperatures

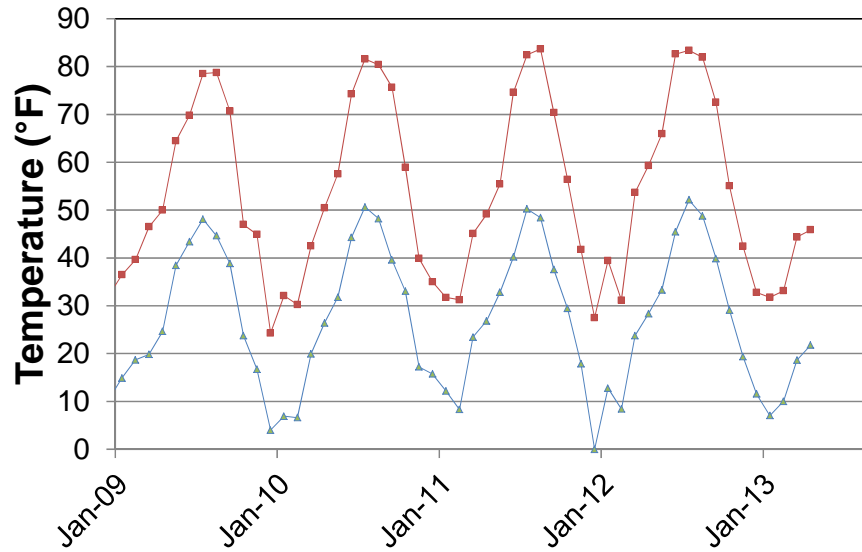


Figure 44. Average daily maximum and minimum temperature in Laramie.

B.2 Average Relative Humidity

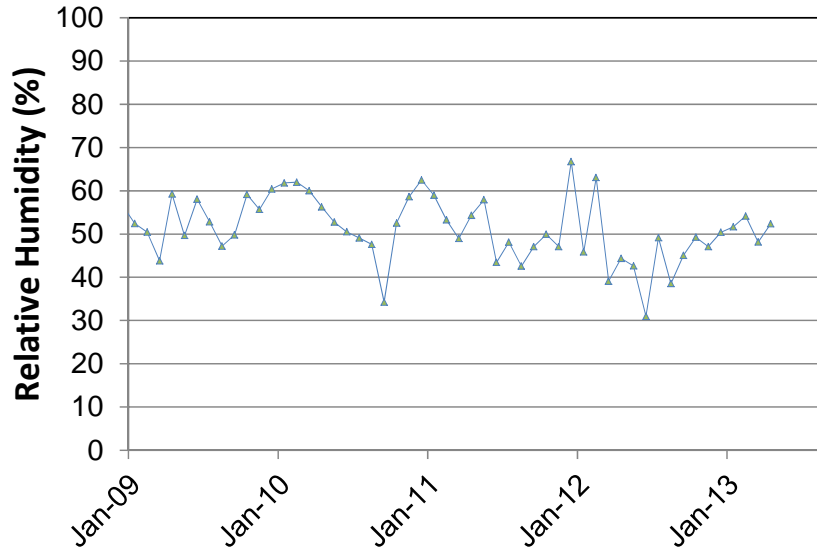


Figure 45. Average daily relative humidity in Laramie.

B.3 Monthly Precipitation

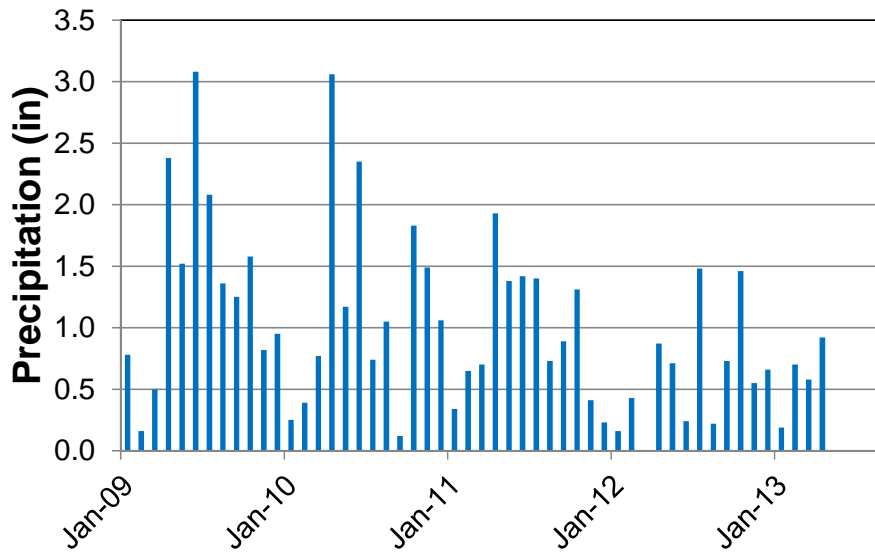


Figure 46. Total monthly precipitation in Laramie.

Appendix C Aggregate Expansions

All aggregates were tested for ASR potential using the Concrete Prism Test (ASTM C1293), the Accelerated Mortar Bar Test (ASTM C1260), the Kinetic Method, a modified Chinese Accelerated Mortar Bar Test (CAMBT), and large scale specimens subjected to outdoor exposure. The results of these tests are presented in this chapter and are listed by aggregate name in alphabetical order.

C.1 Blackrock

C.1.1 CPT Results

Figure 47 shows the concrete prism expansion with respect to time.

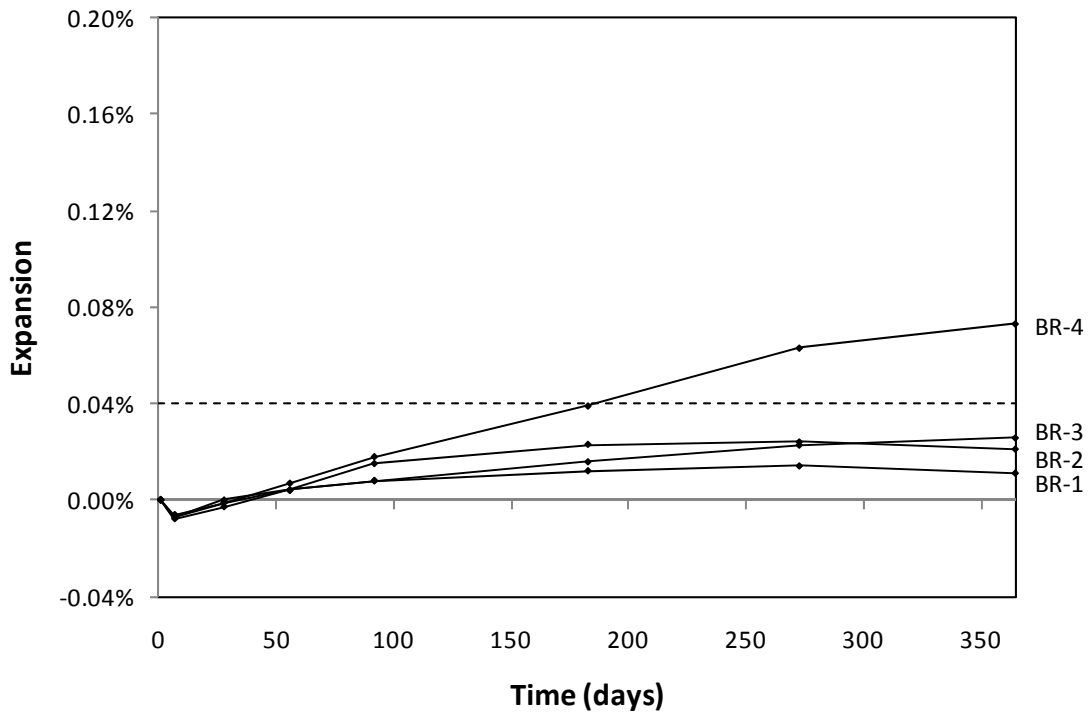


Figure 47. ASTM C1293 results for Blackrock aggregate.

There is good agreement between BR-1, BR-2, and BR-3, but BR-4 displays more reactive behavior. Because the standard only requires three specimens, the average expansion could range from 0.019 percent (if BR-4 is excluded) to 0.040 percent (if BR-1 is excluded). The standard deviation of BR-1, 2, and 3 is 7.64×10^{-5} mm (3.01×10^{-6} inches), so the BR-4 expansion is 5.3 times greater than this standard deviation. The average expansion for all four specimens is 0.033 percent.

The reason for the divergent behavior of BR-4 is unclear and would likely require detailed material testing as well as a petrographic analysis of each specimen. Given the sensitivity of ASR to small changes in the quantity of reactive constituent, it is possible that the aggregate in BR-4 contains a slightly larger proportion of reactive material as compared to the other specimens. This behavior could be an indication of high variability in the aggregate source.



Figure 48. Typical Blackrock prism after test (BR-2 pictured).

C.1.2 AMBT Results

The average expansions for the three mortar bars in each set are shown in Figure 49.

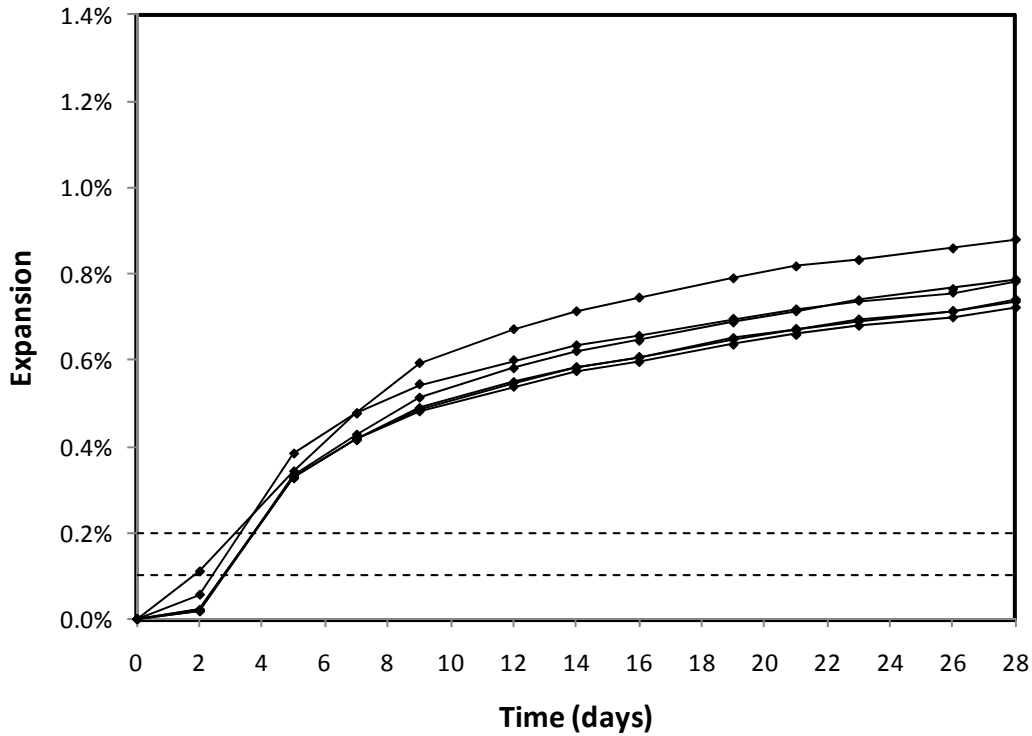


Figure 49. ASTM C1260 average Blackrock mortar bar expansion.

At 14 days after the zero reading the average expansion for all specimens was 0.618 percent which is more than three times greater than the 0.20 percent limit for reactive aggregate.

Therefore, ASTM C1260 classifies the Blackrock aggregate as potentially deleteriously reactive, which indicates that comparison with other test methods is required.

C.1.3 Kinetic Method Results

The values obtained by linear regression are presented in **Error! Reference source not found.**, and a plot showing the quality of the MMF curve approximation is shown in Figure 50.

Table 23. Kinetic Method results for Blackrock aggregate.

$\ln(k)$	-2.343
M	0.781
t_0	2.24

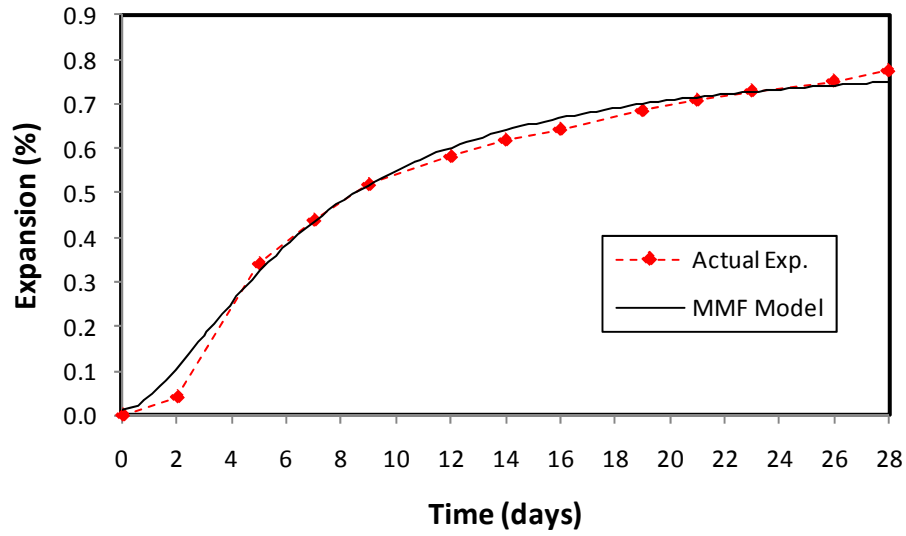


Figure 50. Average actual expansion and MMF approximation for Blackrock aggregate.

$\ln(k)$ is greater than -6 so the Blackrock aggregate is classified as reactive using the kinetic method.

C.1.4 Modified CAMBT Results

There was excellent agreement among the expansions of all three mortar bars which can be seen in Figure 51.

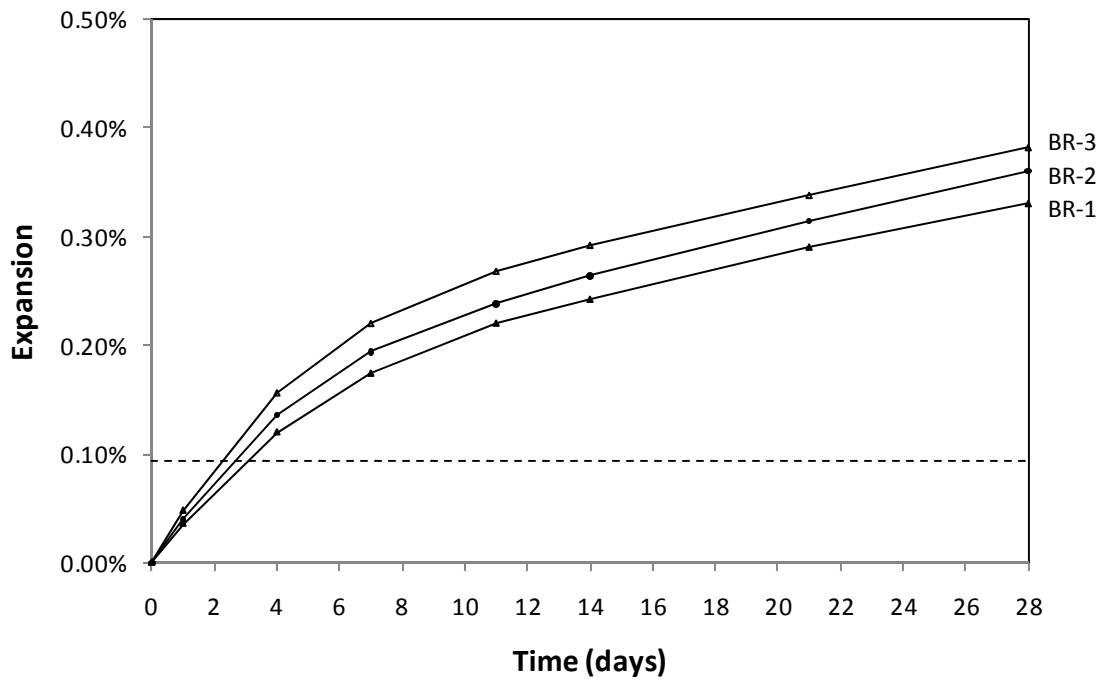


Figure 51. Modified CAMBT mortar bar expansion for Blackrock.

At 14 days after the zero reading the average expansion for the mortar bars was 0.266 percent which exceeds the critical expansion limit of 0.093 percent. Therefore, the modified CAMBT classifies the Blackrock aggregate as reactive.

Visual inspection revealed limited microcracking and almost no open cracks. Given the relatively large expansion that the specimens underwent, the absence of cracks is somewhat surprising. In the pictures of the specimens there seems to be a higher number of visible voids compared to other specimen groups. **Error! Reference source not found.** and **Error! Reference source not found.** show the crack prevalence and void frequency of the typical Blackrock mortar bar.

C.1.5 Summary

The expansion ratio comparison in Figure 52 shows the ratio of measured expansion versus the expansion limit for each accelerated test for the Blackrock aggregate.

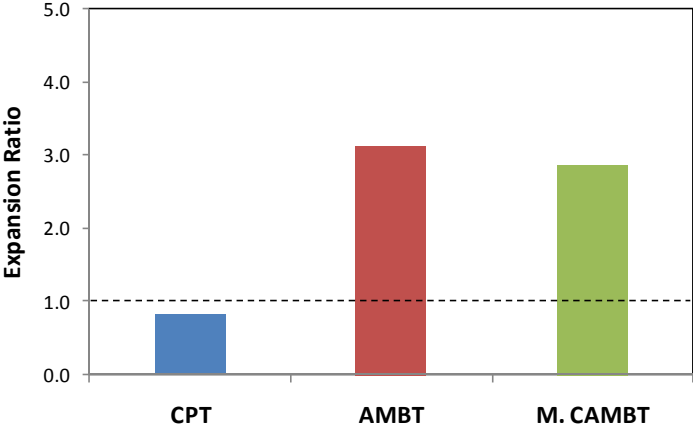


Figure 52. Expansion ratio comparison for Blackrock.

C.2 Devries Farm

C.2.1 CPT Results

The figure below shows specimen expansion with respect to time.

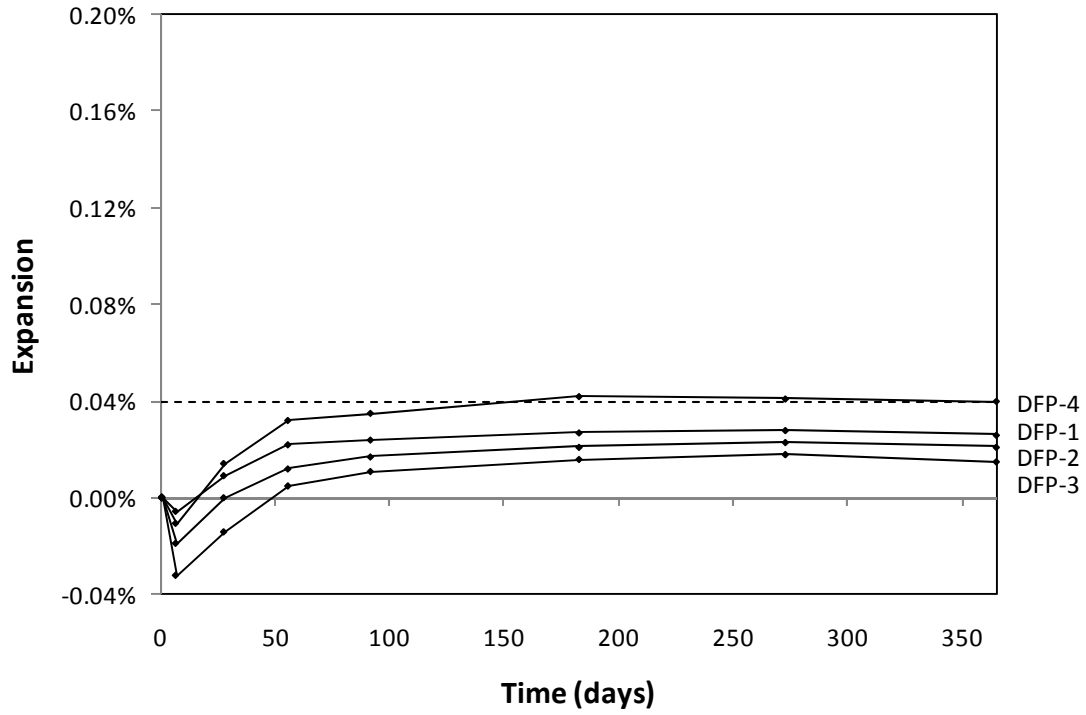


Figure 53. ASTM C1293 results for Devries Farm aggregate.

C.2.2 AMBT Results

The average expansions for the three mortar bars in each set are shown in Figure 54. As can be seen from the graph, there was good correlation between all sets of mortar bars.

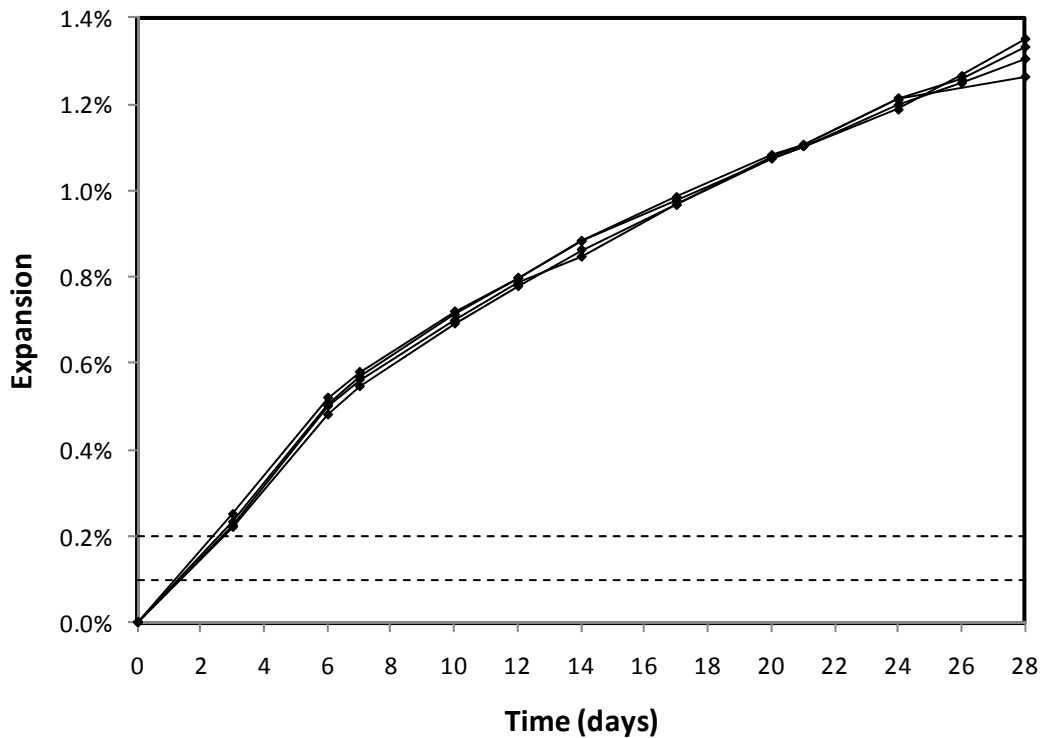


Figure 54. ASTM C1260 average Devries Farm mortar bar expansion.

At 14 days after the zero reading the average expansion for all specimens was 0.869 percent which is more than four times greater than the 0.20 percent limit for reactive aggregate.

Therefore, ASTM C1260 classifies the Devries Farm aggregate as reactive, which indicates that comparison with other test methods is required.

C.2.3 Kinetic Method Results

The values obtained by linear regression are presented in **Error! Reference source not found.**, and a plot showing the quality of the MMF curve approximation is shown in Figure 50.

Table 24. Kinetic Method results for Devries Farm aggregate.

$\ln(k)$	-2.465
M	1.197
t_0	0.28

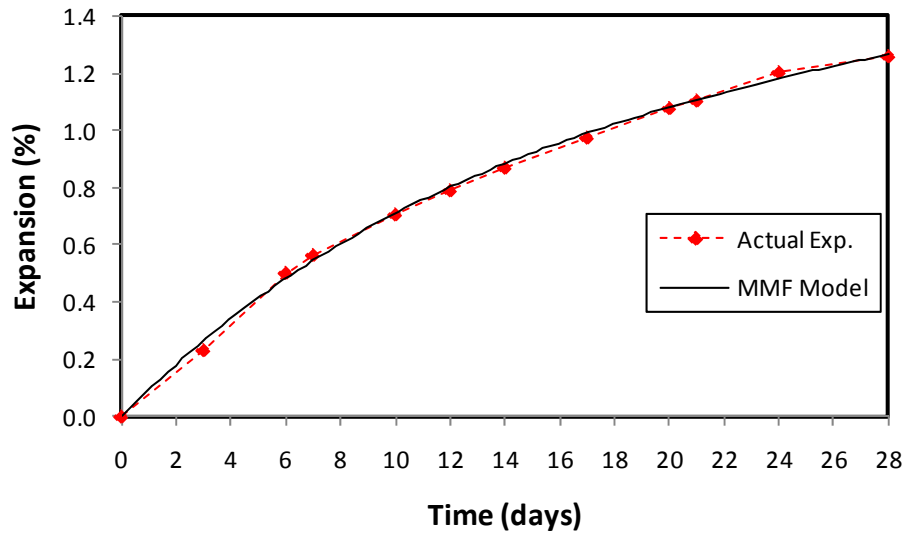


Figure 55. Average actual expansion and MMF approximation for Devries Farm aggregate.

$\ln(k)$ is greater than -6 so the Devries Farm aggregate is classified as reactive using the kinetic method.

C.2.4 Modified CAMBT Results

There was excellent agreement among the expansions of all three mortar bars. The graph of their expansions can be seen in Figure 56.

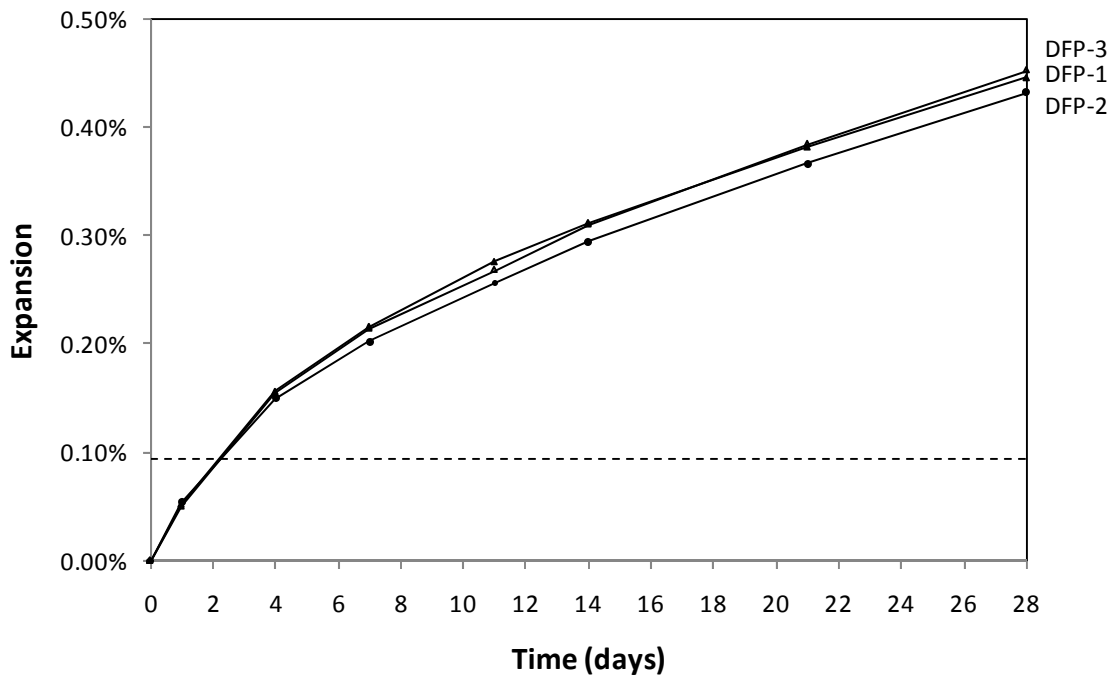


Figure 56. CAMBT Mortar bar expansion for Devries Farm.

At 14 days after the zero reading the average expansion for the mortar bars was 0.305 percent which greatly exceeds the critical expansion limit of 0.093 percent. Therefore, the modified CAMBT classifies the Devries Farm aggregate as reactive.

Figure 57 shows that the mass of the bars increased only during the first day in the NaOH solution and then declined steadily. At the end of 28 days the mass of the specimens were 0.3 to 0.4 percent less than when they entered the NaOH solution.

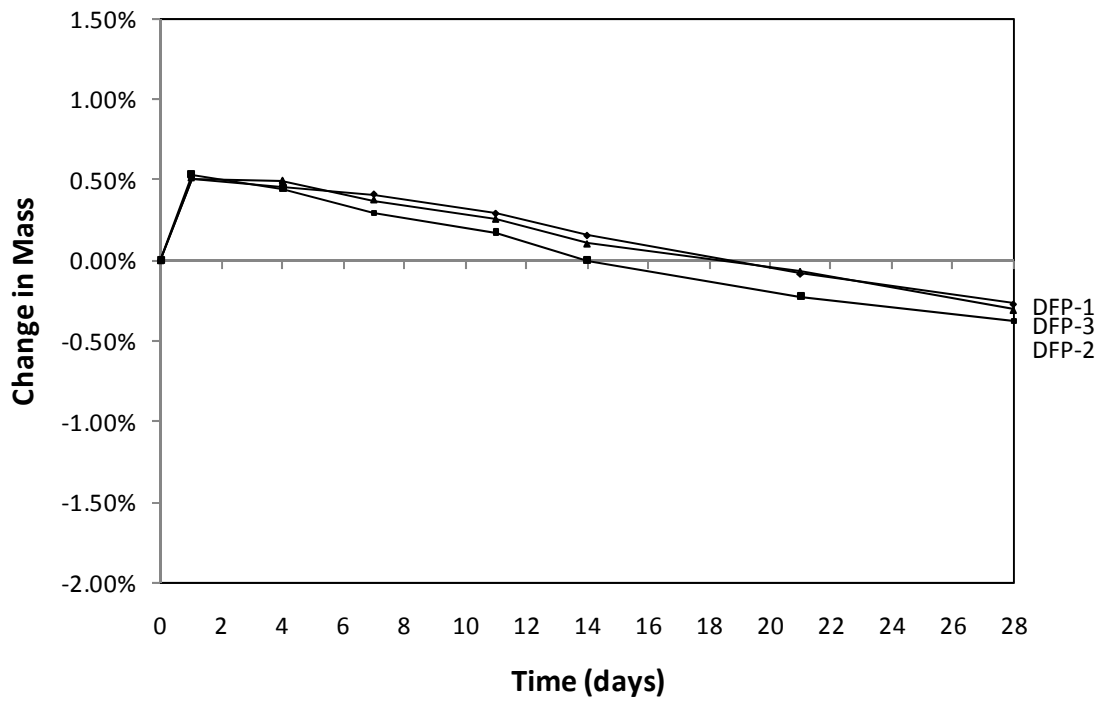


Figure 57. Mass change (%) for Devries Farm mortar bars in the modified CAMBT.

C.2.5 Summary

The expansion ratio comparison in Figure 58 shows the ratio of measured expansion versus the expansion limit for each accelerated test for the Devries Farm aggregate.

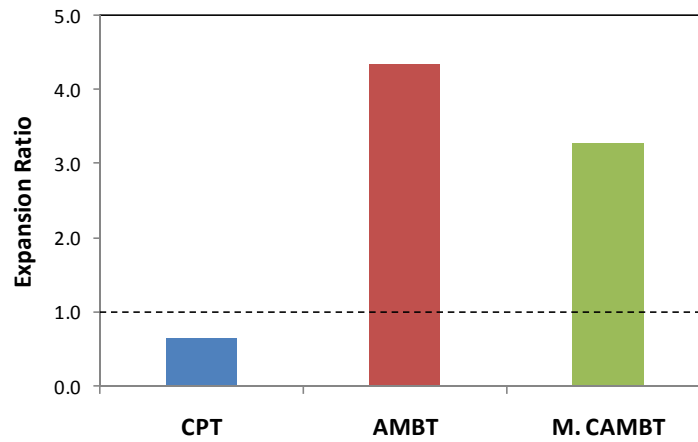


Figure 58. Expansion ratio comparison for Devries Farm.

C.3 Goton

C.3.1 CPT Results

The expansion curves for the Goton specimens are more spread out than other aggregate specimens as can be seen in the figure below.

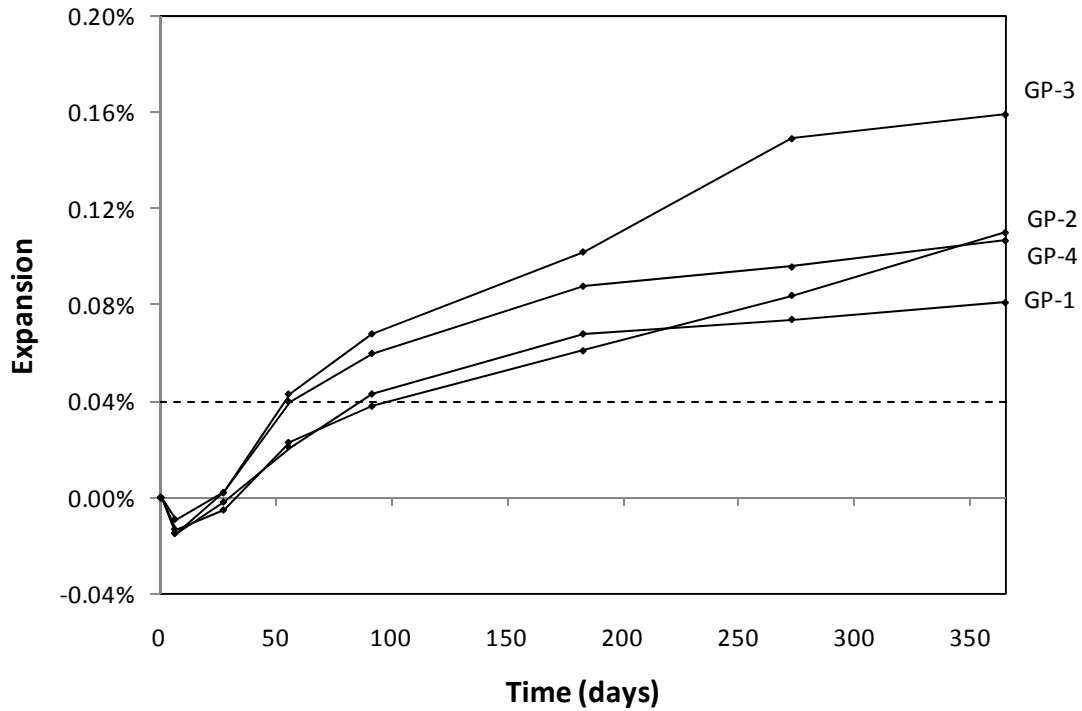


Figure 59. ASTM C1293 results for Goton aggregate.

There was slightly more variation in expansion among the Goton specimens. One reason for this could be that some aggregate on the surface of GP-3 and GP-4 was exposed. Still, all four of the Goton specimens greatly exceeded the expansion limit of 0.04 percent after one year. The average expansion was 0.114 percent, and the Goton aggregate is classified by ASTM C1293 as potentially deleteriously reactive.

C.3.2 AMBT Results

The average expansions for the three mortar bars in each set are shown in Figure 60. As can be seen from the graph, expansion data correlated well in all sets of mortar bars.

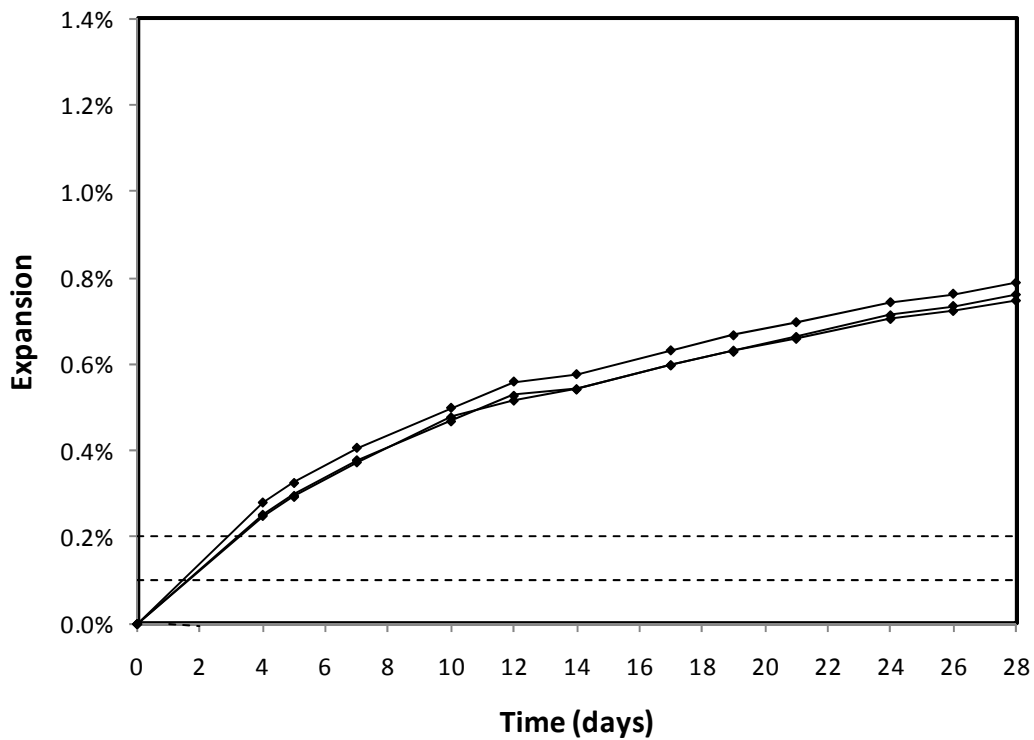


Figure 60. ASTM C1260 average Goton mortar bar expansion.

At 14 days after the zero reading the average expansion for all specimens was 0.554 percent which is nearly three times greater than the 0.20 percent limit for reactive aggregate. Therefore, ASTM C1260 classifies the Goton aggregate as reactive, which indicates that comparison with other test methods is required.

C.3.3 Kinetic Method Results

The values obtained by linear regression are presented in **Error! Reference source not found.**, and a plot showing the quality of the MMF curve approximation is shown in Figure 50.

Table 25. Kinetic Method results for Goton aggregate.

$\ln(k)$	-2.304
M	0.801
t_0	0.00

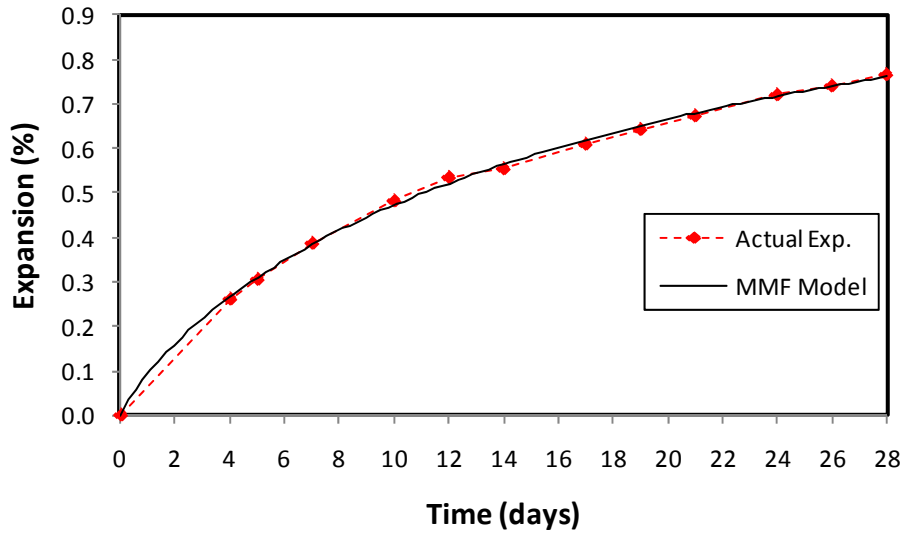


Figure 61. Average actual expansion and MMF approximation for Goton aggregate.

$\ln(k)$ is greater than -6 so the Goton aggregate is classified as reactive using the kinetic method.

C.3.4 Modified CAMBT Results

There was excellent agreement among the expansions of all three mortar bars. To correct for fluctuations in storage temperature, expansion values were adjusted to a normalized temperature of 80° C (176° F). The coefficient of thermal expansion was determined from the difference between the initial reading at room temperature and the zero reading at the elevated temperature.

Measurement was stopped at day 21 for this test, so the 28 day values shown for expansion and mass change (Figure 63) are linear extrapolations of the previous data with some decay included. The accuracy of these extrapolations does not affect the reliability of the test because aggregates are evaluated at day 14. The graph of the mortar bar expansions can be seen in Figure 62.

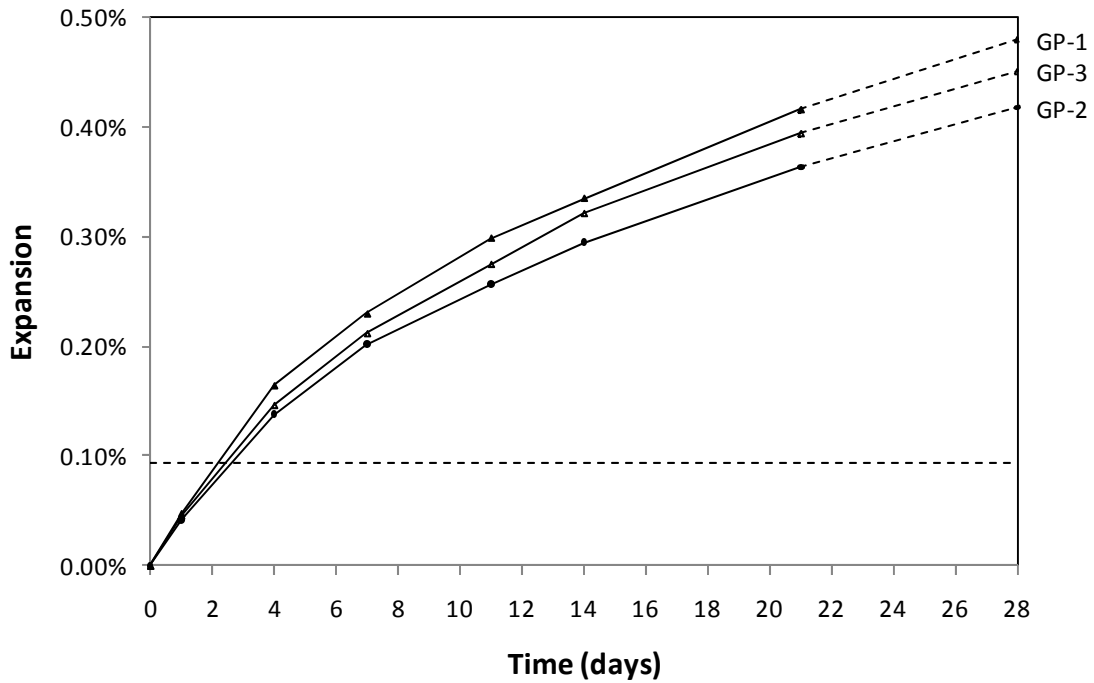


Figure 62. CAMBT Mortar bar expansion for Goton.

At 14 days after the zero reading the average expansion for the mortar bars was 0.317 percent which greatly exceeds the critical expansion limit of 0.093 percent. Therefore, this test classifies the Goton aggregate as reactive.

Figure 63 shows that the mass of the bars increases for the first day and then begins to decrease through the remainder of the test until the mass of the mortar bars are 1.10 – 1.25 percent less at 21 days and an estimated 1.50 – 1.70 percent less at 28 days.

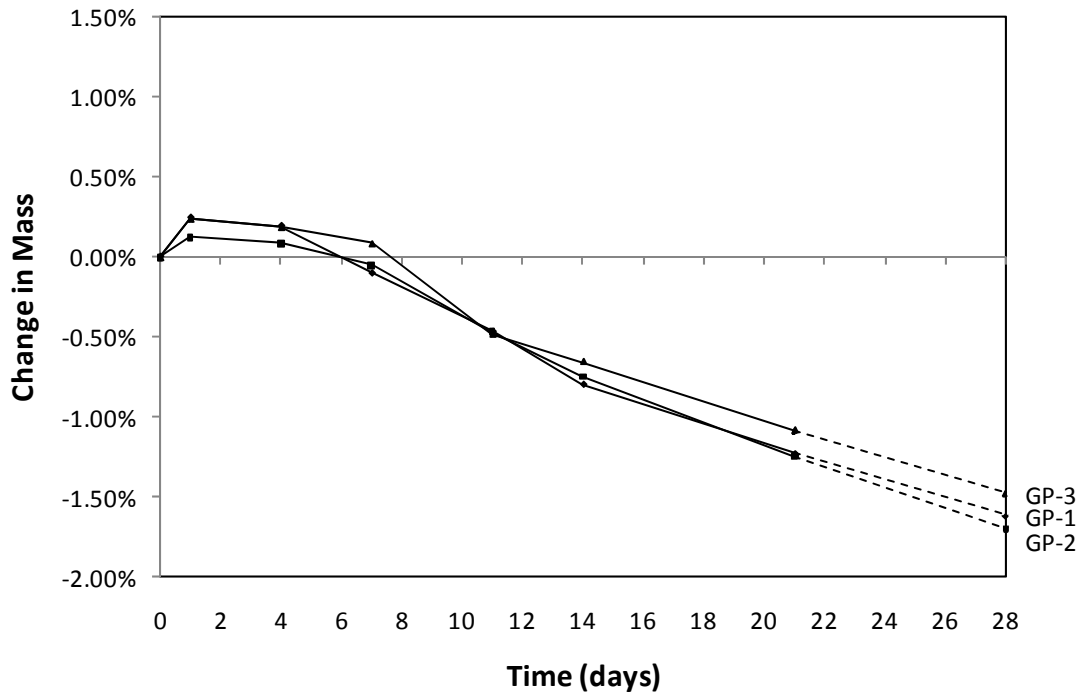


Figure 63. Mass change (%) for Goton mortar bars in the modified CAMBT.

C.3.5 Summary

The expansion ratio comparison in Figure 64 shows the ratio of measured expansion versus the expansion limit for each accelerated test for the Goton aggregate.

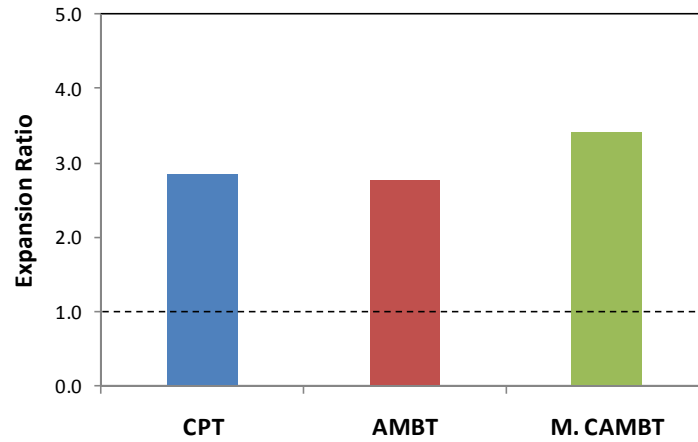


Figure 64. Expansion ratio comparison for Goton.

C.4 Harris

C.4.1 CPT Results

The graph of the expansions can be seen in Figure 65.

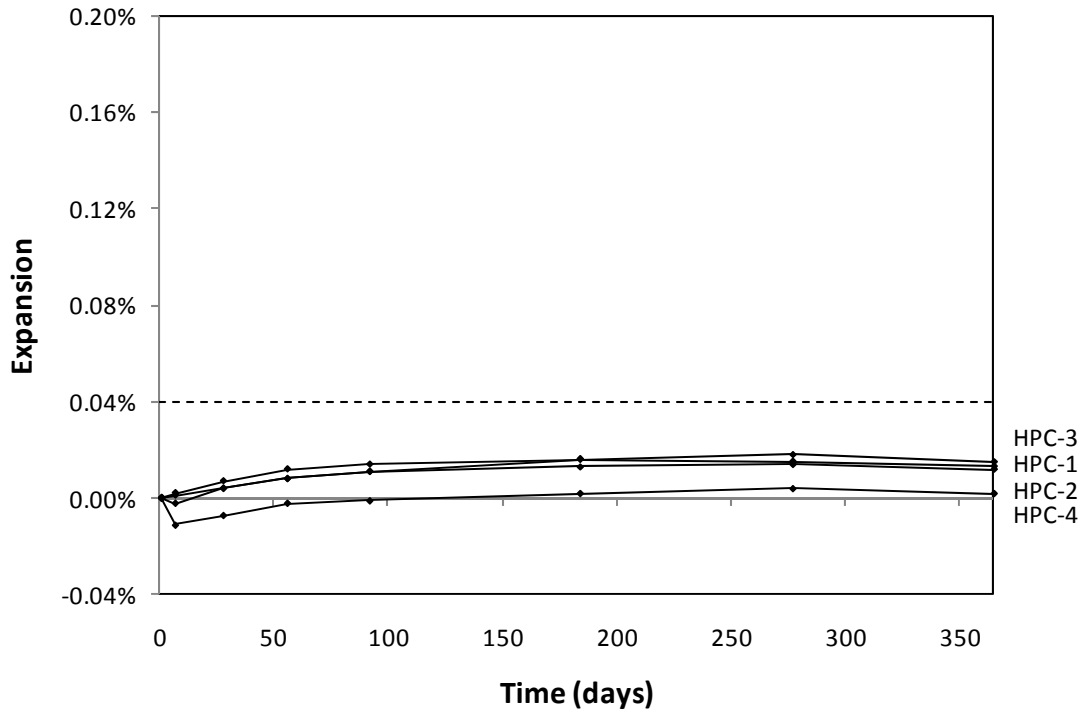


Figure 65. ASTM C1293 expansion for Harris.

There is excellent agreement in the expansions among all four specimens. The average expansion at one year was 0.011 percent which is well below the 0.04 percent limit. Therefore, ASTM C1293 classifies the Harris aggregate as non-reactive.

C.4.2 AMBT Results

The average expansions for the three mortar bars in each set are shown in Figure 66. As can be seen from the graph, expansion data for all sets of mortar bars correlated well with each other.

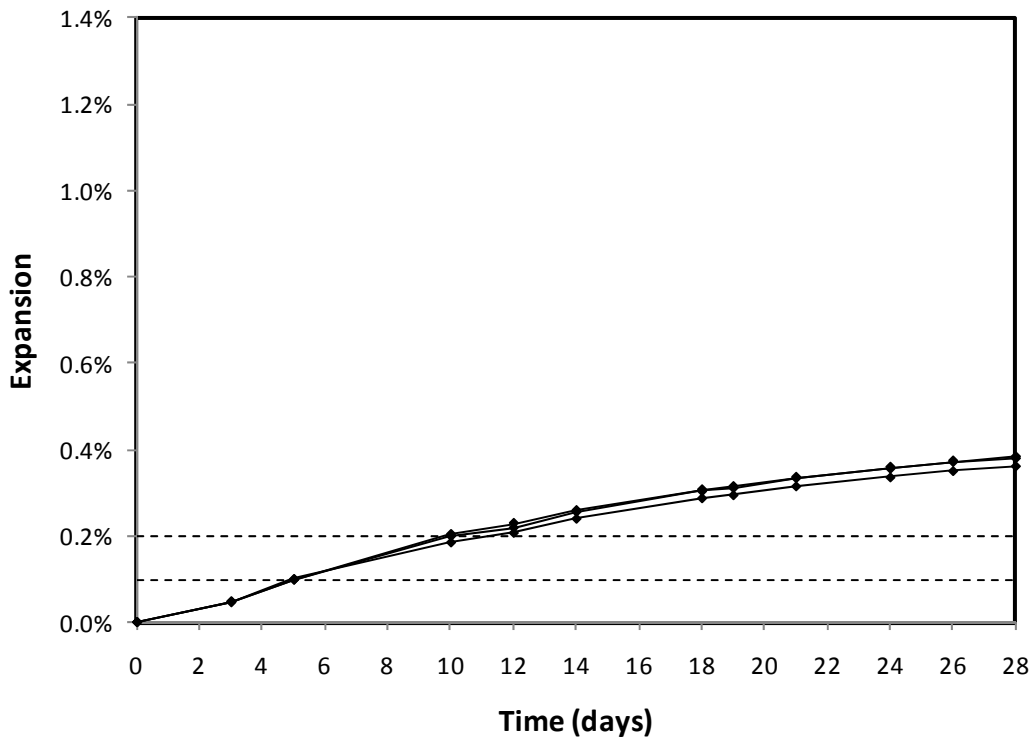


Figure 66. ASTM C1260 average Harris mortar bar expansion.

At 14 days after the zero reading the average expansion for all specimens was 0.252 percent which is slightly greater than the 0.20 percent limit for reactive aggregate. Therefore, ASTM C1260 classifies the Harris aggregate as potentially deleteriously reactive, which indicates that comparison with other test methods is required.

C.4.3 Kinetic Method Results

The values obtained by linear regression are presented in **Error! Reference source not found.**, and a plot showing the quality of the MMF curve approximation is shown in Figure 50.

Table 26. Kinetic Method results for Harris aggregate.

$\ln(k)$	-3.728
M	0.903
t_0	3.08

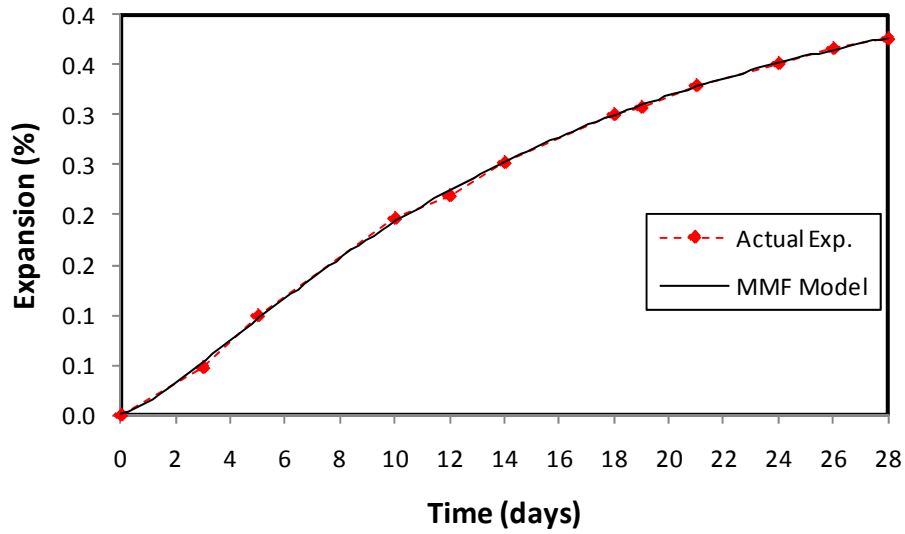


Figure 67. Average actual expansion and MMF approximation for Harris aggregate.

$\ln(k)$ is greater than -6 so the Harris aggregate is classified as reactive using the kinetic method.

C.4.4 Modified CAMBT Results

There was excellent agreement among the expansions of all three mortar bars. The graph of the mortar bar expansions can be seen in Figure 68.

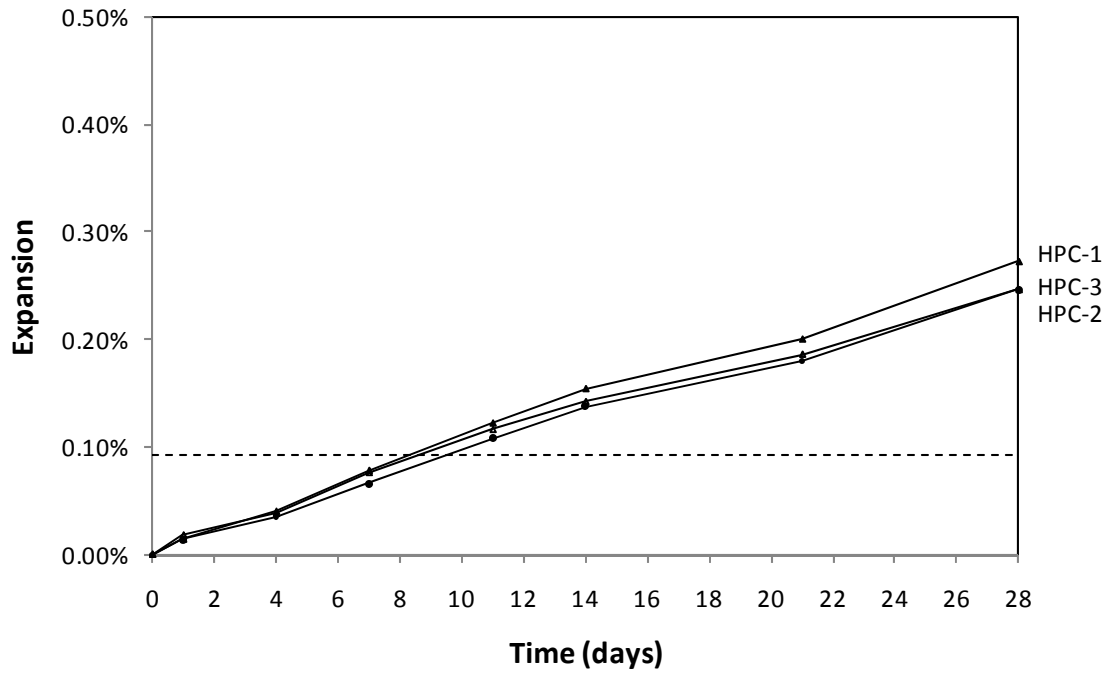


Figure 68. CAMBT Mortar bar expansion for Harris.

At 14 days after the zero reading the average expansion for the mortar bars was 0.145 percent which exceeds the critical expansion limit of 0.093 percent. Therefore, this test classifies the Harris aggregate as reactive.

Figure 69 shows that the mass of the specimens increases for about 14 days and then begins to decrease through the end of the test where the bars are 0.40 – 0.50 percent heavier than at the beginning of the test.

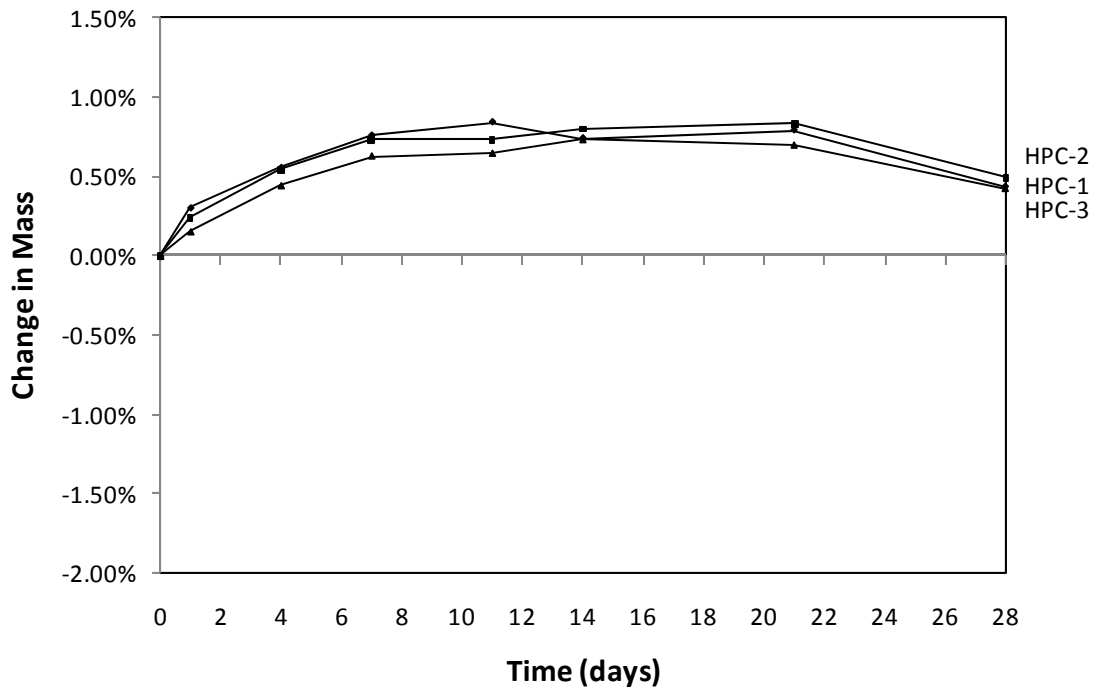


Figure 69. Mass change (%) for Harris mortar bars in the modified CAMBT.

C.4.5 Summary

The expansion ratio comparison in Figure 70 shows the ratio of measured expansion versus the expansion limit for each accelerated test for the Harris aggregate.

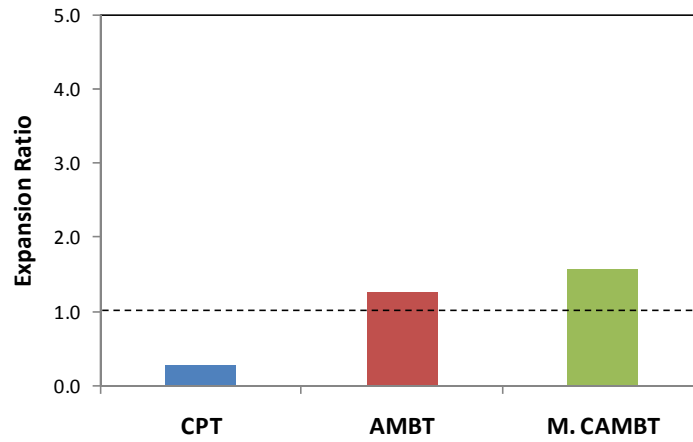


Figure 70. Expansion ratio comparison for Harris.

C.5 Knife River

C.5.1 CPT Results

There is good agreement among the expansions of all four specimens, which is clear in the figure.

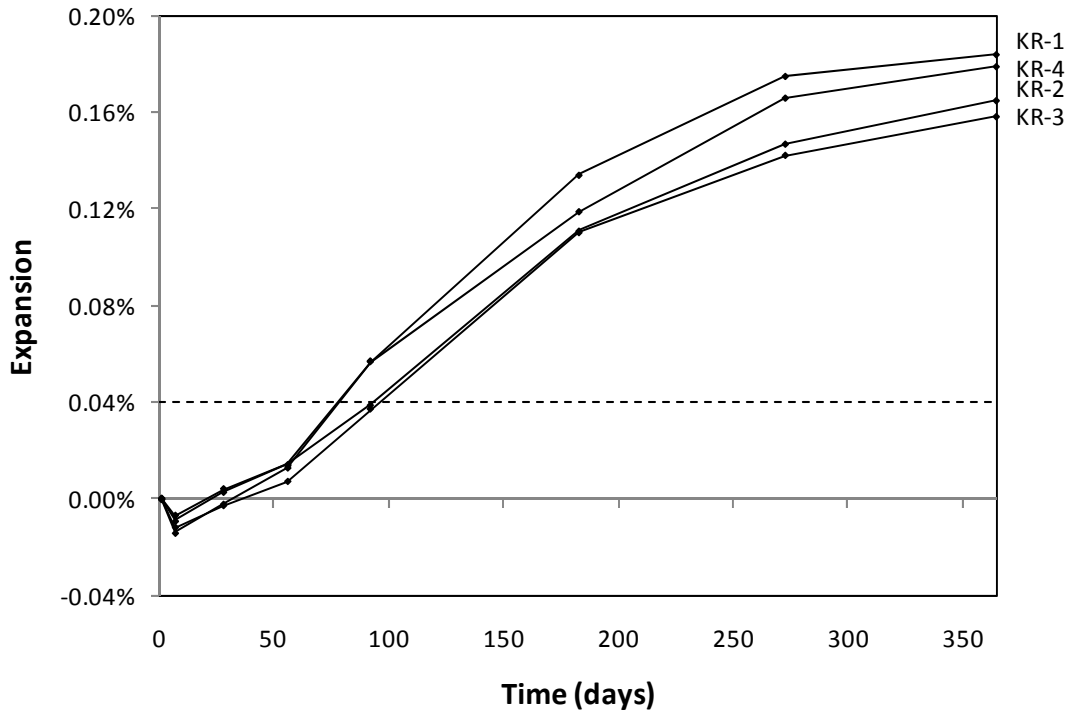


Figure 71. ASTM C1293 results for Knife River aggregate.

The average expansion at one year was 0.172 percent which is significantly greater than the expansion limit. Therefore, ASTM C1293 classifies the Knife River aggregate as potentially deleteriously reactive.

C.5.2 AMBT Results

The average expansions for the three mortar bars in each set are shown in Figure 72. As can be seen from the graph, expansion data for all sets of mortar bars correlated well with each other.

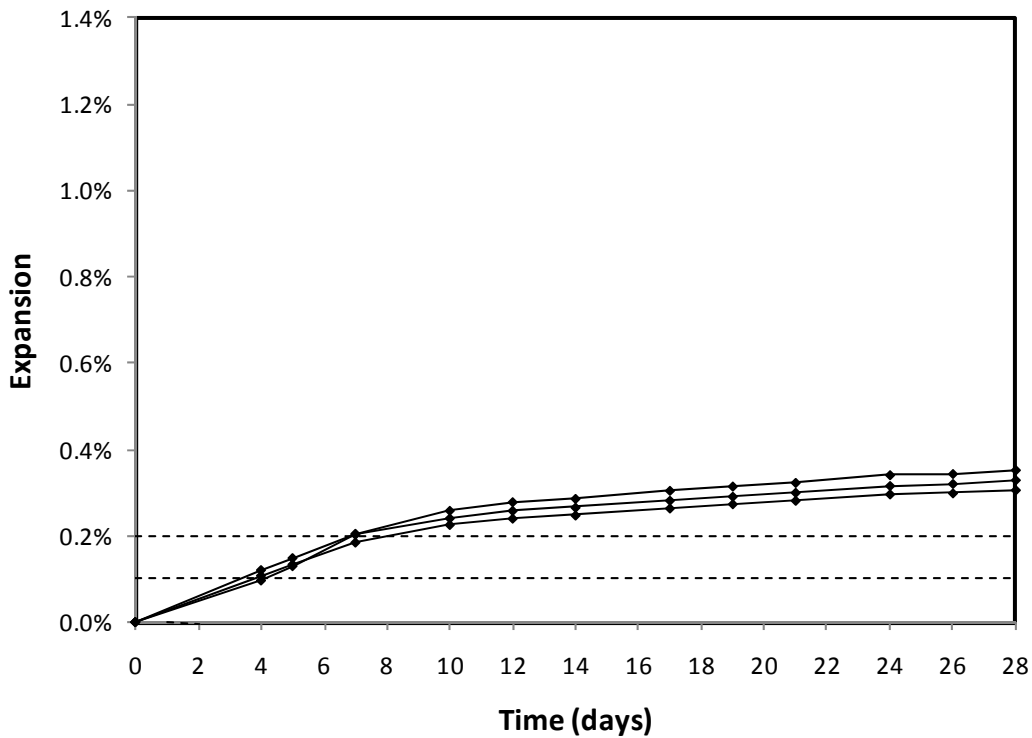


Figure 72. ASTM C1260 average Knife River mortar bar expansion.

At 14 days after the zero reading the average expansion for all specimens was 0.267 percent which is slightly greater than the 0.20 percent limit for reactive aggregate. Therefore, ASTM C1260 classifies the Knife River aggregate as reactive, which indicates that comparison with other test methods is required.

C.5.3 Kinetic Method Results

The values obtained by linear regression are presented in **Error! Reference source not found.**, and a plot showing the quality of the MMF curve approximation is shown in Figure 50.

Table 27. Kinetic Method results for Knife River aggregate.

$\ln(k)$	-3.160
M	0.698
t_0	1.68

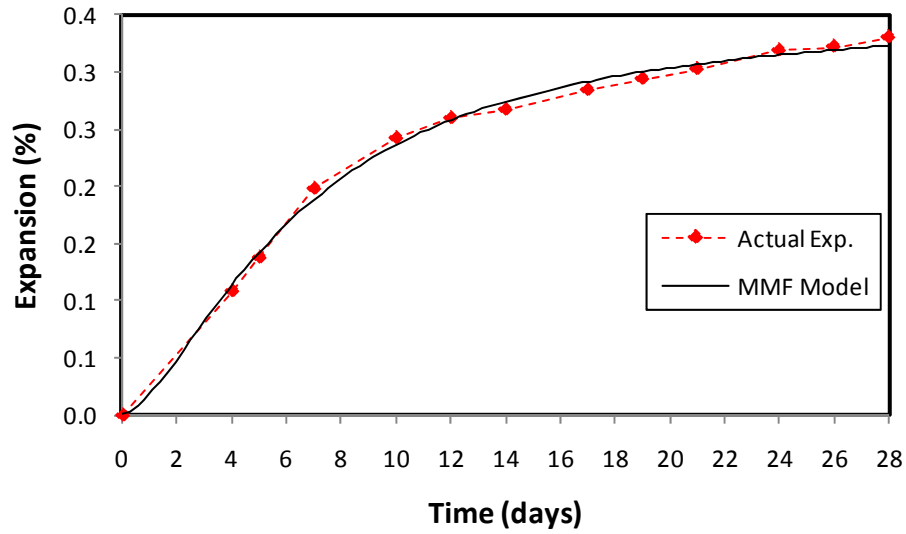


Figure 73. Average actual expansion and MMF approximation for Knife River aggregate.

$Ln(k)$ is greater than -6 so the Knife River aggregate is classified as reactive using the kinetic method.

C.5.4 Modified CAMBT Results

There was excellent agreement among the expansions of all three mortar bars. The graph of their expansions can be seen in Figure 74.

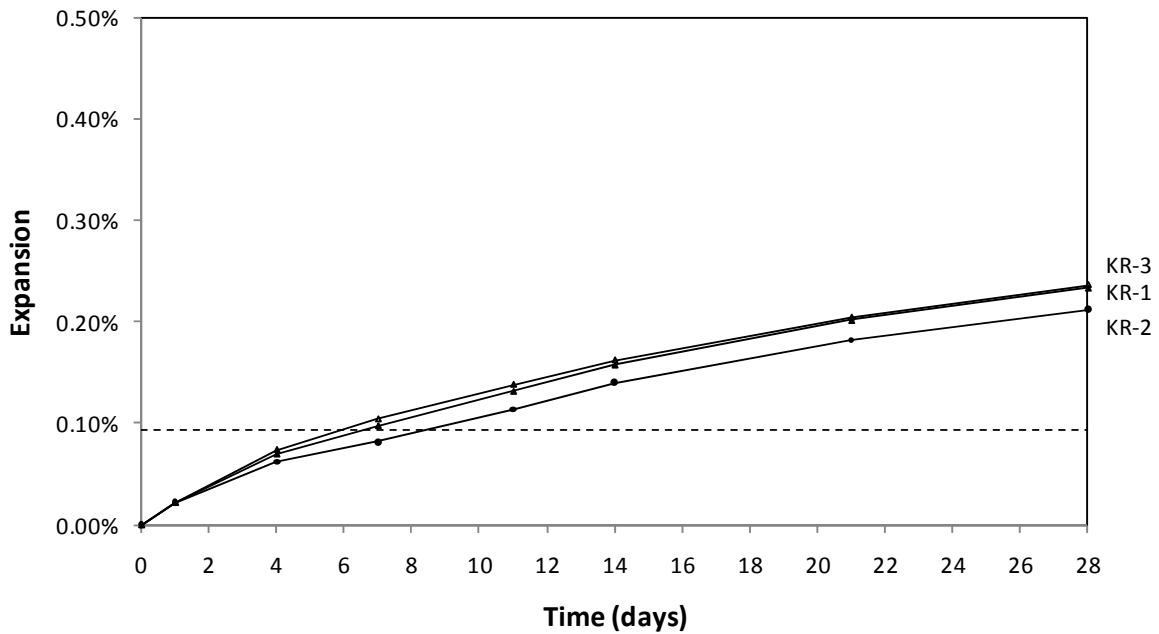


Figure 74. CAMBT Mortar bar expansion for Knife River.

At 14 days after the zero reading the average expansion for the mortar bars was 0.153 percent which exceeds the critical expansion limit of 0.093 percent. Therefore, this test classifies the Knife River aggregate as potentially deleteriously reactive.

Figure 75 shows that except for a short mass loss by two of the bars during day 1, the mass of the bars continues to increase for the duration of the test. At the end of the test, the specimens were 1.0 to 1.3 percent heavier.

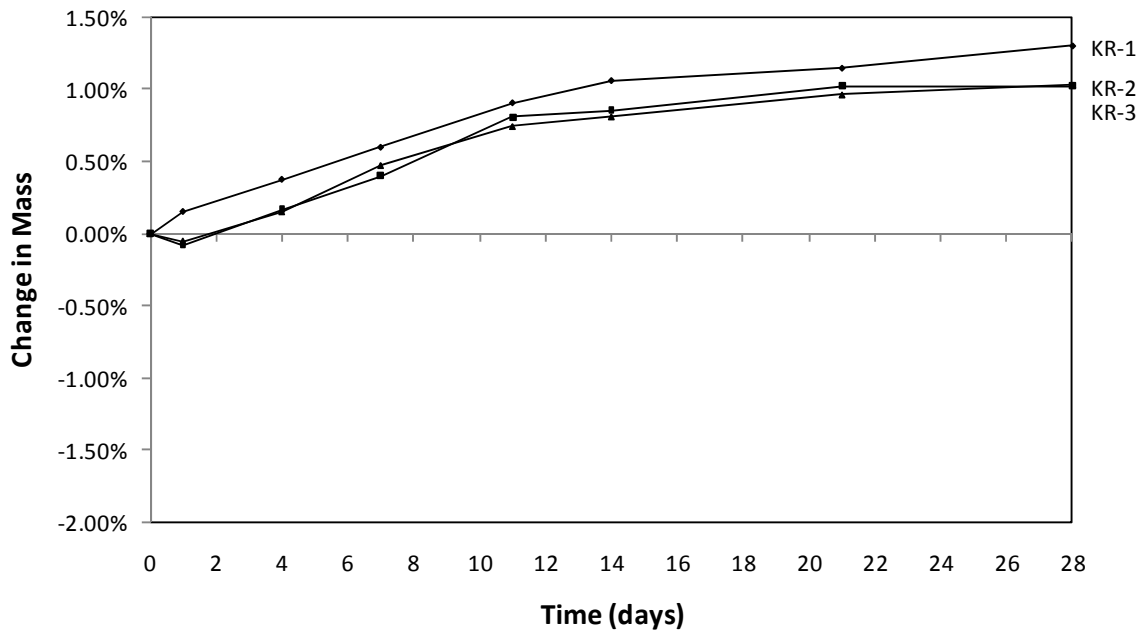


Figure 75. Mass change (%) for Knife River mortar bars in the modified CAMBT.

C.5.5 Summary

The expansion ratio comparison in Figure 76 shows the ratio of measured expansion versus the expansion limit for each accelerated test for the Knife River aggregate.

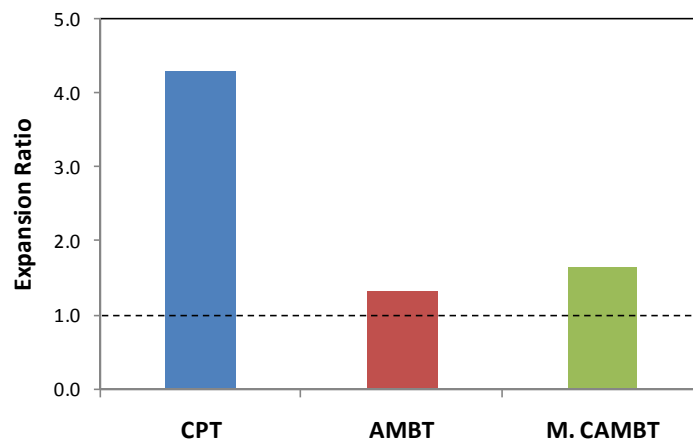


Figure 76. Expansion ratio comparison for Knife River.

C.6 Labarge

C.6.1 CPT Results

The figure below shows the specimen expansion with respect to time.

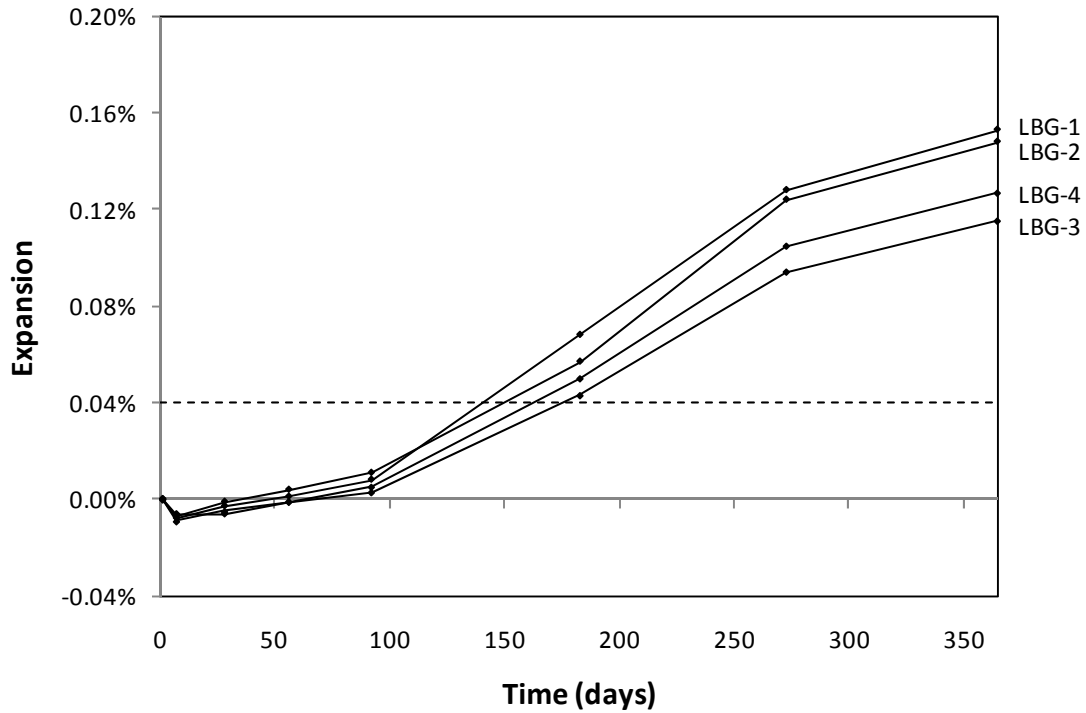


Figure 77. ASTM C1293 results for Labarge aggregate.

There is good agreement among the expansions of all four specimens. The average expansion at one year was 0.136 percent which is significantly greater than the expansion limit. Therefore, ASTM C1293 classifies the Labarge aggregate as potentially deleteriously reactive.

C.6.2 AMBT Results

The average expansions for the three mortar bars in each set are shown in Figure 72.

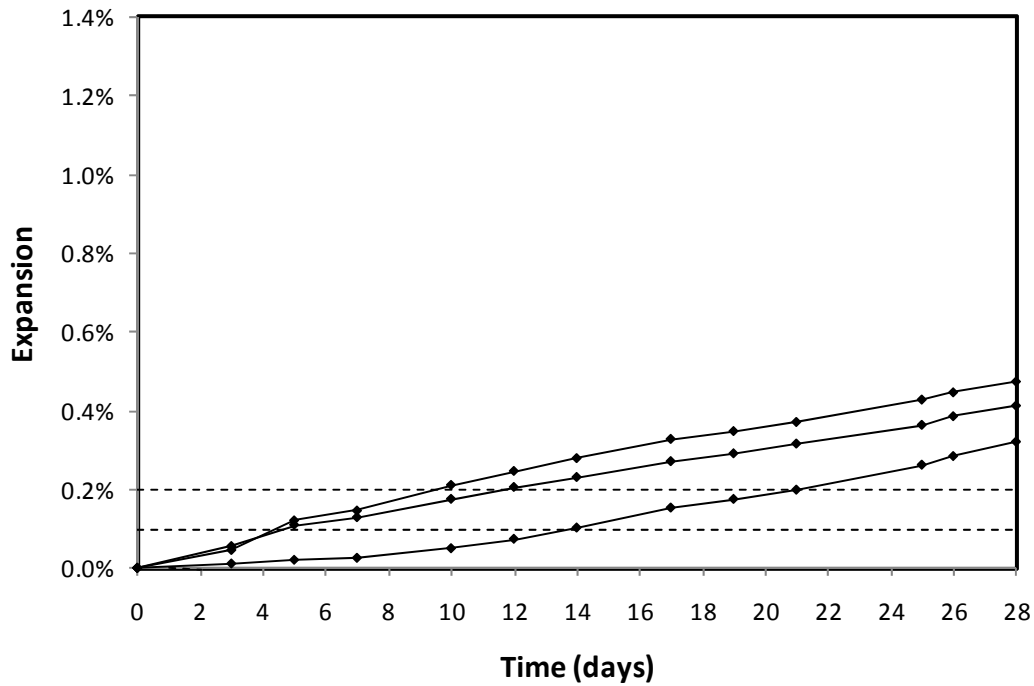


Figure 78. ASTM C1260 average Labarge mortar bar expansion.

At 14 days after the zero reading the average expansion for all specimens was 0.204 percent which is just slightly greater than the 0.20 percent limit for reactive aggregate. Therefore, ASTM C1260 classifies the Labarge aggregate as reactive, which indicates that comparison with other test methods is required.

C.6.3 Kinetic Method Results

The values obtained by linear regression are presented in Table 28, and a plot showing the quality of the MMF curve approximation is shown in Figure 50.

Table 28. Kinetic Method results for Labarge aggregate.

$\ln(k)$	-4.227
M	1.036
t_0	6.16

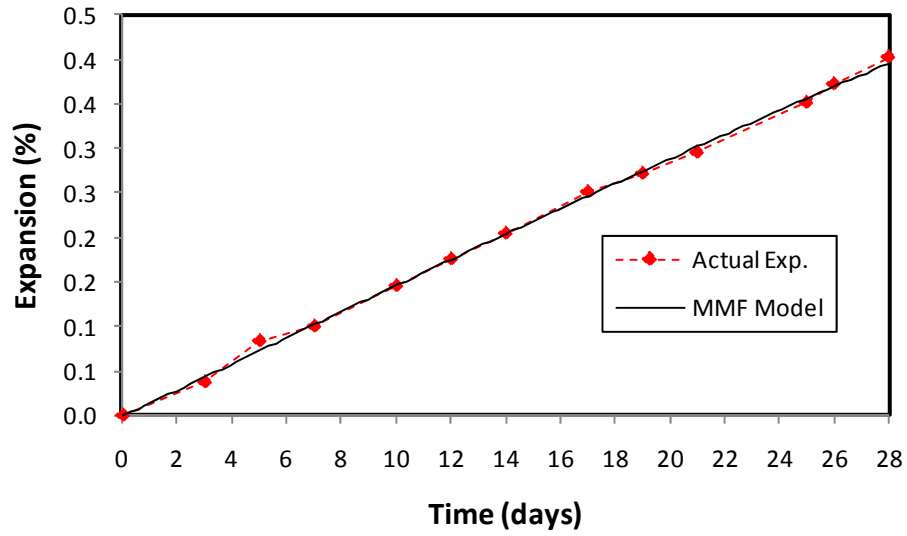


Figure 79. Average actual expansion and MMF approximation for Labarge aggregate.

$\ln(k)$ is greater than -6 so the Labarge aggregate is classified as reactive using the kinetic method.

C.6.4 Modified CAMBT Results

There was excellent agreement among the expansions of all three mortar bars. The graph of their expansions can be seen in Figure 74.

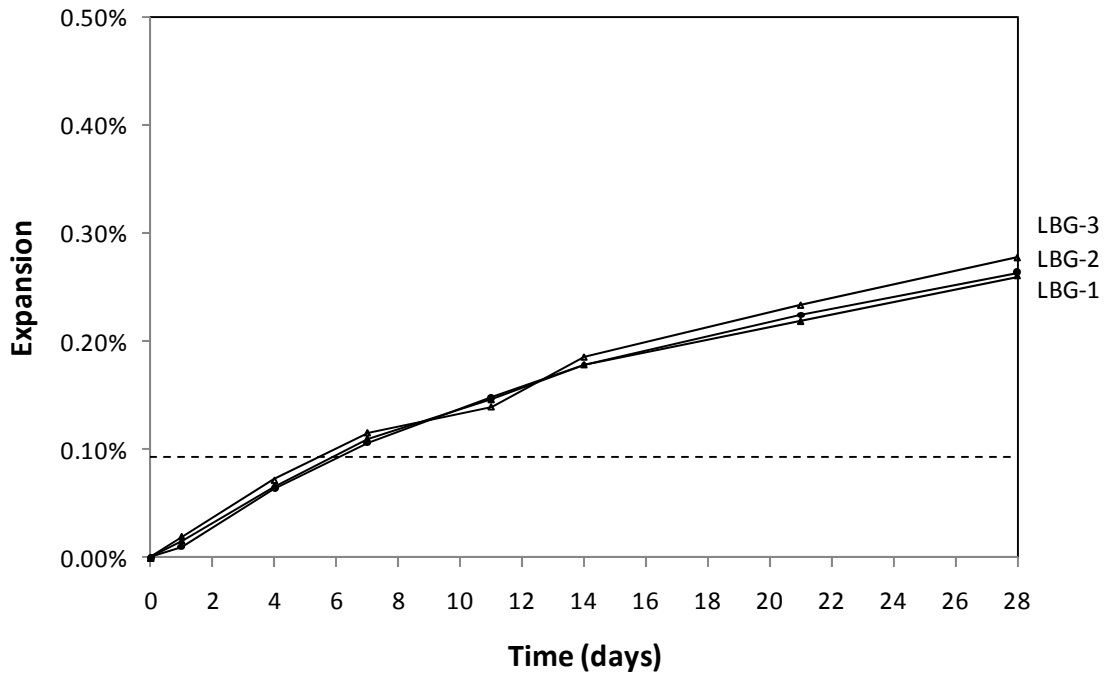


Figure 80. CAMBT Mortar bar expansion for Labarge.

At 14 days after the zero reading the average expansion for the mortar bars was 0.181 percent which exceeds the critical expansion limit of 0.093 percent. Therefore, this test classifies the Labarge aggregate as potentially deleteriously reactive.

Figure 81 shows that the bars gained mass until approximately day 17 and then began to lose mass until, at day 28, the specimens had lost an average of 0.39 percent of their original mass.

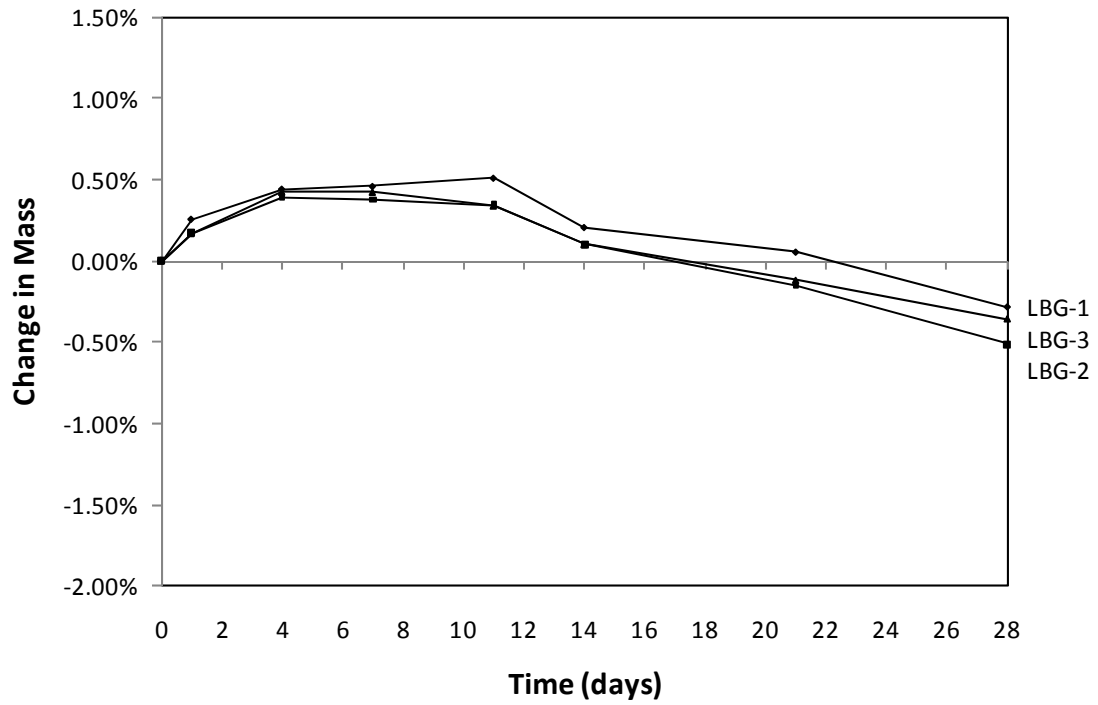


Figure 81. Mass change (%) for Labarge mortar bars in the modified CAMBT.

C.6.5 Summary

The expansion ratio comparison in Figure 82 shows the ratio of measured expansion versus the expansion limit for each accelerated test for the Labarge aggregate.

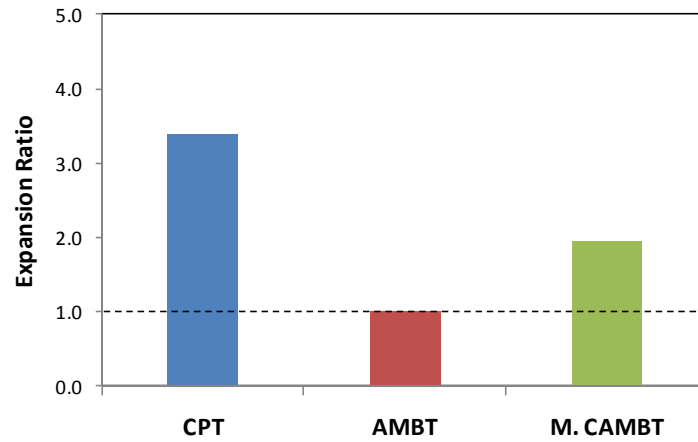


Figure 82. Expansion ratio comparison for Labarge.

C.7 Lamax

C.7.1 CPT Results

The graph of the expansions can be seen in Figure 83.

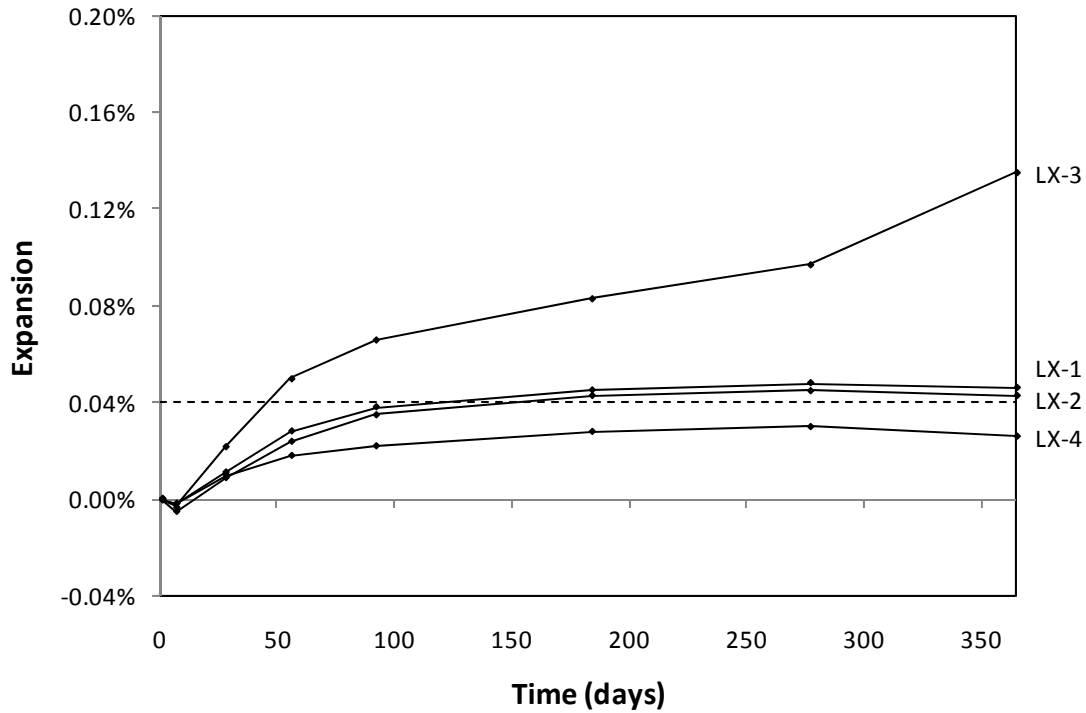


Figure 83. ASTM C1293 expansion for Lamax.

There is good agreement between LX-1, LX-2, and LX-4, but LX-3 displays more reactive behavior. The average expansion for the specimen group that excludes LX-3 is 0.038 percent which would result in a non-reactive classification. However, when LX-3 is included, the group average increases to 0.063 percent which results in a reactive classification. The standard deviation of LX-1, 2, and 4 is 1.08×10^{-4} mm, so LX-3 is 6.7 times greater than this standard deviation.

C.7.2 AMBT Results

The average expansions for the three mortar bars in each set are shown in Figure 84. As can be seen from the graph, expansion data for all sets of mortar bars correlated well with each other.

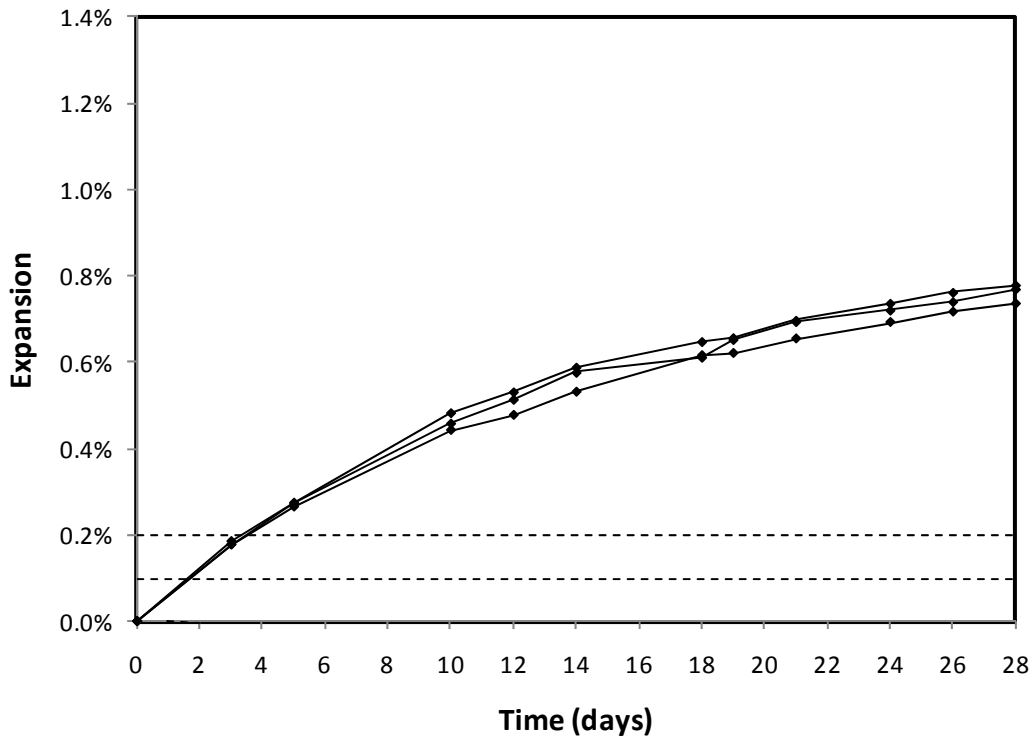


Figure 84. ASTM C1260 average Lamax mortar bar expansion.

At 14 days after the zero reading the average expansion for all specimens was 0.566 percent which is nearly three times greater than the 0.20 percent limit for reactive aggregate. Therefore, ASTM C1260 classifies the Lamax aggregate as reactive, which indicates that comparison with other test methods is required.

C.7.3 Kinetic Method Results

The values obtained by linear regression are presented in Table 29, and a plot showing the quality of the MMF curve approximation is shown in Figure 50.

Table 29. Kinetic Method results for Lamax aggregate.

$\ln(k)$	-2.665
M	0.913
t_0	0.28

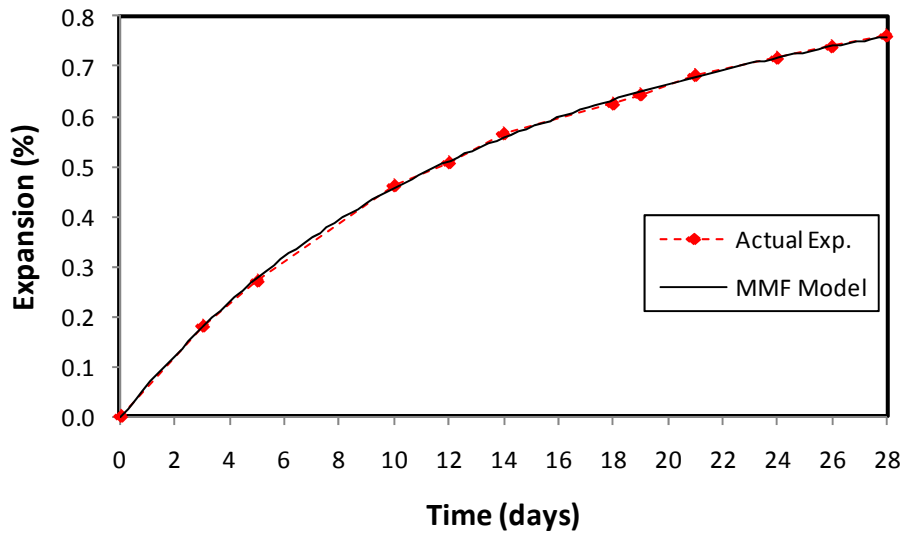


Figure 85. Average actual expansion and MMF approximation for Lamax aggregate.

$\ln(k)$ is greater than -6 so the Lamax aggregate is classified as reactive using the kinetic method.

C.7.4 Modified CAMBT Results

There was excellent agreement among the expansions of all three mortar bars. The graph of their expansions can be seen in Figure 86.

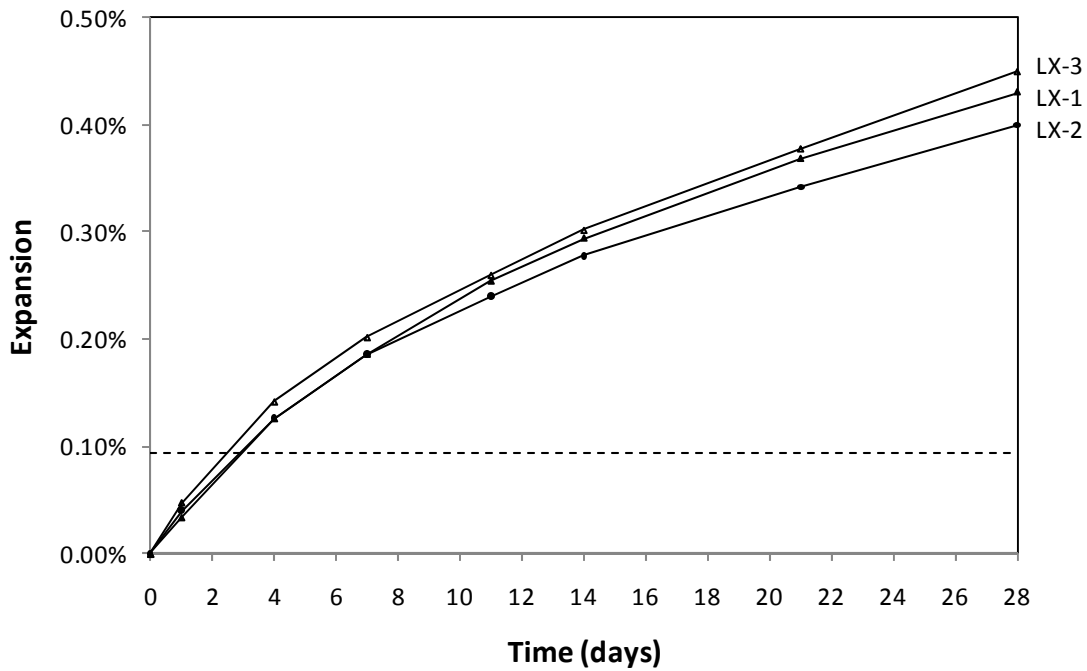


Figure 86. CAMBT Mortar bar expansion for Lamax.

At 14 days after the zero reading the average expansion for the mortar bars was 0.291 percent which greatly exceeds the critical expansion limit of 0.093 percent. Therefore, this test classifies the Lamax aggregate as potentially deleteriously reactive.

Figure 87 shows that the mass of the bars increases for the first few days and then begins to decrease until the day 28 where the mass is about 0.40 – 0.50 percent less than at the beginning of the test.

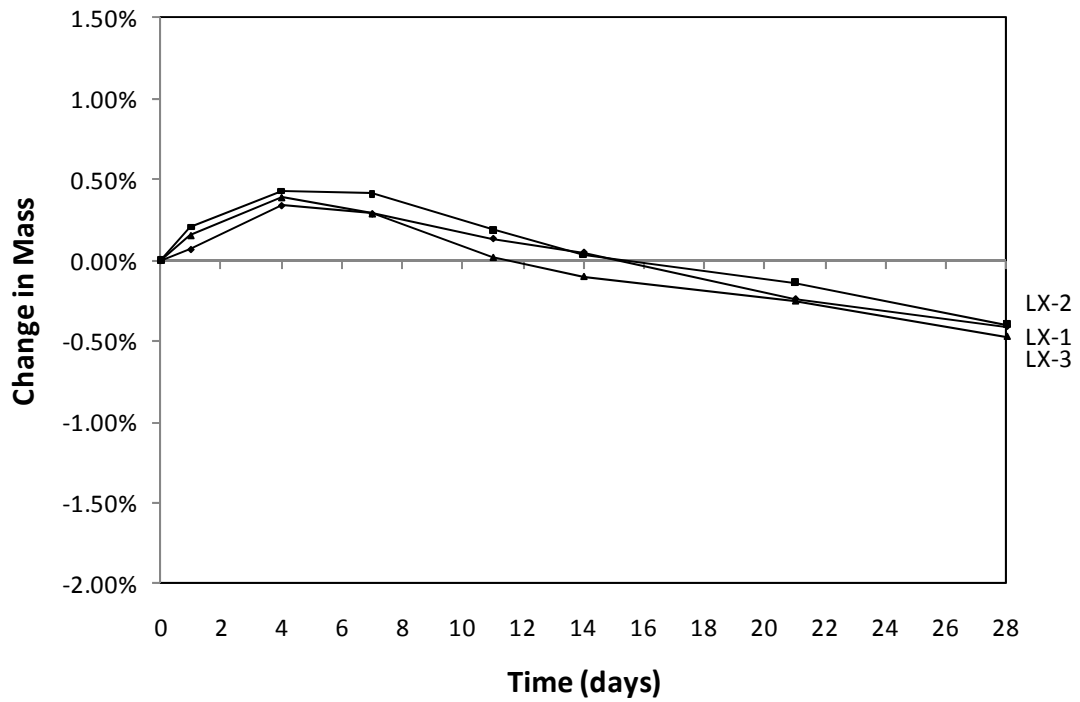


Figure 87. Mass change (%) for Lamax mortar bars in the modified CAMBT.

C.7.5 Summary

The expansion ratio comparison in Figure 88 shows the ratio of measured expansion versus the expansion limit for each accelerated test for the Lamax aggregate.

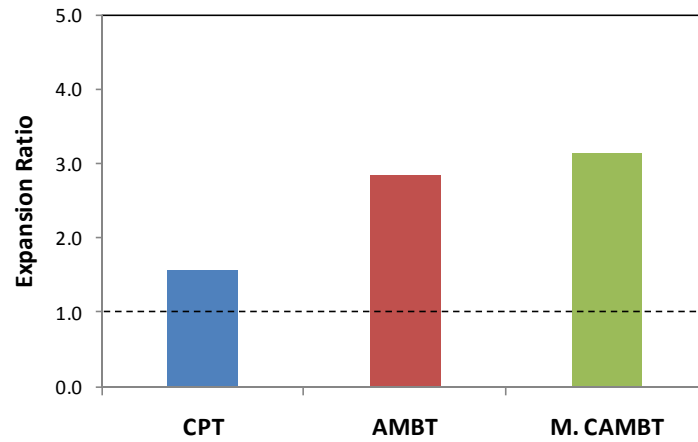


Figure 88. Expansion ratio comparison for Lamax.

C.8 Worland

C.8.1 CPT Results

There is good agreement among the expansions exhibited by the Worland specimens, which is shown in the figure below.

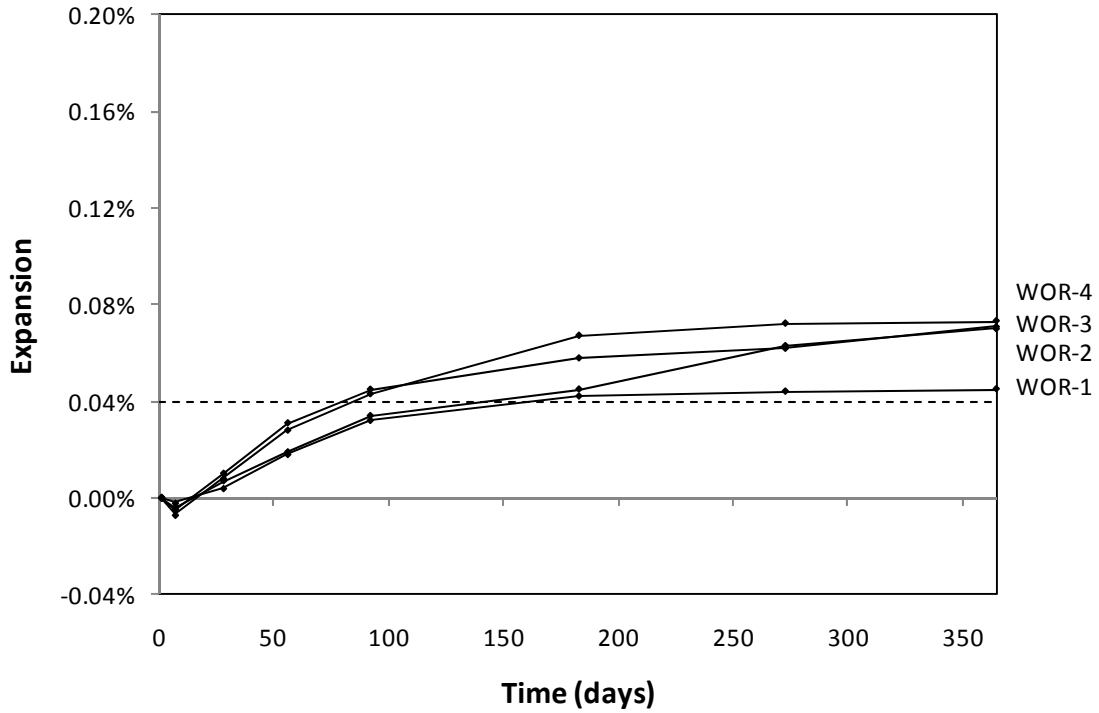


Figure 89. ASTM C1293 results for Worland aggregate.

The average expansion after one year was 0.065 percent which is greater than the expansion limit of 0.04 percent. Therefore, ASTM C1293 classifies Worland aggregate as potentially deleteriously reactive.

C.8.2 AMBT Results

The average expansions for the three mortar bars in each set are shown in Figure 72.

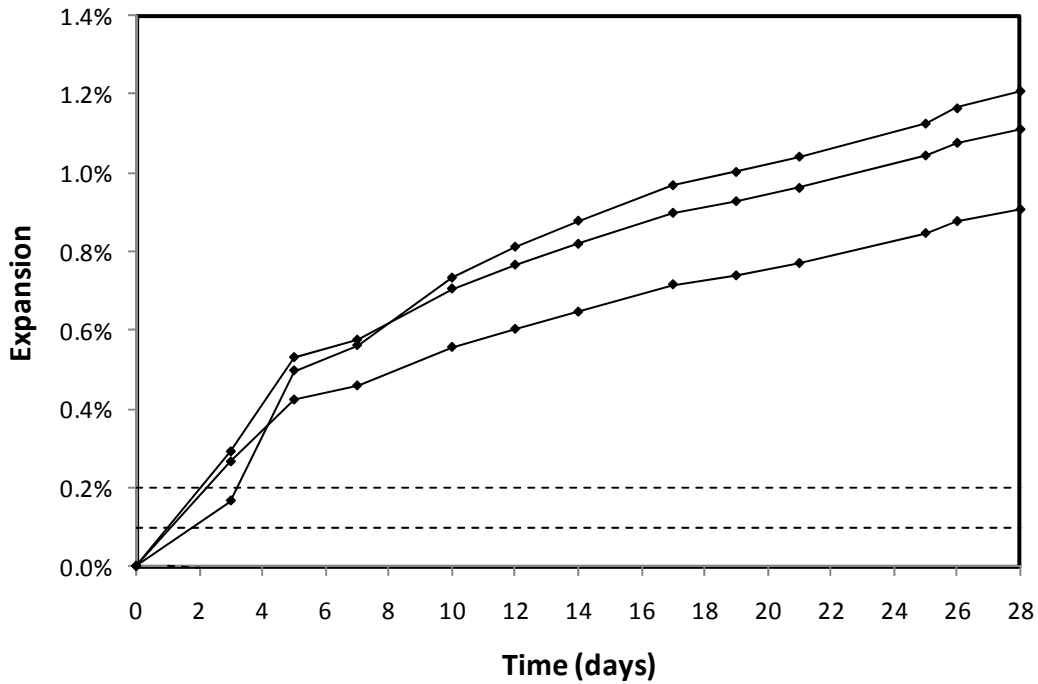


Figure 90. ASTM C1260 average Worland mortar bar expansion.

At 14 days after the zero reading the average expansion for all specimens was 0.781 percent which is nearly four times greater than the 0.20 percent limit for reactive aggregate. Therefore, ASTM C1260 classifies the Worland aggregate as reactive, which indicates that comparison with other test methods is required.

C.8.3 Kinetic Method Results

The values obtained by linear regression are presented in Table 30, and a plot showing the quality of the MMF curve approximation is shown in Figure 50.

Table 30. Kinetic Method results for Worland aggregate.

$\ln(k)$	-2.204
M	1.041
t_0	0.00

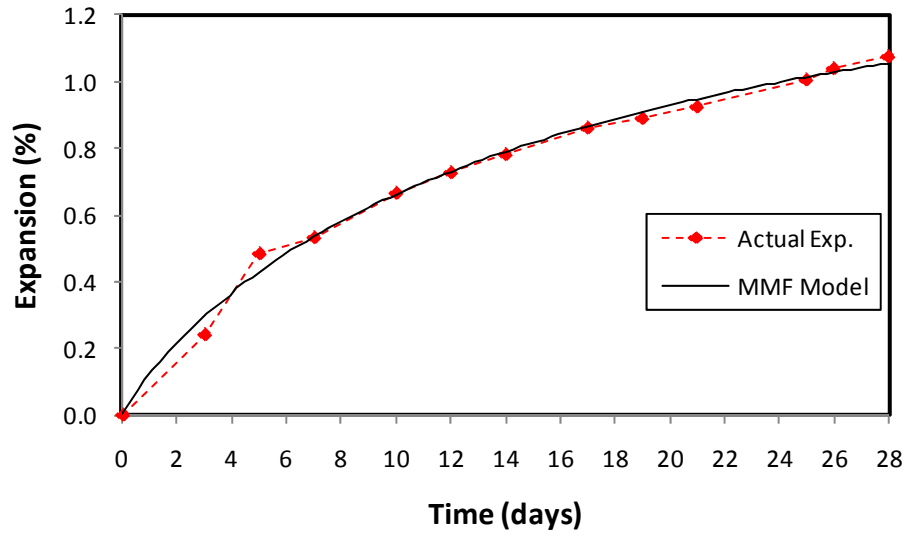


Figure 91. Average actual expansion and MMF approximation for Worland aggregate.

$\ln(k)$ is greater than -6 so the Worland aggregate is classified as reactive using the kinetic method.

C.8.4 Modified CAMBT Results

There was excellent agreement among the expansions of all three mortar bars. The graph of their expansions can be seen in Figure 74.

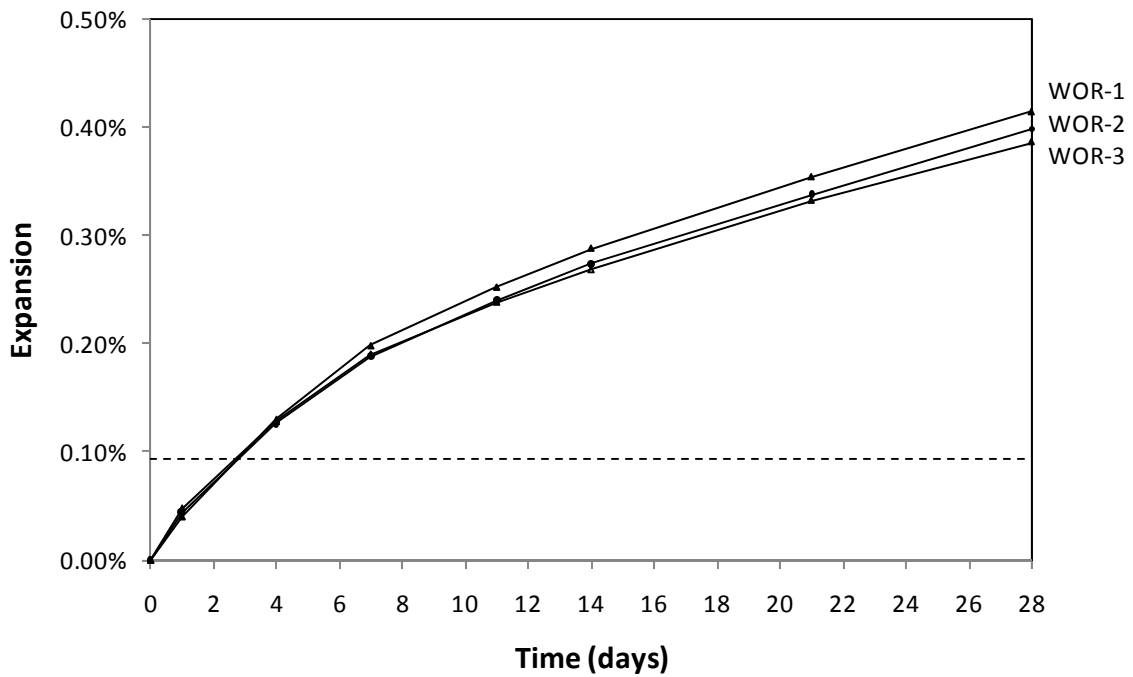


Figure 92. CAMBT Mortar bar expansion for Worland.

At 14 days after the zero reading the average expansion for the mortar bars was 0.277 percent which exceeds the critical expansion limit of 0.093 percent. Therefore, this test classifies the Worland aggregate as potentially deleteriously reactive.

Figure 93 shows that the bars gained mass until approximately day 14 and then began to lose mass until, at day 28, the specimens had lost an average of 0.47 percent of their original mass.

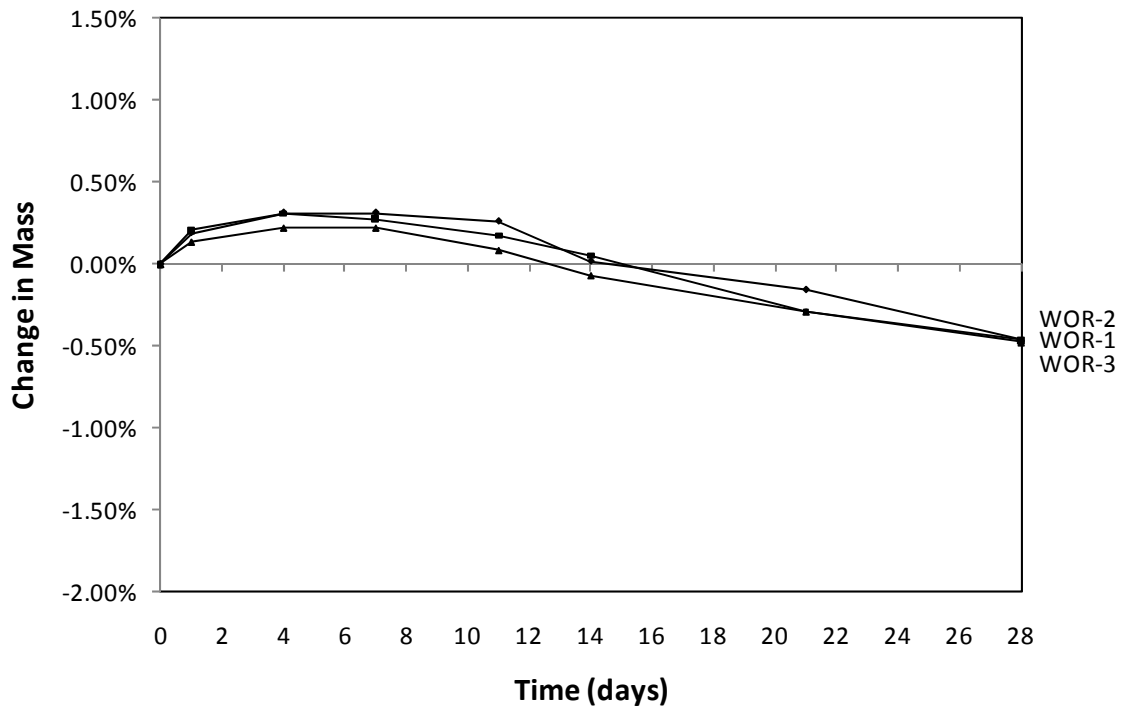


Figure 93. Mass change (%) for Worland mortar bars in the modified CAMBT.

C.8.5 Summary

The expansion ratio comparison in Figure 94 shows the ratio of measured expansion versus the expansion limit for each accelerated test for the Worland aggregate.

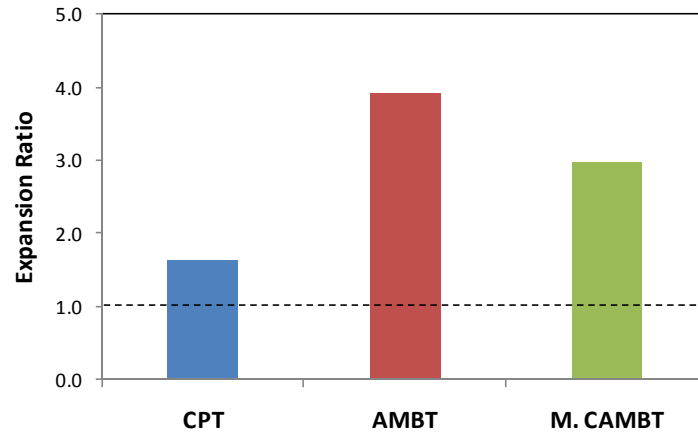
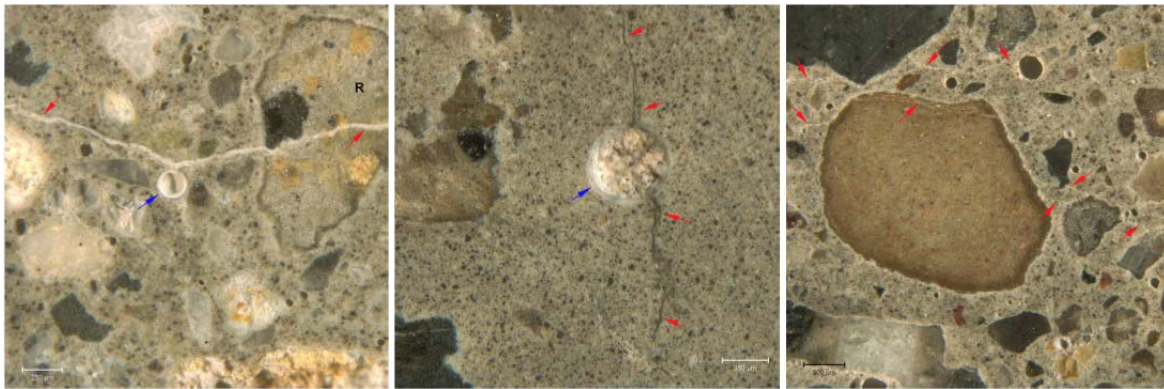


Figure 94. Expansion ratio comparison for Worland.

Appendix D: Petrography Report Summary

A summary of the petrography report by DRP Petrography is presented below. Results are organized alphabetically by aggregate. All text is quoted directly from the DRP interim report.

Black Rock Pit



(a)

(b)

(c)

Figure 95. Black Rock Pit exposure test samples. Reflected light photomicrographs of polished surfaces. Gel-filled microcracks (red arrows) on a) C 1260 mortar bar, b) CAMBT bar and c) C1293 concrete prism. The blue arrows in a) and b) indicate voids lined with gel.

The mortar bars from both the ASTM C 1260 and the CAMBT show severe ASR with abundant cracks and microcracks filled with ASR gel radiating from aggregates and cutting through the paste. The reactive components consist primarily of rhyolite particles; granitic rocks also show evidence of reactivity. Two ASTM C1293 concrete prisms were examined and show evidence of minor to moderate ASR. The rhyolite is the reactive component in the prism. No evidence of ASR was observed in the field specimen.

Devries Farm Pit

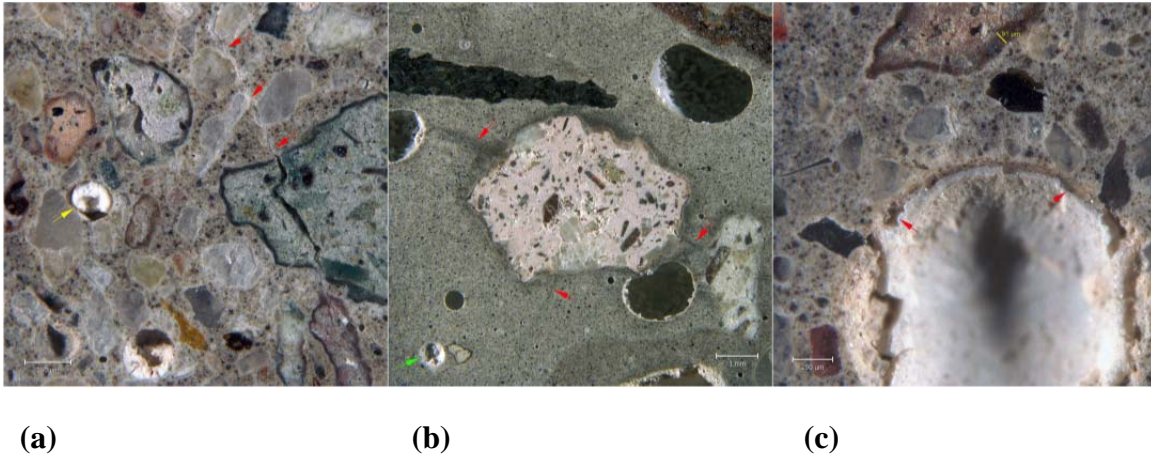


Figure 96. Devries Farm Pit exposure test samples. Reflected light photomicrographs of polished surfaces. Gel-filled microcracks (red arrows) on (a) C1260 mortar bar and (b) CAMBT bar. The yellow and green arrows in (a) and (b), respectively indicate voids lined with gel. In (c) the red arrows indicate gel lining a void and the yellow bar measures a reaction rim on a rhyolite particle on the C 1293 concrete prism.

The mortar bars from both the ASTM C 1260 and the CAMBT show severe ASR with abundant cracks and microcracks filled with ASR gel radiating from aggregates and cutting through the paste. The reactive components consist primarily of rhyolite particles; granitic rocks and quartzites also show evidence of minor ASR, with no significant microcracking observed. Occasional to rare deposits of gel were observed in voids and reaction rims were commonly observed on rhyolite particles, which make up the reactive component in the prism. No evidence of ASR was observed in the field specimen.

Goton Pit

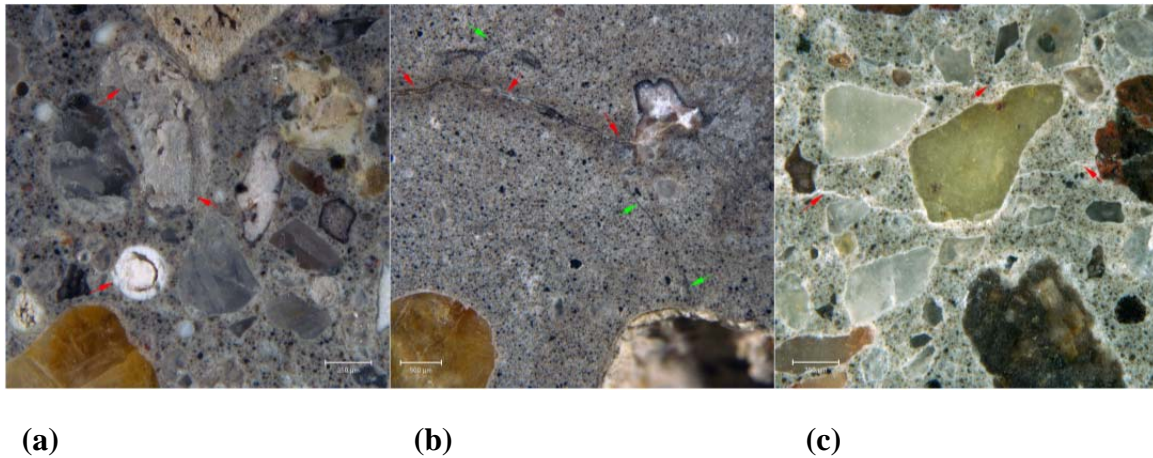


Figure 97. Goton Pit exposure test samples. Reflected light photomicrographs of polished surfaces. (a) Gel in void (red arrows) on C1260 mortar bar. (b) Hairline crack (red arrows) and microcrack (green arrows) filled with gel on CAMBT bar. (c) Microcracks (red arrows) on C1293 prism.

The mortar bars from the ASTM C1260 and CAMBT show moderate and severe ASR, respectively. The C1260 mortar bar showed very minor hairline macroscopic cracking; microcracks filled with ASR gel were rarely to occasionally observed and deposits of gel in voids were occasionally observed. The CAMBT bar showed abundant cracks and microcracks filled with ASR gel radiating from aggregates and cutting through the paste. The reactive components consist primarily of rhyolite particles; granitic rocks and quartzites also show evidence of reactivity. The ASTM C1293 concrete prism showed evidence of minor ASR, with no significant microcracking observed. Occasional to rare deposits of gel were observed in voids and reaction rims were commonly observed on rhyolite particles which make up the reactive component in the prism. No evidence of ASR was observed in the field specimen.

Harris Pit

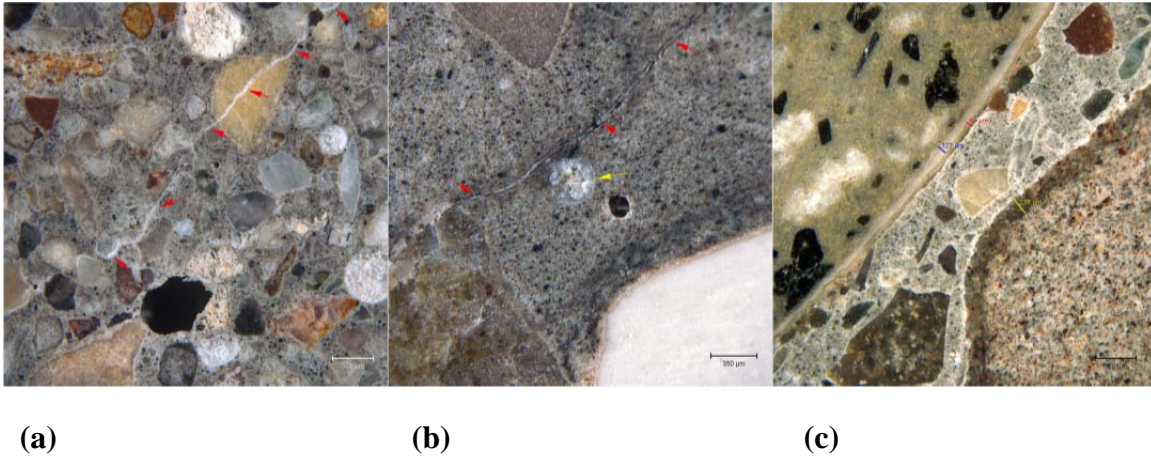
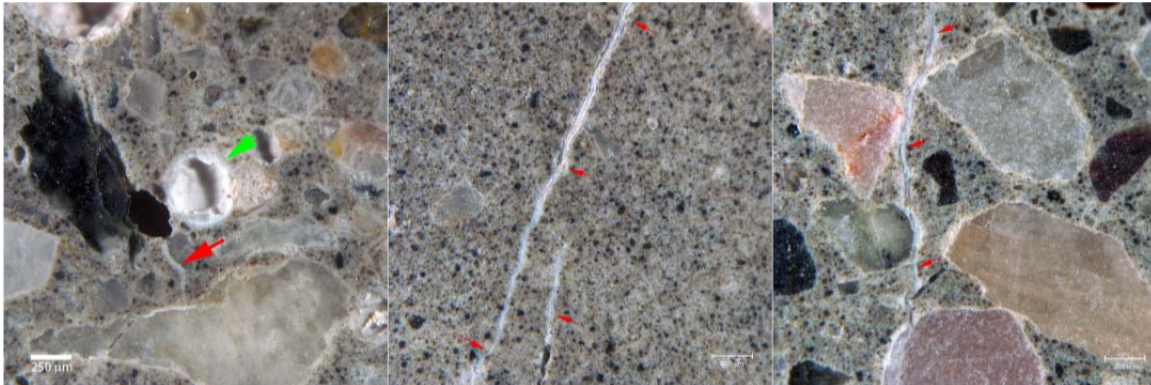


Figure 98. Harris Pit exposure test samples. Reflected light photomicrographs of polished surfaces. (a) Gel in microcracks (red arrows) on C1260 mortar bar. (b) Microcrack (red arrows) and void (yellow arrow) filled with gel on CAMBT bar. (c) Reaction rims on aggregate on C1293 prism.

The mortar bars from the ASTM C1260 and the CAMBT show moderate and severe ASR, respectively. The C1260 mortar bar showed no macroscopic cracks; microcracks filled with ASR gel were rarely to occasionally observed and deposits of gel in voids were occasionally observed. In the CAMBT bar, cracks and microcracks filled with ASR gel were commonly observed radiating from aggregates and cutting through the paste. The reactive components consist primarily of granite, rhyolite and quartzite particles. The ASTM C1293 concrete prism showed traces of evidence ASR, with no significant cracking or microcracking observed. Trace amounts of gel were observed in rare voids and reaction rims were occasionally observed on rhyolite and quartzite particles. No evidence of ASR was observed in the field specimen.

Knife River Pit



(a)

(b)

(c)

Figure 99. Knife River Pit exposure test samples. Reflected light photomicrographs of polished surfaces. (a) Gel in microcracks (red arrow) and in void (green arrow) on C1260 mortar bar. (b) Microcracks (red arrow) filled with gel on CAMBT bar. (c) Microcrack filled with gel (red arrows) on C1293 prism.

The mortar bars from the ASTM C1260 and the CAMBT show moderate and severe ASR, respectively. The C1260 mortar bar showed no macroscopic cracks; microcracks filled with ASR gel were rarely to occasionally observed and deposits of gel in voids were occasionally observed. In the CAMBT bar, cracks and microcracks filled with ASR gel were commonly observed radiating from aggregates and cutting through the paste. The reactive components consist primarily of granite, rhyolite and quartzite particles. The ASTM C1293 concrete prism showed negligible ASR, with no significant cracking or microcracking observed. Trace amounts of gel were observed in rare voids and reaction rims were occasionally observed on rhyolite and quartzite particles. No evidence of ASR was observed in either core.

Labarge Pit

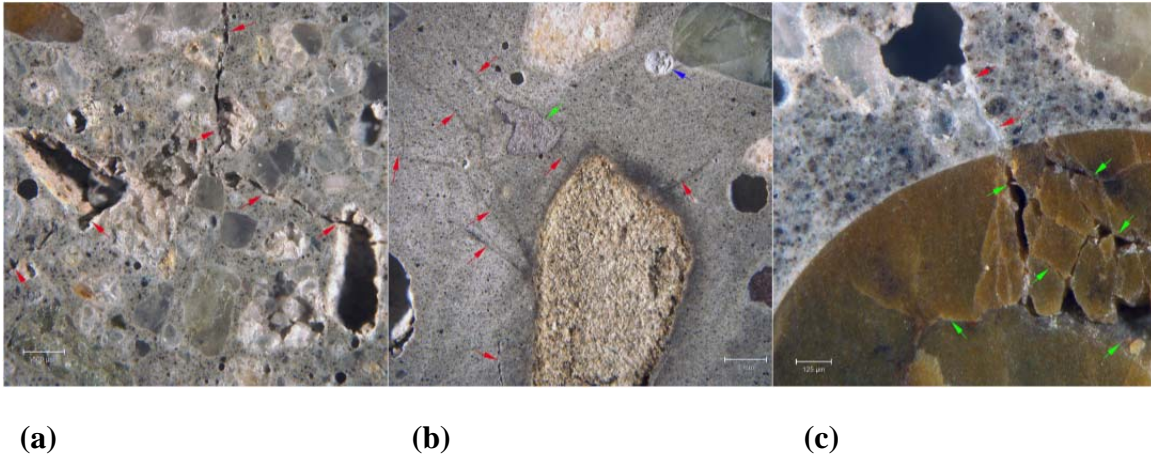


Figure 100. Labarge Pit exposure test samples. Reflected light photomicrographs of polished surfaces. (a) Gel in microcracks (red arrow) radiating from aggregate particle on C1260 mortar bar. (b) Microcracks (red arrows) filled with gel radiating from pitted quartzite particle on CAMBT bar. (c) Microcrack filled with gel (red arrows) on C1293 prism.

The mortar bars from the ASTM C1260 and the CAMBT show severe ASR, with abundant hairline cracks and microcracks filled with ASR gel and gel present in voids. Both granite and quartzite show evidence of reactivity. The ASTM C1293 concrete prism shows minor to moderate ASR. No significant cracking was observed but microcracks cutting the paste and filled with ASR gel were occasionally observed and reaction rims were commonly observed on granite and quartzite particles. No evidence of ASR was observed in the field specimen.

Lamax Pit

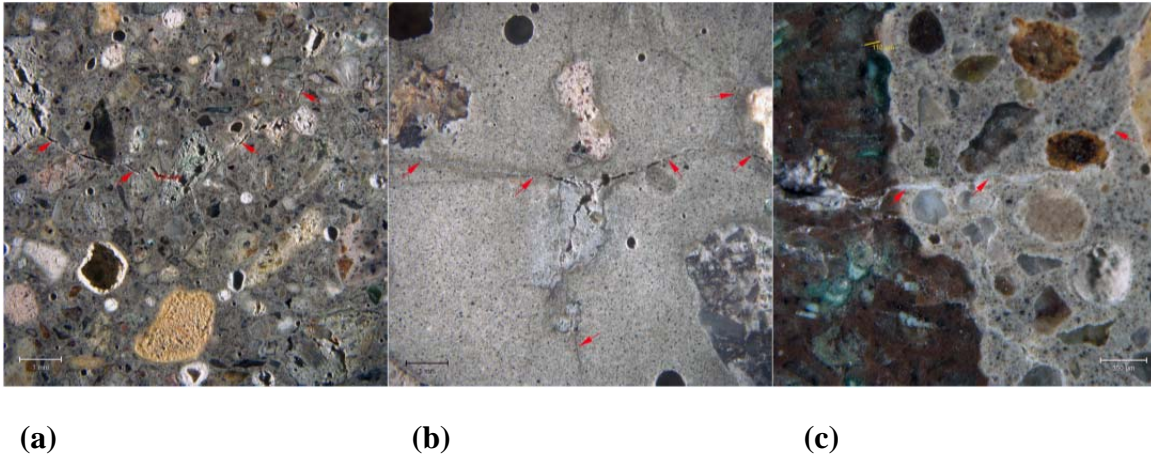


Figure 101. Lamax Pit exposure test samples. Reflected light photomicrographs of polished surfaces. (a) Gel in microcracks (red arrow) radiating from rhyolite particle on C1260 mortar bar. (b) Microcracks (red arrows) filled with gel radiating from rhyolite particle on CAMBT bar. (c) Microcrack filled with gel (red arrows) cutting from rhyolite particle into the paste on C1293 prism.

The mortar bars from the ASTM C1260 and the CAMBT show severe ASR, with abundant hairline cracks and microcracks filled with ASR gel cutting from rhyolite and granite particles, deposits of gel present in voids and extensive pitting of quartzite particles. The rhyolite, granite and quartzite show evidence of reactivity. The ASTM C1293 concrete prism shows minor to moderate ASR. No significant cracking was observed but microcracks cutting the paste and filled with ASR gel were occasionally observed and reaction rims were commonly observed on granite and quartzite particles. No evidence of ASR was observed in the field specimen.

Worland (BLM) Pit

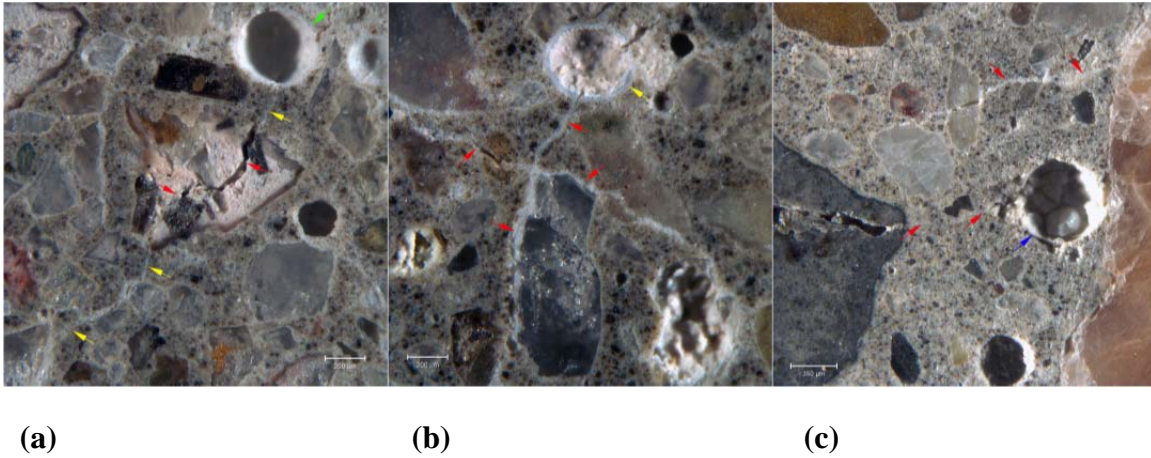


Figure 102. Worland (BLM) Pit exposure test samples. Reflected light photomicrographs of polished surfaces. (a) Microcracks (yellow arrows) radiating from rhyolite particle on C1260 mortar bar; the red bars show internal microcracks in the particle. (b) Microcracks (red arrows) filled with gel cutting through the paste on CAMBT bar. The yellow arrow highlights deposit of gel rimming a void. (c) Microcracks filled with gel (red arrows) cutting from rhyolite particle into the paste on C1293 prism. Blue arrow highlights void with gel.

The mortar bars from the ASTM C1260 and the CAMBT show moderate and severe ASR, respectively. The C1260 mortar bar showed no macroscopic cracks associated with ASR; microcracks filled with ASR gel were occasionally observed and deposits of gel in voids were occasionally observed. In the CAMBT bar, cracks and an extensive network of microcracks filled with ASR gel were commonly observed radiation from rhyolite particles and cutting through the paste. The reactive components consist primarily of rhyolite, quartzite and granite. The ASTM C1293 concrete prism showed traces of evidence of ASR, with no significant cracking or microcracking observed. Trace amounts of gel were observed in rare voids and reaction rims were occasionally observed on rhyolite and quartzite particles. No evidence of ASR was observed in the field specimen.